STABILITY ANALYSIS OF A COUPLED STRUCTURE: A RAILWAY
TUNNEL AND A ROAD CUT SLOPE

A THESIS SUBMITTED TO
THE GRADUATE SCHOOL OF APPLIED AND NATURAL SCIENCES
OF
MIDDLE EAST TECHNICAL UNIVERSITY

BY

BURCU ÜNLÜTÜRK

IN PARTIAL FULFILLMENT OF THE REQUIREMENTS
FOR
THE DEGREE OF MASTER OF SCIENCE
IN
MINING ENGINEERING

JULY 2018

Approval of the thesis:

STABILITY ANALYSIS OF A COUPLED STRUCTURE: A RAILWAY TUNNEL AND A ROAD CUT SLOPE

submitted by **BURCU ÜNLÜTÜRK** in partial fulfillment of the requirements for the degree of **Master of Science in Mining Engineering Department, Middle East Technical University** by,

Prof. Dr. Halil Kalıpçılar
Dean, Graduate School of **Natural and Applied Sciences**

Prof. Dr. Celal Karpuz
Head of Department, **Mining Engineering**

Assoc. Prof. Dr. H. Aydın Bilgin
Supervisor, **Mining Engineering Dept., METU**

Examining Committee Members:

Asst. Prof. Dr. İ. Ferid Öge
Mining Engineering Dept., Muğla Sıtkı Koçman University

Assoc. Prof. Dr. H. Aydın Bilgin
Mining Engineering Dept., METU

Asst. Prof. Dr. Mustafa Erkayaoğlu
Mining Engineering Dept., METU

Date: 12.07.2018

I hereby declare that all information in this document has been obtained and presented in accordance with academic rules and ethical conduct. I also declare that, as required by these rules and conduct, I have fully cited and referenced all material and results that are not original to this work.

Name, Last name : Burcu Ünlütürk

Signature :

ABSTRACT

STABILITY ANALYSIS OF A COUPLED STRUCTURE: A RAILWAY TUNNEL AND A ROAD CUT SLOPE

Ünlütürk, Burcu
M.Sc., Department of Mining Engineering
Supervisor: Assoc. Prof. Dr. Hasan Aydın Bilgin

July 2018, 106 pages

A road-cut slope is planned for the construction of a new highway at Zonguldak province. This slope will be excavated by bench blasting method in close proximity to the No 50 Turkish State Railway Tunnel which is a masonry lined 84 years old tunnel in service. The excavation will continue until –approximately- 56 m horizontal and 55 m vertical distances remain to the tunnel lining. The plane failure risk of the slope and the damage risk of the tunnel are two major risks. Investigating stability of the slope and determination of strains and displacements around the tunnel caused by the rock excavation by using plane strain analysis are crucial to assess the safety of these coupled structures, the tunnel and the slope itself. In this thesis, the stability analysis of the road-cut slope and the probability of any damage on the rock structure around the tunnel and the masonry lining caused by the excavation of the benches are examined with two-dimensional plane strain finite element program RS^2 with shear strength reduction technique.

Keywords: *Tunnel Stability, Slope Stability, Finite Element, Shear Strength Reduction, Mohr-Coulomb, Turkish State Railways, Zonguldak*

ÖZ

BİR DEMİRYOLU TÜNELİNİN VE BİR YOL ŞEVİNİN STABİLİTESİNİN İKİLİ ANALİZİ

Ünlütürk, Burcu
Yüksek Lisans, Maden Mühendisliği Bölümü
Tez Yöneticisi: Doç. Dr. Hasan Aydın Bilgin

Temmuz 2018, 106 sayfa

Zonguldak İli'nde yeni bir karayolu inşası için yol yarması yapılarak bir şev oluşturulması planlanmıştır. Şev kazısı, kullanımda olan, 84 yıllık, taş kemer kaplamalı, 50 Numaralı Türkiye Cumhuriyeti Devlet Demiyolları Tüneli'ne çok yakın mesafe içinde basamak patlatması yöntemiyle yapılacaktır. Şev kazısı tünel kaplamasına yaklaşık 56 m yatay uzaklık, 55 m düşey mesafe kalana değin devam edecektir. Şevde düzlem kayma ve tünelde hasar oluşma olasılıkları iki ana tehlikedir. Düzlem birim deformasyon analiz yöntemi kullanılarak kaya kazısının tünel çevresinde oluşturacağı birim deformasyonlar ile deplasmanların tayini ve şev duraylılığının araştırılması bu ikili yapının güvenilirliğine karar verilebilmesi için hayati önemdedir. Bu tez çalışmasında, basamak kazıları yapılması sonucunda tünel kaplamasında ve tüneli çevreleyen kaya kütlesinde oluşabilecek hasar olasılıkları ve yol yarması şevinin duraylılık durumu iki boyutlu düzlem birim deformasyon sonlu elemanlar yazılımı RS^2 kullanılarak makaslama dayanımı azaltma yöntemiyle incelenmiştir.

Anahtar Kelimeler: *Tünel Stabilitesi, Şev Stabilitesi, Sonlu Elemanlar, Kesme Dayanamı Azaltma, Mohr-Coulomb, Türkiye Cumhuriyeti Devlet Demiryolları, Zonguldak*

ACKNOWLEDGEMENTS

To my mother

TABLE OF CONTENTS

LIST OF TABLES

TABLES

LIST OF FIGURES

FIGURES

xiv

LIST OF ABBREVIATIONS

CSRF	Critical Strength Reduction Factor
FEM	Finite Element Method
GSI	Geological Strength Index
LEM	Limit Equilibrium Method
RMR	Rock Mass Rating
RQD	Rock Quality Designation
SF	Safety Factor
SRF	Strength Reduction Factor
SSR	Shear Strength Reduction
UCS	Uniaxial Compression Strength

CHAPTER 1

INTRODUCTION

1.1 Background Information

Transportation, one of the most essential requirements of humankind, has evolved together with the development of vehicle technology. Railways became popular in 19th century, after the Industrial Revolution (Peters, E. et.al, 2016). Road and other infrastructure constructions are still in progress to supply the society with this crucial service and will continue with the increasing population and need of mobility. This will give rise to the requirement of completing these projects in shorter durations and in the safest manner, therefore stability investigations on the designs have to be conducted to ensure the safety of these structures.

In this thesis, a coupled stability analysis was conducted for a road-cut slope and a railway tunnel before the slope construction. The subject tunnel is No 50 Turkish State Railway Tunnel, constructed in 1934 (TCDD, 2017) and the excavation of the mentioned road-cut slope was completed at the time of the submission of this thesis on the route of Zonguldak-Amasra-Kurucaşile Highway between Km 26+590 and Km 26+700.

The aforementioned tunnel is a shallow railway tunnel, which has been in service for the last 84 years, and it is still stable after the slope construction. The mountainous tunnel is masonry lined and the inner view of the tunnel is given in Figure 1 and the outer view of the tunnel is given in Figure 2.

Figure 1. Inner view of the tunnel

Figure 2. General view of the east portal of the tunnel and the surrounding rock

The road-cut slope, which was excavated by bench blasting, resulted in stress relief and variation in the stress distribution within the rock mass surrounding the tunnel. The removal of the rock mass may cause both slope instability and deformations around the tunnel. Hence, to investigate these risks, coupled stability analysis was conducted based on the planned slope profile with the current tunnel geometry. The plan view of the road-cut slope can be seen in Figure 3.

The vertical sections of the slope taken at each 10th meter of the route containing the tunnel were analyzed to investigate the possible failure surface for the slope and whether the tunnel will be enclosed or not in case any slope failure occurs. In order to investigate the possibility of a slope instability and the corresponding damage on the tunnel, planned profiles for the road-cut slope were modelled in the finite element software RS^2 considering two-dimensional plane-strain conditions. This software allows users to compute stresses and displacements on rock mass models, and with an embedded application that enables users to use Shear Strength Reduction (SSR) technique, to analyze failure planes and to estimate the Factor of Safety (SF) with the Critical Strength Reduction Factor (CSRF). Shear strength reduction can be basically explained as gradual decrease of the shear strength parameters which are cohesion and friction angle until the point of failure (CSRF). It is possible to see the failure plane on the computed outputs of the model, and stresses and displacements can be analyzed on these outputs.

In the analysis, slopes were investigated for displacement and failure, then the location of the slope failure plane was identified to observe if the tunnel was also influenced by the failure. If the slope failure plane covers the tunnel, then other strength reduction stages were investigated until the failure plane did not cover the tunnel. At that stage, the displacements on the slope and around the tunnel were investigated to evaluate the stability of the coupled structure. At the stage in which the coupled system was stable, SF was calculated for the system.
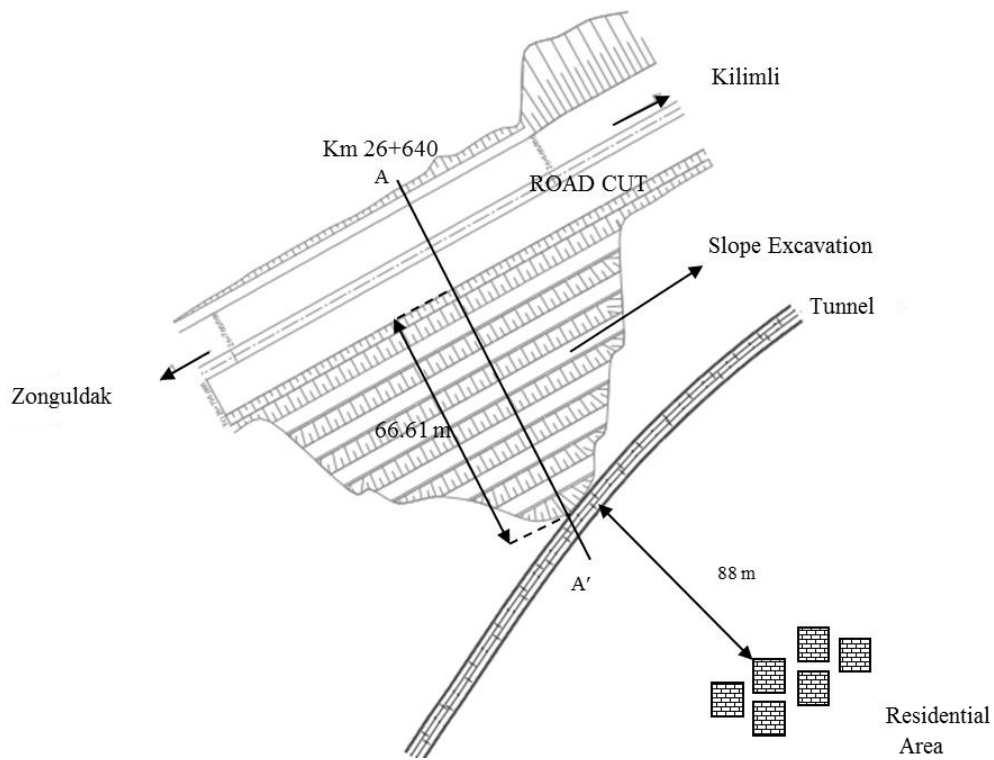
Figure 3. Plan view of the slope profile – tunnel is included

1.2 Problem Statement

A road-cut slope will be excavated by bench blasting on the transition zone of Zonguldak-Amasra-Kurucaşile highway between the sections of Km 26+590 and Km 26+700. There is a tunnel in service below the excavation which might be affected by the slope construction. Stability of the slope must be investigated to assess if any slope failure will occur or not, and in the case of a possible slope failure, the location of the failure surface must be investigated. Additionally, this excavation will cause stress relief around the tunnel below it and might lead to deformations and convergence around the tunnel. Hence, investigation of deformations and changes around the No 50 Turkish State Railway Tunnel must be examined and disturbance and damage of these changes must be evaluated to overcome the risk of failure for both structures.

4

1.3 Objective

In road constructions, road cuts are common in mountainous areas to overcome instability of the natural slopes where road excavations are performed. In this thesis, stability of a coupled structure; a road cut slope and a railway tunnel is examined. The tunnel is 84 years-old masonry lined No 50 Turkish state Railway Tunnel and is on the route of Zonguldak Amasra Kurucaşile roadway. It is in Kilimli region, between Km 26+590 and Km 26+700. The aim of this thesis is to model the coupled structure and assess its stability with Finite Element Software (FEM) software. The stability investigations are performed as the following:

i. Examination of the stability of the road-cut slope and rock mass covering the tunnel.

ii. Investigation of deformation and convergence amounts on the tunnel's sidewalls, shoulders, and roof.

The scope of this research study is using FEM to analyze and evaluate the stability of the No 50 Turkish State Railways Tunnel and the road-cut slope after the excavations.

1.4 Research Methodology

The case study is assessed in three steps. First, a short literature review is conducted to select the suitable method for slope stability assessment and geotechnical information about the study area is collected from reports and on site investigations.

Secondly, based on the knowledge collected from the aforementioned review, the slope-tunnel structure is modelled in a finite element analysis software and stability analysis is conducted with RS^2.

Finally, the results of the analysis are evaluated regarding deformations on the slope, location of the failure plane, and deformations around the tunnel which were utilized to decide on the safety factor of the slope.

1.5 Limitations

A number of limitations have been defined in order to achieve the aim of this thesis within the limited time and available resources. The most significant one is related to the physical and mechanical properties of the rock that the system belongs. These are taken from a geotechnical report prepared by Mega Mühendislik Müşavirlik Ltd for the neighboring tunnel structure. This aforementioned tunnel is between Km 25+290 and Km 25+656 and is around 900 m away from the entrance of No 50 Turkish State Railway Tunnel. After the onsite investigations it was decided that the rock masses have the same character and structure.

1.6 Structure of the Thesis

Including this chapter, this thesis consists of seven chapters containing information about literature survey, research area, data collection, methodology and case analysis, results and discussion, and conclusions and recommendations.

CHAPTER 2

LITERATURE SURVEY

Stability investigation of natural and man-made slopes is a significant topic in rock mechanics. In road constructions, road cuts are common in mountainous areas to overcome instability of the natural slopes where road excavations are performed, therefore stability of slopes has been a focus of various researches. Assessing slope stability is one the significant issues in geotechnical engineering (Farshidfar & Nayeri, 2015). Slope stability investigation is simply assessing the stress amount that a slope is able to manage before it fails and a slope is either natural or man-made, assuring the stability of it is of paramount importance as the failure of it might result in human and financial loses. The most important parameter affecting these analyses is the accuracy of the geotechnical data.

For the slope stability analysis, design based safety factor is calculated to determine how close a slope is to fail (Hammah et.al., 2004).

There are several methods used for slope stability analysis and determining the SF, limit equilibrium method (LEM) and the FEM are the most commonly used ones. For slope stability, LEM is a traditional and well established method for engineers and researchers, which was proposed by Bishop in 1955, and modified by Spencer (1967) and many others, but determining the failure plane is challenging in this method as stated by Sternik in 2013, and Farshidfar and Nayeri in 2015. FEM became increasingly popular in stability analysis with the introduction of the (time) SSR technique because of its flexibility and power as mentioned by Griffith and Lane in

1999, and has been improved significantly with time (Farshidfar & Nayeri, 2015). Since it is proved by many studies, a comparison of the SF from Shear Strength Reduction (SSR) technique and LEM shows that the results are similar, the biggest advantage of no need to decide on the failure plane in FEM makes the technique preferable (Murianni & Federico, 2011).

Furthermore, the overall advantages of SSR technique with FEM is explained in the following by Griffith & Lane and as cited in Hammah et. al. in Proceedings of EUROCK 53rd Geomechanics Colloquium 2004.

1. As mentioned before, the pre-assumption of shape and location of failure is unnecessary, as the failure occurs naturally where the material cannot support the generated shear stress.
2. If the stress-strain data is reliable then the FEM solutions provides information about deformation and displacement amounts.
3. It is capable of modelling progressive failure .

SSR technique is best suited for Mohr-Coulomb failure criterion due to its easiness (Hammah & Curran, 2007). In SSR technique strength parameters of the slope, namely, cohesion and internal friction angle are gradually reduced until the slope fails within perfect elasto-plasticity (Zheng et. al., 2009). In other words, SRF increases incrementally until collapse occurs (Chatterjee & Elkadi, 2012). The shear strength of the original material in Mohr-Coulomb failure criterion is calculated using the formula below, where τ is shear stress, c is cohesion, σ is normal stress and ϕ is internal friction angle:

$$\tau = c + \sigma tan\phi$$

The reduced shear strength is calculated with the following formula in which SRF is the factor that the strength parameters are divided.

$$\tau = \frac{c}{SRF} + \frac{\sigma tan\phi}{SRF}$$

8

This method can be explained in the following sequence:

1. Calculation of FEM model
2. Reduction of the strength parameters
3. If the run converges to a solution than it is the SF of the structure, if it does not converge than it is unstable (Hammah et.al. 2005).

In many of the slope stability analysis, safety factor is used to describe the how close or far away that the slope is from failing (Hammah et.al. 2005). The stage in which the slope instability occurs is the stage that the reduction factor is critical (CSRF) and this is taken to be the safety factor of the slope (Hammah & Curran, 2007). The SF in SSR technique can be explained as the ratio of the initial shear strength of the material to shear strength of the material at CSRF.

CHAPTER 3

GENERAL INFORMATION ABOUT THE STUDY AREA AND GEOTECHNICAL STUDIES

3.1 Research Area

The No 50 Turkish State Railway Tunnel is located in Kilimli, Zonguldak, and is on the route of the Zonguldak-Amasra-Kurucaşile Highway, between Km 26+590 and Km 26+700. It is 7 km away from Zonguldak city center and 70 km away from Bartın.

Figure 4. Location of the study area (http://zonguldak.bel.tr/ulasim-2/)

3.2 Data Collection and Processing

3.2.1 Geological and Geotechnical Information

The No 50 Turkish State Railway Tunnel is adjacent to Aslankayası Highway Tunnels that is between Km 25+290 and Km 25+656. On site investigations resulted in the following decisions; joints, dipping of the joints, bedding planes of the rock mass surrounding the Aslankayası Tunnels exhibit rather similar characteristics and structure of the rock mass that is covering the No 50 Turkish State Railway Tunnel. Figure 5 and Figure 6 represent the rock mass of the study area and the Aslankayası Tunnels, respectively, and were taken during onsite investigations. After the site visits, it was concluded that the geotechnical studies conducted by Mega Mühendislik Müşavirlik Ltd in 2014 for Aslankayası Tunnels can also be used for this study.

The rock mass covering the tunnel is named as Kilimli formation. It is coded as Kk in Aslankayası Tunnels Geologic-Geotechnical Report and consists of sandy limestone, sandstone, siltstone, claystone, clayey limestone and marl. The preliminary geology-geotechnical report was done for Aslankayası Tunnels by Mega Mühendislik Müşavirlik Tic. Ltd. Şti. in 2014. In the report, samples were taken from different rock types and required tests were conducted on these specimens to decide rock mass classification of the samples regarding Rock Mass Rating (RMR), Q System, Geological Strength Index (GSI) and New Austrian Tunneling Method (NATM).

*Figure 5. Rock mass structure at Kilimli, Zonguldak No 50 Turkish State Railway
Tunnel and slope excavation site*

Figure 6. Rock mass structure at Kilimli, Zonguldak Aslankayası Tunnels site

3.2.1.1 Geological Information about the Study Area

The region of the research is mainly characterized by limestone, mudstone, sandstone, conglomerate and shale. Different researchers studied this area such as Charles, Kaya, Tüysüz, Akbaş and many others as mentioned in Şener (2007).

Kilimli formation (Kk), which lies on top of İnaltı formation, consists of clayey limestone, sandstone, siltstone, claystone, and marl. The formation is divided into 3 categories and investigated separately. Yellow colored quartz sandstones are named as Velibey member, glauconitic sandstone and clayey limestone are considered as Sapça member, and the levels consisting of marl are considered to be Tasmaca member.

Kilimli formation demonstrates an alternation of limestone with sand, sandstone, siltstone, and claystone. It has a grey yellowish color and the bedding planes have low to medium thickness.

In the study area, outcrops of Sapça member (Kk's) can be seen. Sandstone, claystone, siltstone alternation consists of low amount of sandy clayey limestone levels.

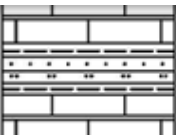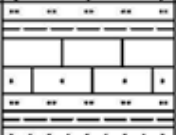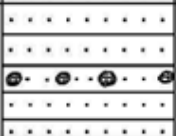The stratigraphy of the Kilimli formation is given in Figure 7.

Figure 7. Stratigraphy of Kilimli formation

3.2.1.2 Geotechnical Information

The geotechnical tests were conducted by Mega Mühendislik Müşavirlik Ltd. Şti. in accordance with site investigations and strength tests done on the specimens taken from the site. In the geotechnical report, the results of the laboratory tests on the specimens taken from the rock mass, Uniaxial Compressive Strength values, deformation modulus, unit weight etc., and tables regarding rock mass classification systems, namely, RMR, Q, GSI and NATM are given.

The data in the report is used to decide the lowered elasticity modulus in ROCDATA with the use of GSI. This lowered deformation modulus is controlling the displacement amount and distribution around the slope and the tunnel. In ROCDATA software, disturbance factor is required, for this case, as the tunnel was excavated before, it was taken as 0. Moreover, Kilimli formation consists of clay, hence dilation angle was taken as zero for the analysis. This ROCDATA data input and output is given in Appendix A.

The rock data used in RS^2 models can be seen from Table 1.

Table 1. Material properties of the rock mass- used in modelling (Mega Mühendislik Müşavirlik Ltd Şti, 2014)

Material Properties	
GSI	47
RMR	49
Q-Tunneling quality index	1.25
NATM	B2 Class
Compressive strength of rock mass (MPa)	2.62
Modulus of deformation (MPa)	2547
Poisson's ratio	0.26
Unit weight (kN/m3)	26
Peak cohesion (MPa)	0.51
Peak friction angle (°)	47.5
Peak tensile strength (MPa)	0.26
Residual cohesion (MPa)	0.3
Residual friction angle (°)	40
Residual tensile strength (MPa)	0.2

CHAPTER 4

METHODOLOGY AND CASE ANALYSIS

4.1 Rock Classification Systems

Stability analyses on rock structures require reliable geotechnical data, therefore the data obtained can be used in rock mass classification for analysis. For the classification of surrounding rock mass around the tunnel, which will be excavated RMR, GSI, and Q systems are used. Moreover, the result of these classification analyses were used for modelling the structure in FEM, RS^2.

4.1.1 Rock Mass Rating (RMR) System

This rock mass classification system, RMR, which was introduced by Bienawski in 1973, and developed in years uses six parameters of rock for classification. These are

i.   Uniaxial Compressive Strength,

ii.   Rock quality designation

iii.   Discontinuity spacing

iv.   Discontinuity conditions (length, separation, smoothness, infilling, weathering)

v.   Groundwater conditions

vi.   Discontinuity orientation (Hoek et. al., 2000).

Aforementioned parameters can be obtained during on-site investigations as well as laboratory experiments from the boreholes. The system uses these parameters to provide a rating for the rock mass that has been studied.

As a result of the site investigation and laboratory test results it was concluded that the rock mass covering the tunnel is a fair rock in RMR system.

4.1.2 Geological Strength Index

Geological Strength Index (GSI) is commonly used in designing of slopes and tunnels. This system is based on rock strength and deformation parameters. GSI value of a rock gives an overall representation of the geotechnical quality of a rock mass. It requires field observation to decide on blockiness and jointing properties etc. (Hong et.al., 2017).

4.1.3 Rock Tunneling Quality Index, Q

Norwegian Geotechnical Institute and Barton et.al. (1974) introduced a tunneling Quality Index, Q, to be used in determining rock mass characteristics and support categorizations of tunnels (Hoek et.al., 2000). This Q value is determined with the following formula Jn is the joint set number, Jr is roughness number of the joints and Ja is the alteration number where Jw is the joint water parameter, in addition, SRF is stress reduction factor.

$$Q = \frac{RQD}{J_n} x \frac{J_r}{J_a} x \frac{J_w}{SRF}$$

4.2 Modelling

The analyses were done with Mohr-Coulomb failure criterion. The values mentioned in Data Collection and Analysis chapter were used as inputs for the model. Additionally, as the formation consists of claystone, the dilatancy angle was taken as

0°, and the disturbance factor required for lowering the elasticity modulus was taken as 0, as the tunnel is excavated before, and no additional degradation of the mass parameters by disturbance factor was required.

Additionally, due to the onsite investigations no spring no water discharge is observed, moreover during the blast hole drilling operations, holes were observed to be dry, and in the analysis ground water is not included.

Furthermore,

FEM was selected to investigate the stability of the slope. SSR technique which is embedded in the RS^2 software was used to determine the failure surface of the slope, and accordingly, the situation of the tunnel was considered. The SRF of the stage in which the tunnel was not covered by the failure plane was selected and checked for displacement rates on the slope and around the tunnel, if the deformation amounts did not result in collapse then that stage was selected as which the coupled system is stable and SF of the coupled system calculated.

SRF and CSRF should not be considered directly as safety factor. First of all, these constants are the reduction rates of cohesion and internal friction angle of the limit equilibrium point of a slope failure. On the other hand, the strength reduction factor obtained at critical point when the model fails is equal to the SF of the system (Rocscience Inc., 2017).

To illustrate, if the slope failure situation occurs when the shear strength parameters of the rock mass of the slope is reduced by dividing them with 2.40, then CSRF is equal to 2.40. This CSRF can be considered and used, for this limit equilibrium case, as SF. Another example can be given for the same slope as follows; failure and deformation values will be significantly small in quantity and less in density when compared to the stage SRF=2.40 since no reduction is done on shear strength parameters at the stage SRF=1. In modeling stage SRF=1, when deformations around the tunnel and the slope, the absence or presence of yielding points and planes, their intensity and distribution are investigated it will be seen that the strength parameters are not reduced and a more stable model is created. In this case, SF=2.40/1=2.4.

19

Furthermore, if the shear strength parameters are divided by 1.50 and the situation at this stage is examined for stability, then SF at this stage is SF=2.40/1.50=1.60. The safety factors for the coupled structure were calculated accordingly.

Coupled stability analyses were carried out for the slope-tunnel system by investigating CSRF, SRF, and SF of the planned slope by FEM in RS^2 software with the embedded application Shear Strength Reduction (SSR). Stability of the slope and failure planes are checked with SSR technique for all sections including the tunnel. Both slope and tunnel deformations were analyzed for the possibility of instability of the slope and the tunnel.

In detail the following steps are done for the assessments:

1. Analysis were conducted for each 10th m of the tunnel-slope model
2. CSRF was evaluated for each cross-section, location of the failure plane of the slope and displacements were analyzed
3. Failure plane of the slope at CSRF was investigated for the possibility of covering the tunnel
4. The stage where the tunnel was not covered by the failure plane was selected for further investigation
5. Deformations around the tunnel were analyzed for the selected SRF stage in this step to investigate the possibility of tunnel instability due to road cut
6. SF of the coupled system was calculated

The model was created with plastic material and failure criteria used was Mohr-Coulomb. The material properties were used as input in RS^2 are given in Figure 8.
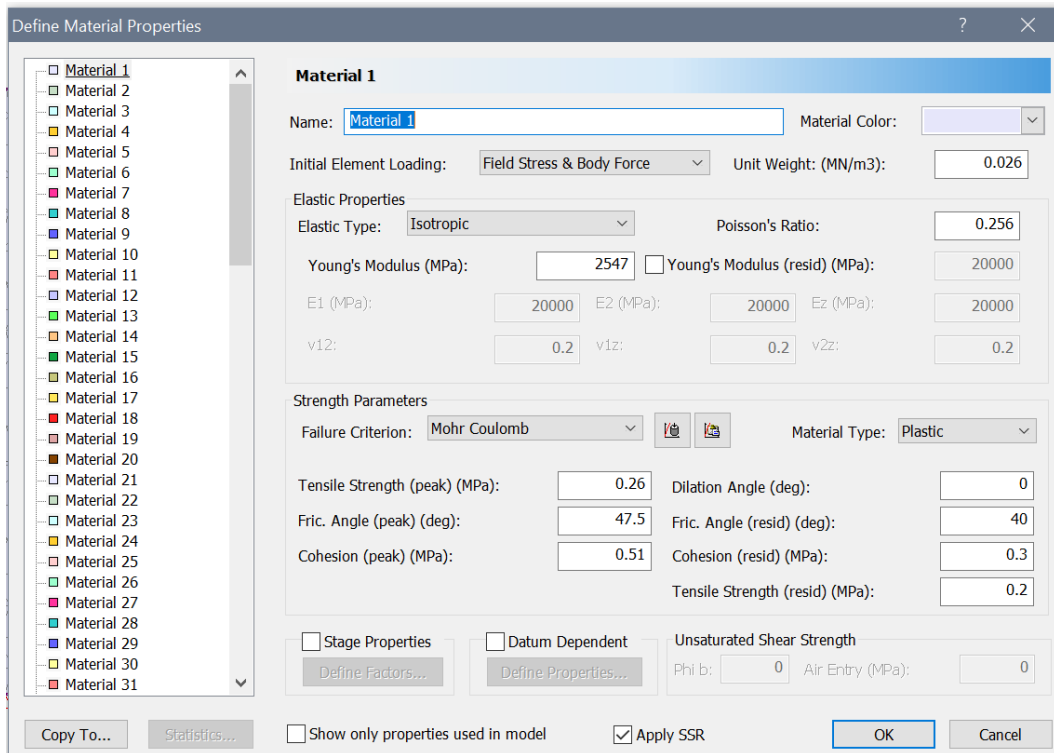
Figure 8. Material properties used in RS² for the analysis

The field stress properties used in the model are shown on Figure 9.
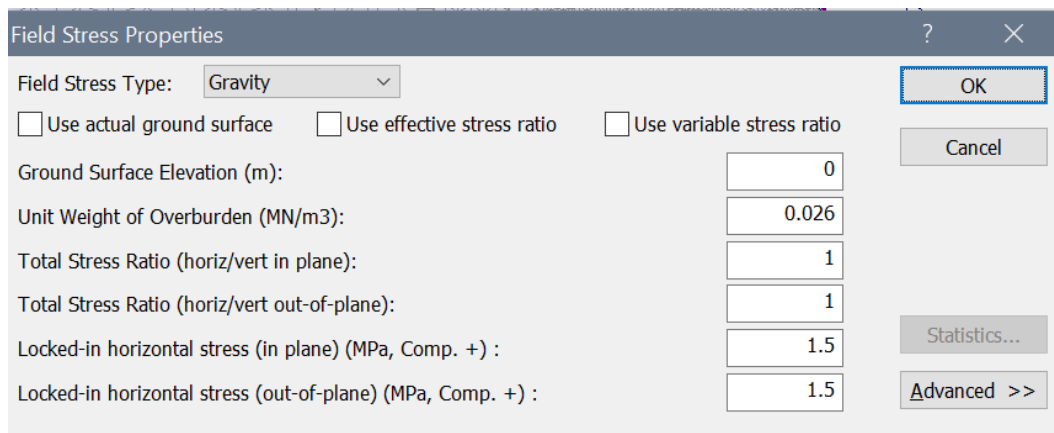

Figure 9. Field stress properties used for the model in RS2 for the analysis

CHAPTER 5

RESULTS AND DISCUSSION

All sections of the road-cut slope through the tunnel were investigated for slope and tunnel stability. This was realized by checking CSRF, SFR, and SF of the road-cut for each 10th m section. Secondly, the deformation amounts on the slope and the failure plane for each section were investigated to assess rock mass movement. Moreover, tunnel deformations were analyzed to assess instability cases.

In this section, analysis and discussions regarding the stability investigation are given in detail for the most critical section at Km 26+640. The modelling results of the sections are discussed under this chapter, but the modelling and analysis of the other sections are given in the Appendix 2.

The most critical section is selected by the following criteria:

1. The highest overburden above the tunnel, vertically

2. Closest distance to the tunnel from the planned road-cut slope profile, horizontally

5.1 Slope Stability Assessment of 26+640 Km

The most critical section of the planned slope-cut at Km 26+640 was analyzed to assess the stability of the slope and the tunnel, and the results are discussed in this section. That chainage was selected as the most critical section because of the shortest horizontal distance between slope profile and the tunnel, which is around 56 m, and the highest overburden thickness above the tunnel, for which the vertical distance to

23

the roof of the tunnel is around 55m – the highest overburden amount along the tunnel route. Figure 10 and Figure 11 are cross sectional views and a plan view of the coupled structure for the critical section respectively.
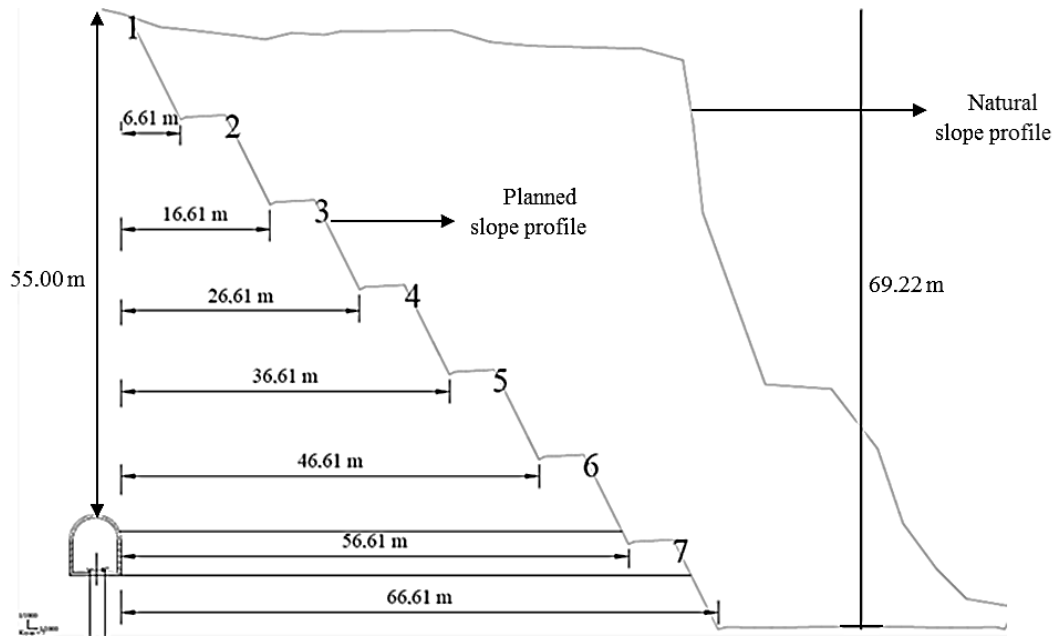
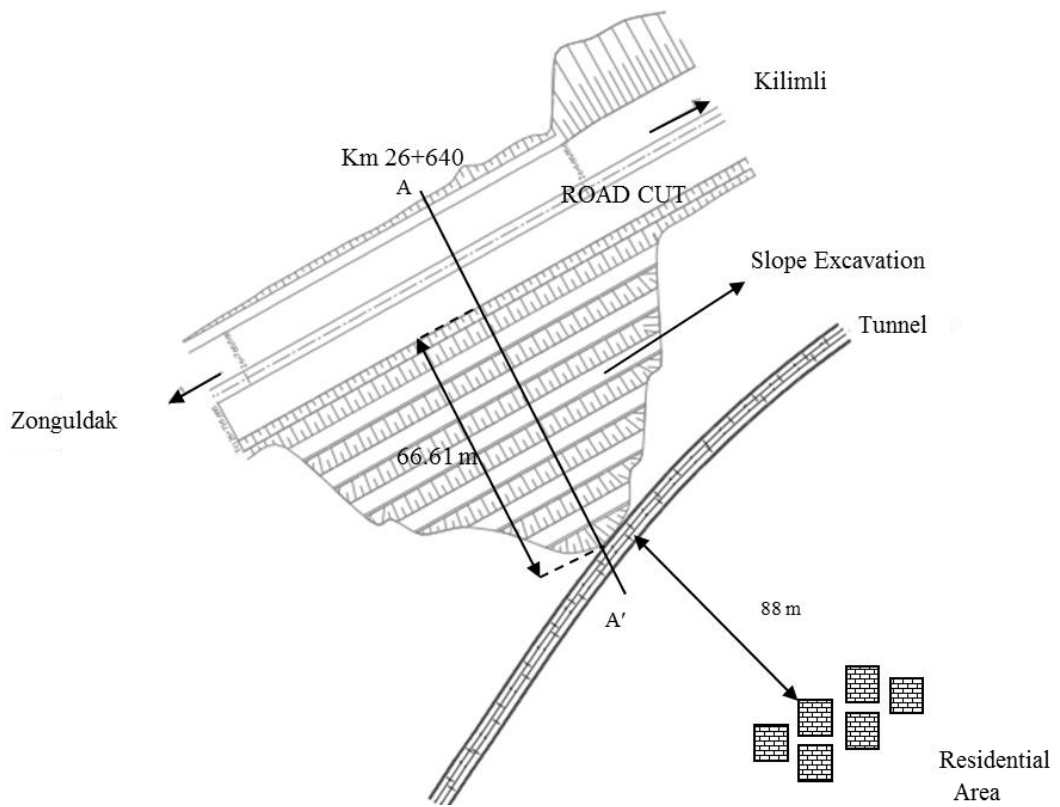*Figure 10. Cross-sectional view of the tunnel of the critical Km 26+640, section (A-A')*

Figure 11. Plan view of the tunnel of the critical Km 26+640 section (A-A').

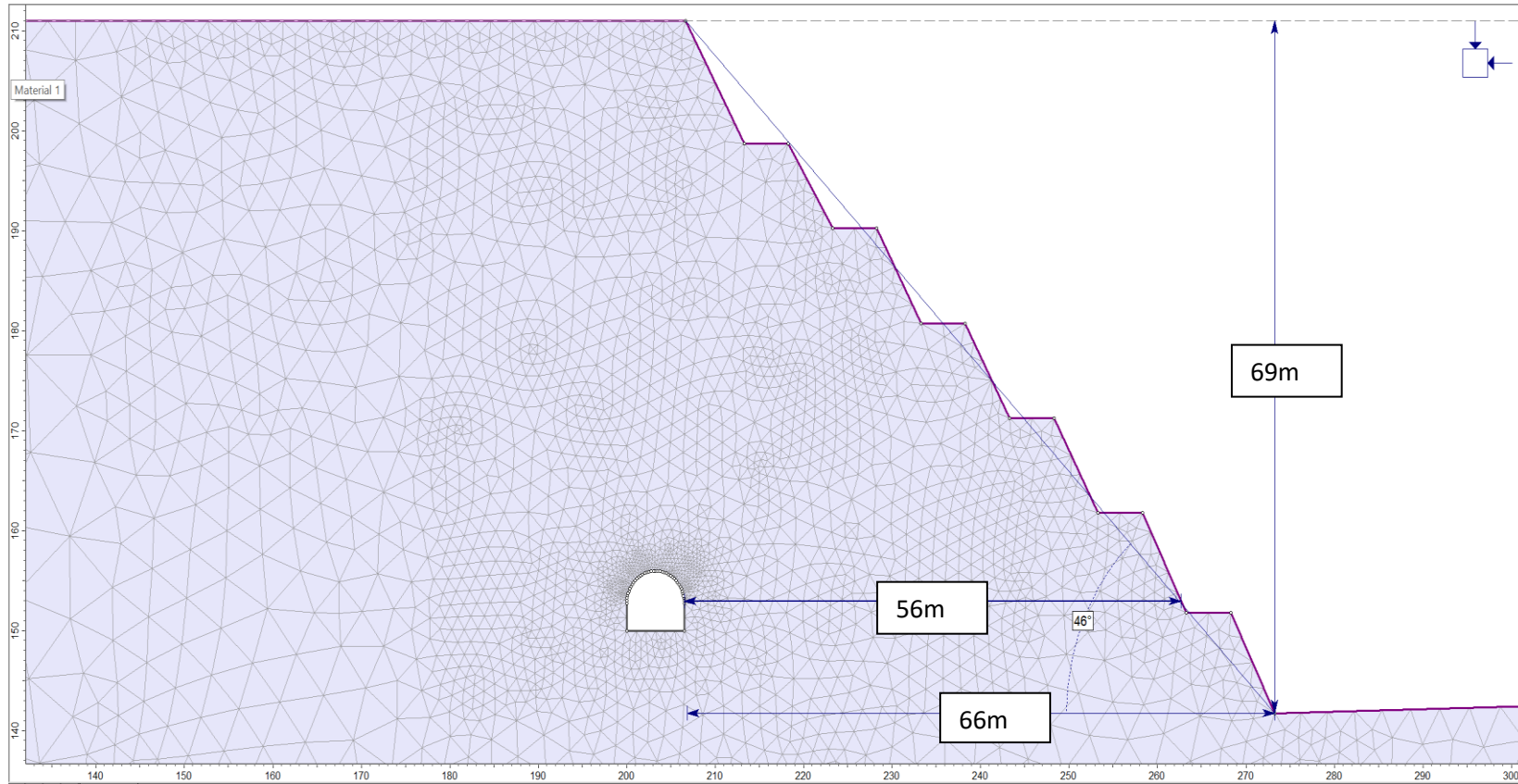The numerical model of the slope cut at Km 26+640 is given in Figure 12.

Figure 12. Slope dimensions and finite element model of the planned slope profile, section A-A', Km 26+640

After the creation of the model in RS^2, stability analyses were conducted to assess the slope stability of the most critical section.

Figure 13 shows the shear strain distribution in the rock mass and the possible failure surface of the slope for the stage CSRF=2.40. The failure plane shown in the figure was generated by the analysis of the maximum shear strain distribution in the model.

At this stage failure plane of the slope is covering the tunnel so, even though, CSRF=2.40 (SF=2.40) is a high safety factor, any failure in the slope cut will affect the tunnel and it is not a desired situation. Therefore, other stages were investigated to see where the failure plane was not covering the tunnel, and for that stage the displacements around the tunnel were assessed to see if the deformation amount might cause collapse of the tunnel or not. Then, the stage where the SRF=1.50 was decided to be investigated. In Figure 14 the failure mechanism by SSR can be observed on the contours of the maximum shear strain. In this stage, SRF=1.50 means that the strength factors, cohesion and friction angle were divided by 1.50. Hence the safety factor at this stage is SF=CSRF/SRF=2.40/1.50=1.60.

In this case study, coupled stability of the slope and the tunnel had to be investigated together. In other words, since it is a coupled system, stability of the slope and the tunnel could not be assessed separately. Hence, further investigation was required when the CSRF=2.40 was calculated, and it is actually found that the stability of both systems were ensured in the stage SRF=1.50 and the coupled safety factor for the system was calculated to be 1.60.

In Figure 15, the displacements of the slope are shown for the most critical state, CSRF=2.40. Displacement amounts on the slope are around 9-10 cm, and the failure plane encloses the railway tunnel. For a slope with a height of around 50 m, these magnitudes of deformation are not likely to cause any failure, since the limit equilibrium (failure) state is obtained by decreasing the strength factors by a factor of 2.40.

Displacement vectors and amounts calculated at SRF=1.50 are given in Figure 16. Displacement magnitudes decreased to 1-2 cm, hence the slope can be considered safe since the SF is 1.60 (SF=CSRF/SRF=2.40/1.50=1.60).
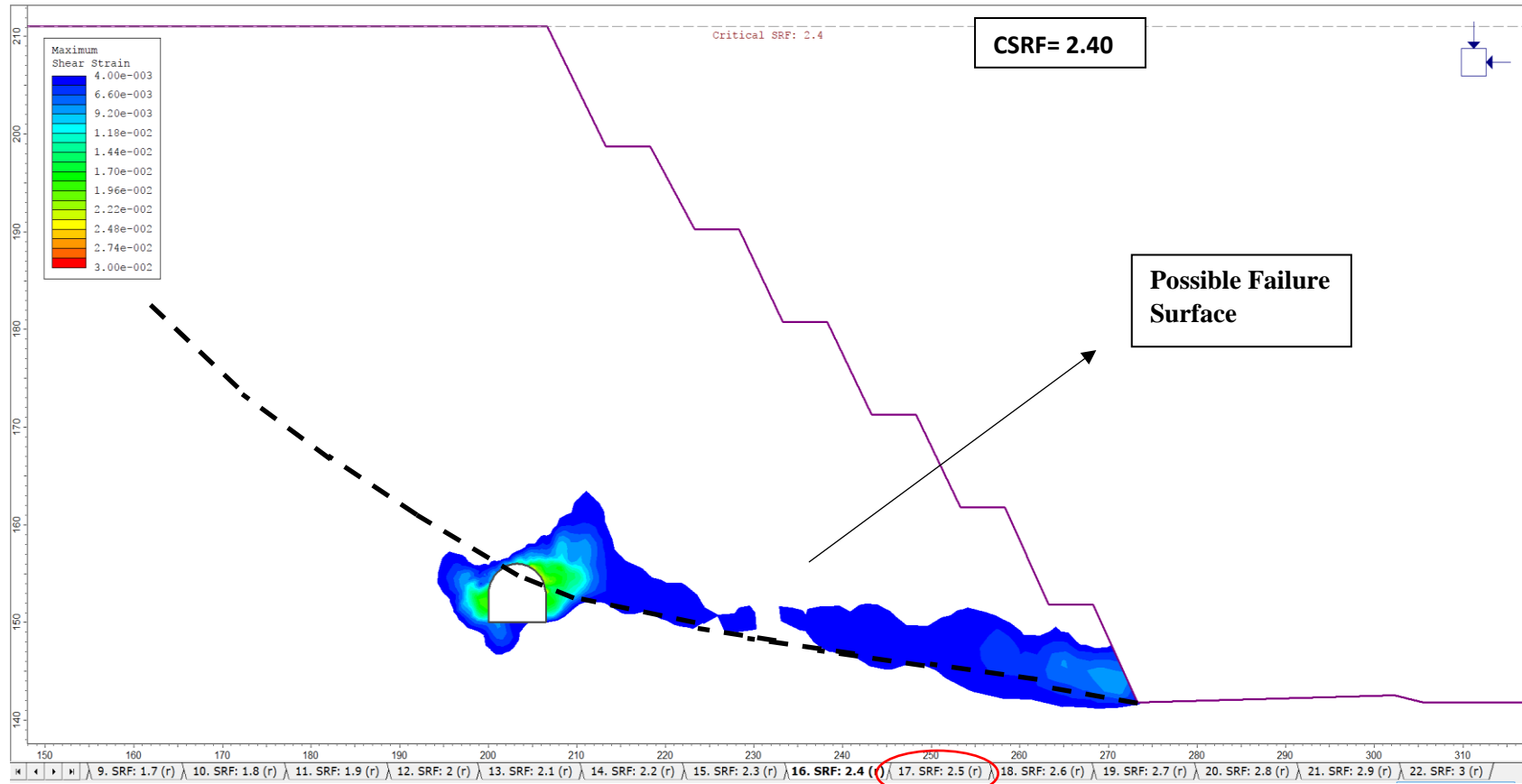
Figure 13. Maximum shear strain distribution and possible failure surface after critical strength reduction of (CSRF) 2.40 at Km 26+640
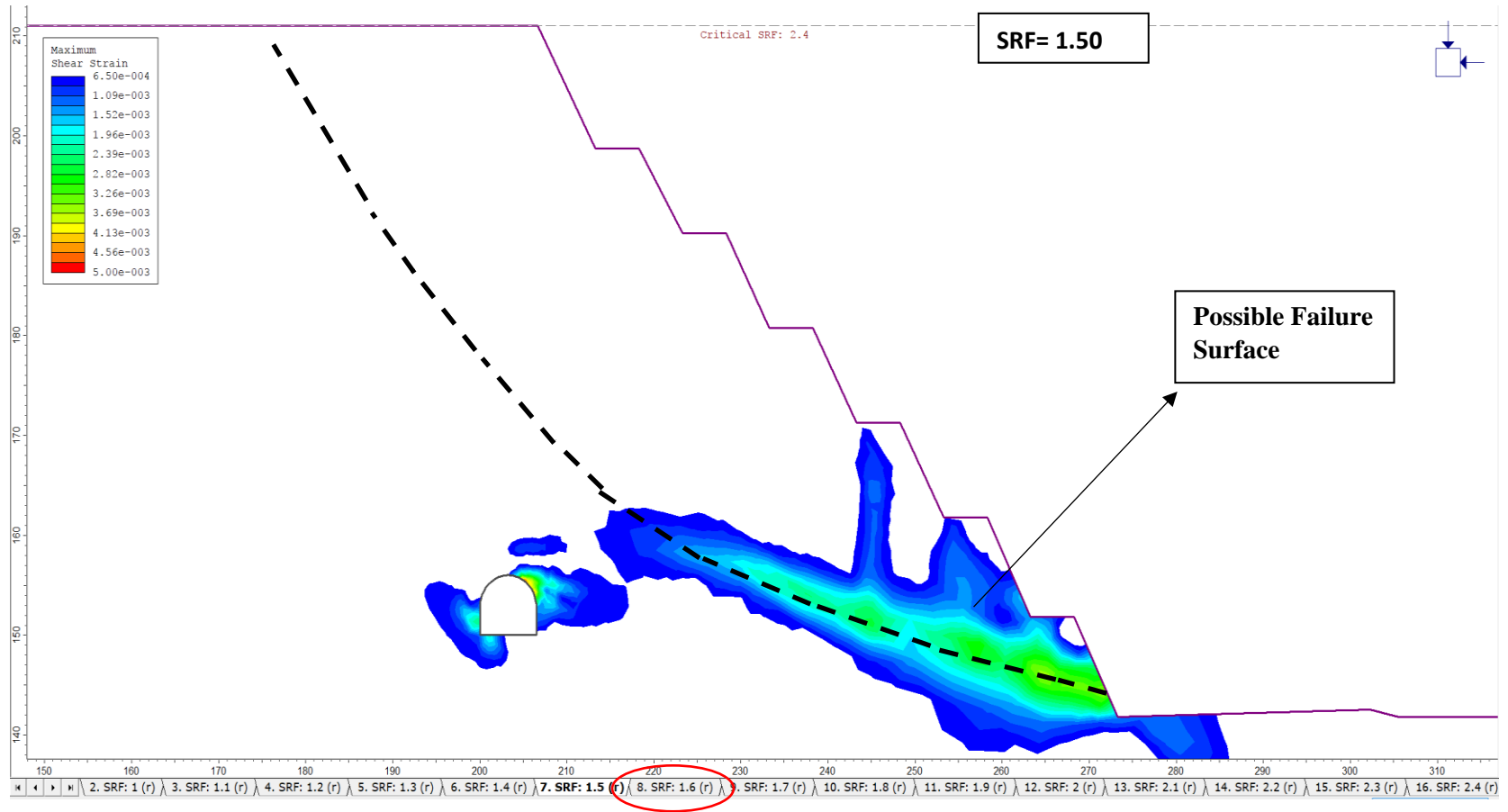
Figure 14.Maximum shear strain distribution and possible failure surface after strength reduction of (SRF) 1.50 at Km 26+640
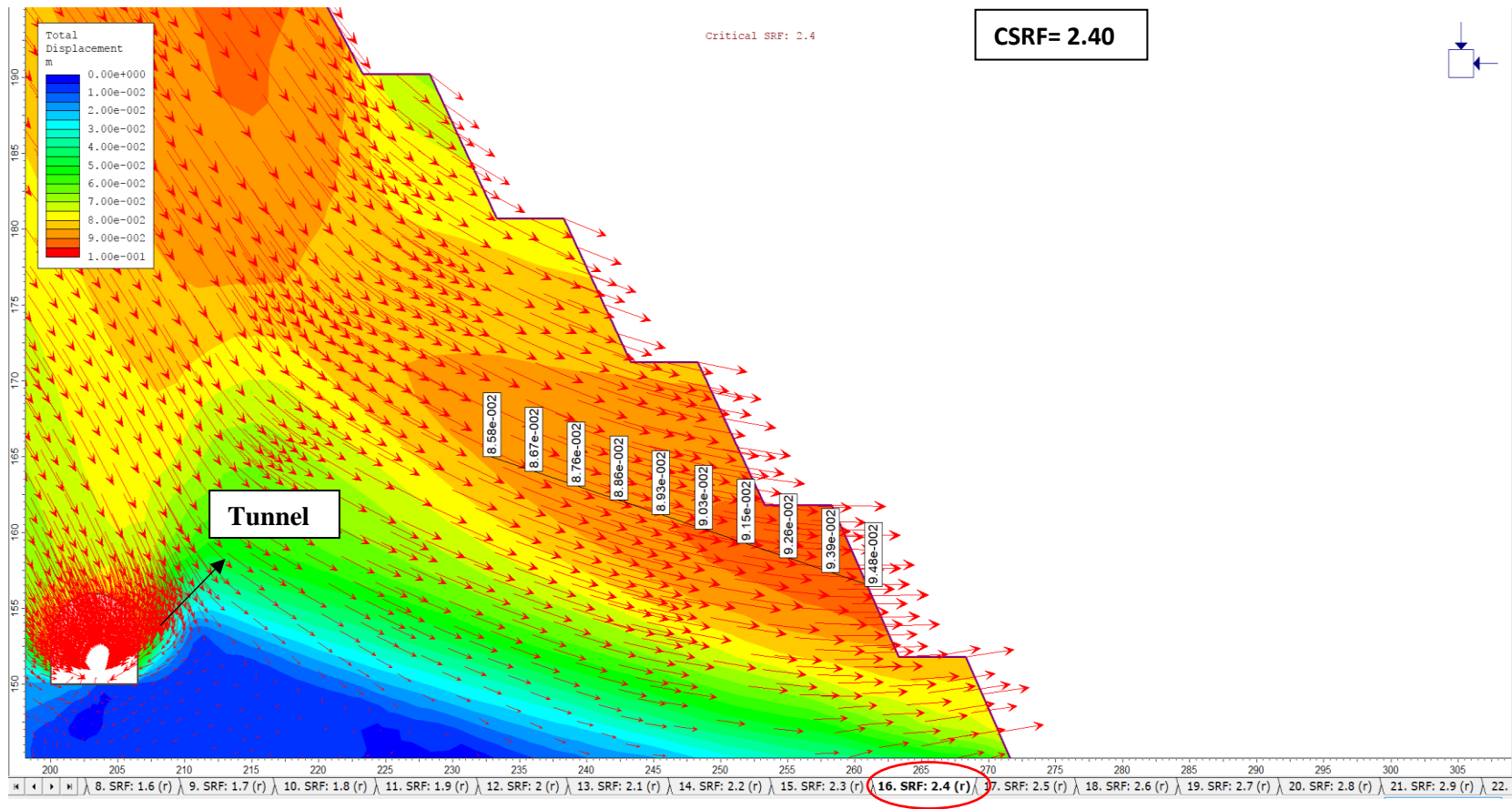
Figure 15. Displacement vectors and displacement magnitudes within planned slope cut at the CSRF=2.40 at Km 26+640
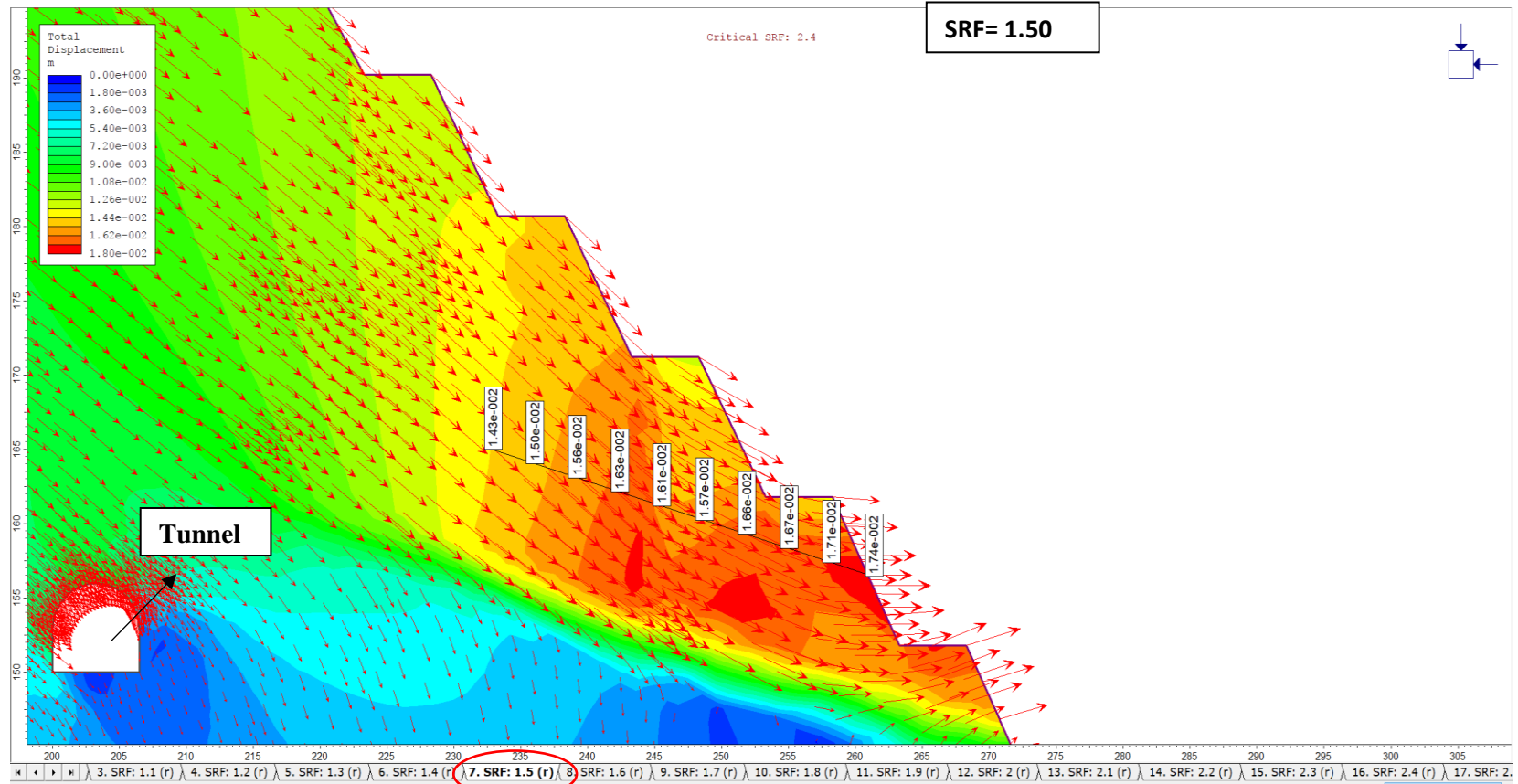
Figure 16. Displacement vectors and displacement magnitudes within the planned slope cut at the SRF=1.50 at Km 26+240

5.2 Tunnel Stability

The deformations around the tunnel were investigated for CSRF=2.40 stage and for the selected stage, SRF=1.50. Deformations around the tunnel for CSRF=2.40 and SF=1.50 are shown in Figure 17 and Figure 18, respectively. For the critical stage (limit equilibrium or failure, CSRF=2.40 case) the displacements likely occur around the tunnel were calculated between 3 cm and 8 cm (Figure 17), and according to NATM Classification, where the rock mass is discussed as B2 – very friable rock – failure of the tunnel is likely to occur. Instability of the tunnel having 6.5 m width can only occur when the displacements around it may reach 3 to 5 cm or beyond. Therefore, no damage is expected unless the CSRF value equals 2.40. Additionally, the SRF=1.50 case was investigated and the displacements at the tunnel crown and shoulders are calculated to vary between 0.3 and 0.7 cm (Figure 18). Displacement amounts around 3-7 mm for the case SRF=1.50, are about one tenth of the those calculated for CSRF=2.40 case. SRF=1.50 case led to a coupled factor of safety of 1.60 (SF=CSRF/SRF=2.40/1.50=1.60). Displacements varying from 3 mm to 7 mm will not cause any failure of the tunnel, moreover, the failure plane of the slope is not covering the tunnel (Figure 14). Hence no failure at the boundary of the tunnel is expected even though the strength factors, namely cohesion and friction angle, are decreased by 1.50 (in case of SRF=1.50).
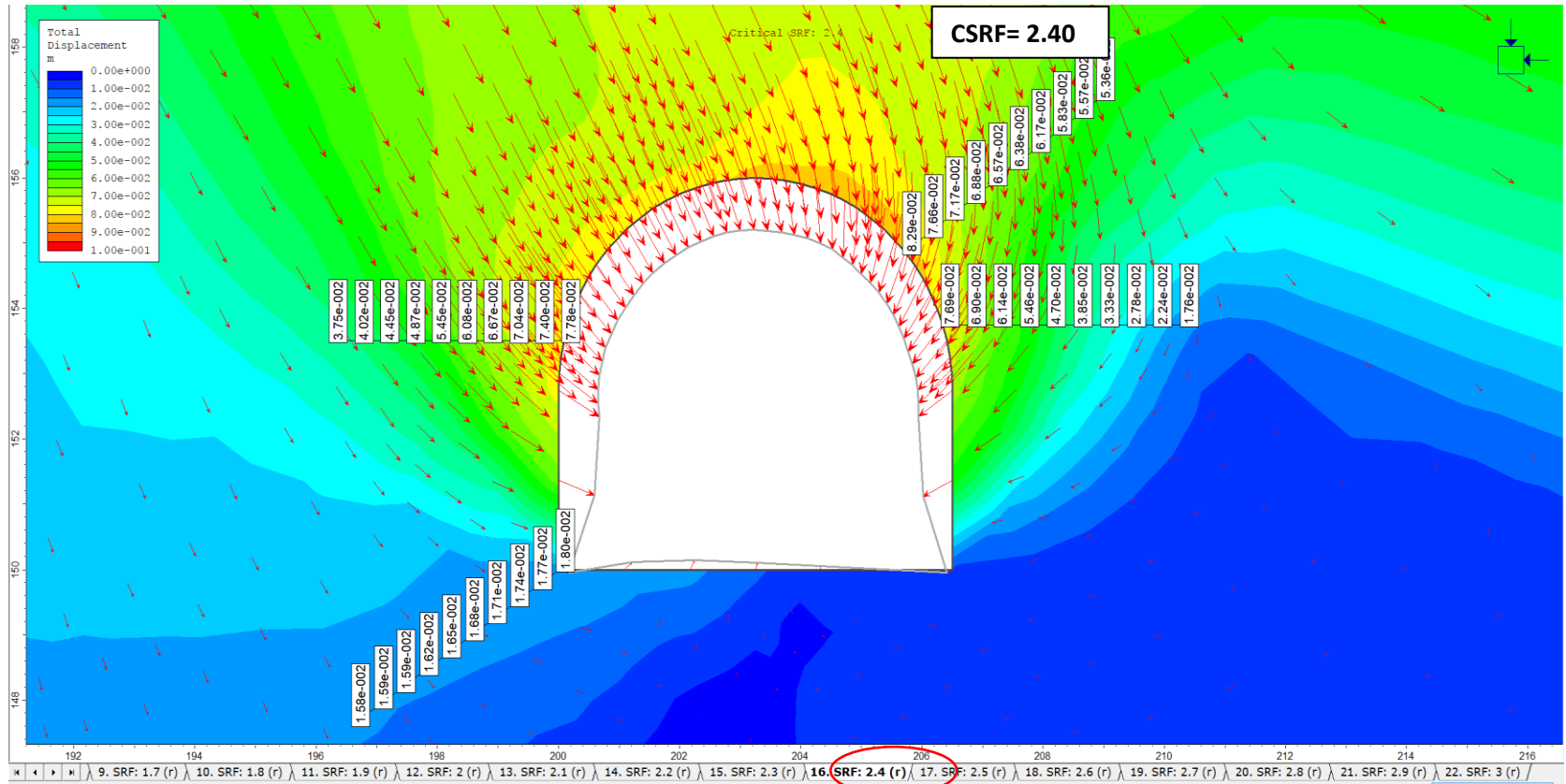
Figure 17. Displacement amounts around the tunnel at the CSRF=2.40 at Km 26+640
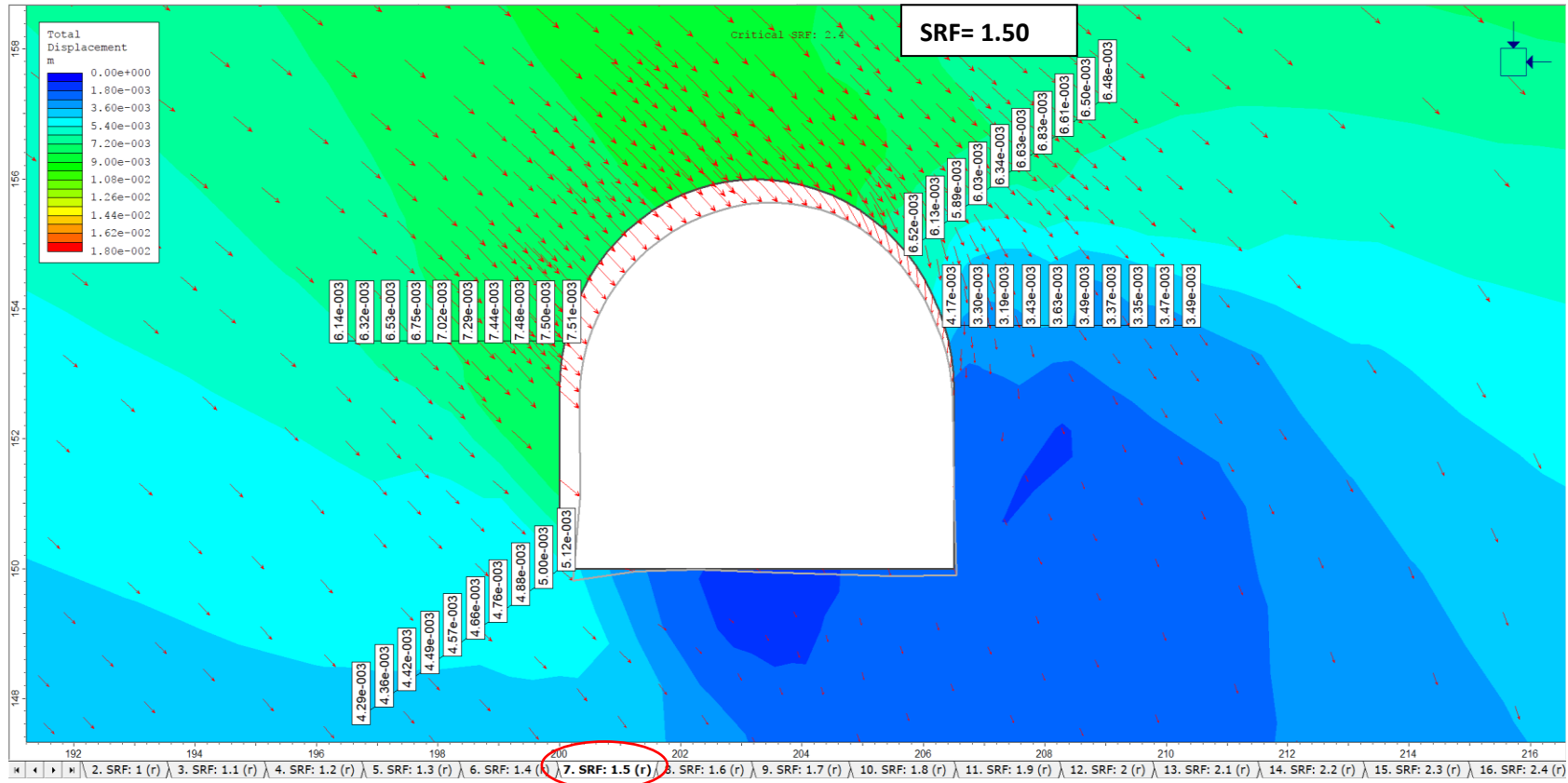
Figure 18. Displacement amounts around the tunnel at the SRF=1.50 at Km 26+640

In Table 2, the CSRF and the SF values calculated for each 10th m section for the coupled system are provided. The selected stage SRF=1.5 was used for all the other sections assessed as it was decided to be used for the most critical section, and to provide accuracy in the calculations. In the appendix, computation results for each section at their critical stage and SF=1.5 are given.

Table 2. The CRSF and SF for the coupled system in analyzed cross-sections

Cross - Section (Km)	CSRF	SF
26+600	2.5	1.67
26+610	2.6	1.73
26+620	2.4	1.60
26+630	2.6	1.73
26+640	2.4	1.60
26+650	2.7	1.80
26+660	3.3	2.20
26+670	2.9	1.93
26+680	3.5	2.33
26+690	4	2.67

Table 3. The displacement amounts around the tunnel at the CSRF and SF of the cross-sections

Cross - Section (Km)	Displacement amounts around the tunnel at CSRF (cm)	Displacement amounts around the tunnel at aimed SF (cm)
26+600	1-9	0.2-2
26+610	0.2-9	0.5-2
26+620	2-9	0.3-1
26+630	2-7	0.3-0.6
26+640	2-8	0.3-0.7
26+650	3-20	0.3-0-7
26+660	0.2-1	0.01-0.2
26+670	1-7	0.4-0.6
26+680	1-0.7	0.2-0-6
26+690	0.7-3	0.07-0.3

CHAPTER 6

CONCLUSIONS AND RECOMMENDATIONS

In this thesis, coupled stability analysis of a planned road-cut slope and a railway tunnel is conducted since the slope excavation above and at the side of the tunnel will cause stress relief around the tunnel.

Structures were analyzed in one coupled system and the stability analysis were conducted with FEM. The software used was RS^2 and the shear strength reduction technique that is embedded in the software was implemented to conduct the stability analysis on the structure.

Firstly, the structure was modelled in the software and computations were done according to SSR technique. Then, displacements on the slope and the possible failure surface of it were evaluated at the CSRF, which was the stage in which the structure fails. As the failure plane of the slope was covering the tunnel at these stages for every modelled section, other stages where the slope structure was stable and the tunnel was not covered by the failure plane of that was selected for further investigation of the coupled system. That stage was evaluated again, according to the slope stability and failure plane. In addition, the tunnel deformations were assessed for tunnel stability. At these stages, the safety factor of the coupled system was calculated.

The analysis started with the critical section 26+640 Km and conducted for each 10th m section along the route. The safety factors of each system is calculated for their critical stage and coupled stage. The conclusions are listed in the following:

- SF of the coupled structure at the most critical section is 1.60.
- The highest coupled SF is found as 2.67.

- The lowest coupled SF calculated is 1.60.
- The lowest SF found for the slope is 2.3.
- The highest SF found for the slope is 3.5.

Since the lowest SF for the slope was higher than 2.0, which is the defined limit in the Disaster Regulation for Highway Engineering Structures which contains other engineering structure in Appendix 9 (Bayındırlık ve İskan Bakanlığı, 2006), the slope was found safe. Moreover, the displacements assessed around the tunnel in each analyzed section for the related coupled SF shows that the deformations are in the range of 0-2 cm, which will not cause the failure of the tunnel. The lowest coupled SF is higher than 1.5, which is commonly accepted as a reliable SF for engineering constructions.

The SSR method is easy to be implemented in FEM as the software is user friendly. After understanding what is affecting the rock structures' strength, the method is beneficial to use, as it does not require assumptions on how the structure will fail. It is beneficial over LEM, and only rock properties are utilized. This method has been widely used and many studies were conducted with this method on stability of the structures.

In further modelling gravitational constant may be included in modelling for pseudo dynamic analysis. Hence, more detailed geotechnical data can be collected.

In case of water table presence, it should be included in modelling.

REFERENCES

Bayındırlık ve İskan Bakanlığı. (2006, 12 07). *Resmi Gazete.* Retrieved from Karayolu Mühendislik Yapıları için Afet Yönetmeliği: http://www.resmigazete.gov.tr/eskiler/2006/12/20061207-5.htm

Bihop, A. (1955). The use of the slip circle in the stability analysis of slopes. *Geotechnique, 5*, 7-17.

Chatterjee, P., & Elkadi, A. (2012). *Strenght Reduction Analysis.* Netherlands: TNO DIANA BV.

Farshidfar, N., & Nayeri, A. (2015). Slope Stability Analysis by Shear Strength Reduction Method. *Journal of Civil Engineering and Urbanism, 5*(1), 35-37.

Griffiths, D., & Lane, P. (1999). Slope Stability Analysis by finite elements. *Geotechnique, 49*(3), 387-403.

Hammah, R., Curran, J. H., Yacoub, T., & Corkum, B. (2004). Stability Analysis of Rock Slopes using the Finite Element Method. *Proceedings of the EUROCK 2004 & 53rd Geomechanics Colloquium*(1), 783-789.

Hammah, R., Curran, J., Yacoub, T., & Corkum, B. (2005). The Shear Strength Reduction Method for the Generalized Hoek-Brown Criterion. *Alaska Rocks 2005, the 40th U.S. Symposium on Rock Mechanics: Rock Mechanics for Energy, Mineral, Infrastructure Development in teh Northern Regions.* Anchorage, Alaska.

Hammah, R., T., Y., & Curran, J. (2007). Servicability-Based Slope Factor of Safety using the Shear Strength Reduction Method. *11th ISRM Congress Proceedings* . Lisbon: International Society for Rock Mechanics and Rock Engineering.

Hoek, E., Kaiser, P., & Bawden, W. (2000). *Support of Underground Excavations in Hard Rock* . CRC Press.

Hong, K., Han, E., & Kang, K. (2017). Determination of geological strength index of jointed rock mass based on image processing. *Journal of Rock Mechanics and Geotechnical Engineering, 9*(4), 702-708.

Mega Muhendislik Musavirlik Tic. Ltd. Sti. (2014). *Aslankayasi Tuneli - Tunel On PROJE Jeolojik Jeoteknik Etut Raporu.* Ankara.

Murianni, A., & Federico, A. (2011). A comparison between the limit equilibrium method and the shear strength reduction technique for slope stability analyses. *13th Conference of the IACMAG, Computional Advances in Numerical and Analytical Methods.*

Peters, Edward; Parker, N. Geoffrey; Weinstein, Donald; ,McMillan Salmon, John; Herrin, Judith Eleanor; Russell, Geoffrey ; Treasure, Richards; Stig Sørensen, Marie-Louise. (n.d.). *The Industrial Revolution.* Retrieved July 13, 2018, from Encyclopedia Britannica: https://www.britannica.com/topic/history-of-Europe/The-Industrial-Revolution#ref311007

Rocscience Inc. (2017, 10 13). *Shear Strenght Reduction Overview.* Retrieved from www.rocscience.com/help/phase2/webhelp/phase2_model/Shear_Strenght_Reduction_Overview

Şener, S. (2007). Amasra Yöresi (Bati Karadeniz) Üst Jura-Alt Kretase İnalti Kireçtaşlarinin Bentik Foraminifer Paleontolojisi. Retrıeved from acikarsiv.ankara.edu.tr/browse/24958/sıbelsener.pdf

Sternik, K. (2013). Comparison of Slope Stability Precitions by Gravity Increase and Shear Strength Reduction Methods. *Technical Transactions Environment Engineering*(1-s), 121-130.

(2017, January). TCDD. (B. Unluturk, Interviewer)

Zheng, Y., Tang, X., Zhao, S., Deng, C., & Lei, W. (2009). Strength reduction and step loading finite element approaches in geotechnical engineering . *Journal of Rock Mechanics and Geotechnical Engineering, 1*(1), 21-30.

APPENDICES

A. DATA RELATIVE TO CHAPTER 3

Under the section Data Collection and Processing the data calculated with ROCDATA which was used for analyses in RS^2 software was mentioned in Appendix 1. In Figure 19 the input data and the output data are provided.
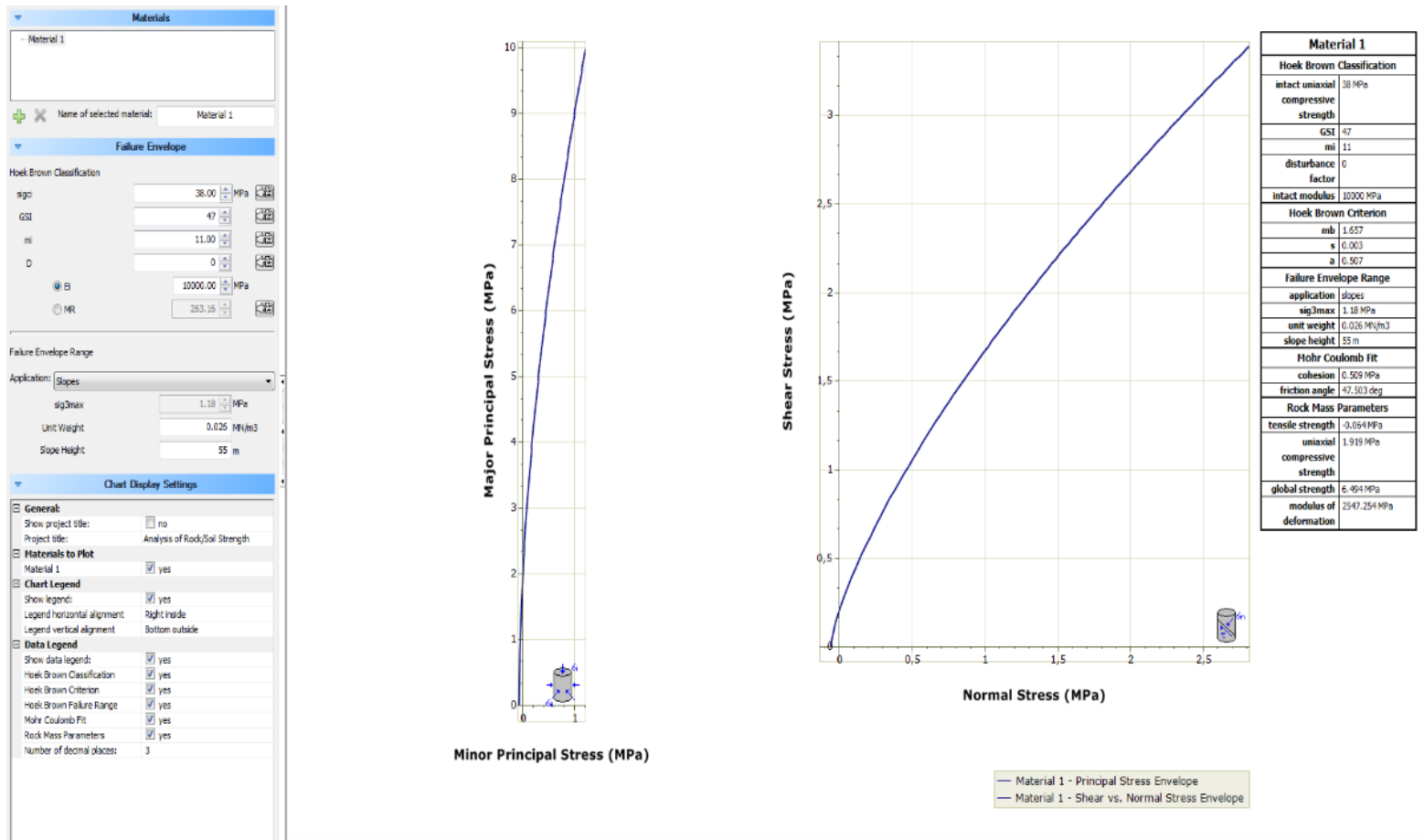
Figure 19. ROCDATA – input and output data

B. COMPUTATION RESULTS FOR EACH CROSS-SECTION

In Appendix 2, the cross-sectional modelling of the slope profiles and the results obtained from the analyses of the coupled structure profiles 26+600, 26+610, 26+620, 26+630, 26+650, 26+660, 26+670, 26+680 and 26+690 are presented. In addition, the models and the results of analyses for each cross-section are given in the following order; FE mesh model and the dimensions of the slope profile under consideration, maximum shear strain distribution, and location of the failure plane at CSRF for related slope section, maximum shear strain distribution and location of the failure plane at SRF=1.5 for the same section, displacement vectors and magnitudes at CSRF for related slope section, displacement vectors and magnitudes of the slope at SRF=1.5, displacement magnitudes around the tunnel at CSRF for related section, displacement magnitudes around the tunnel at SRF 1.5.

Km 26+600
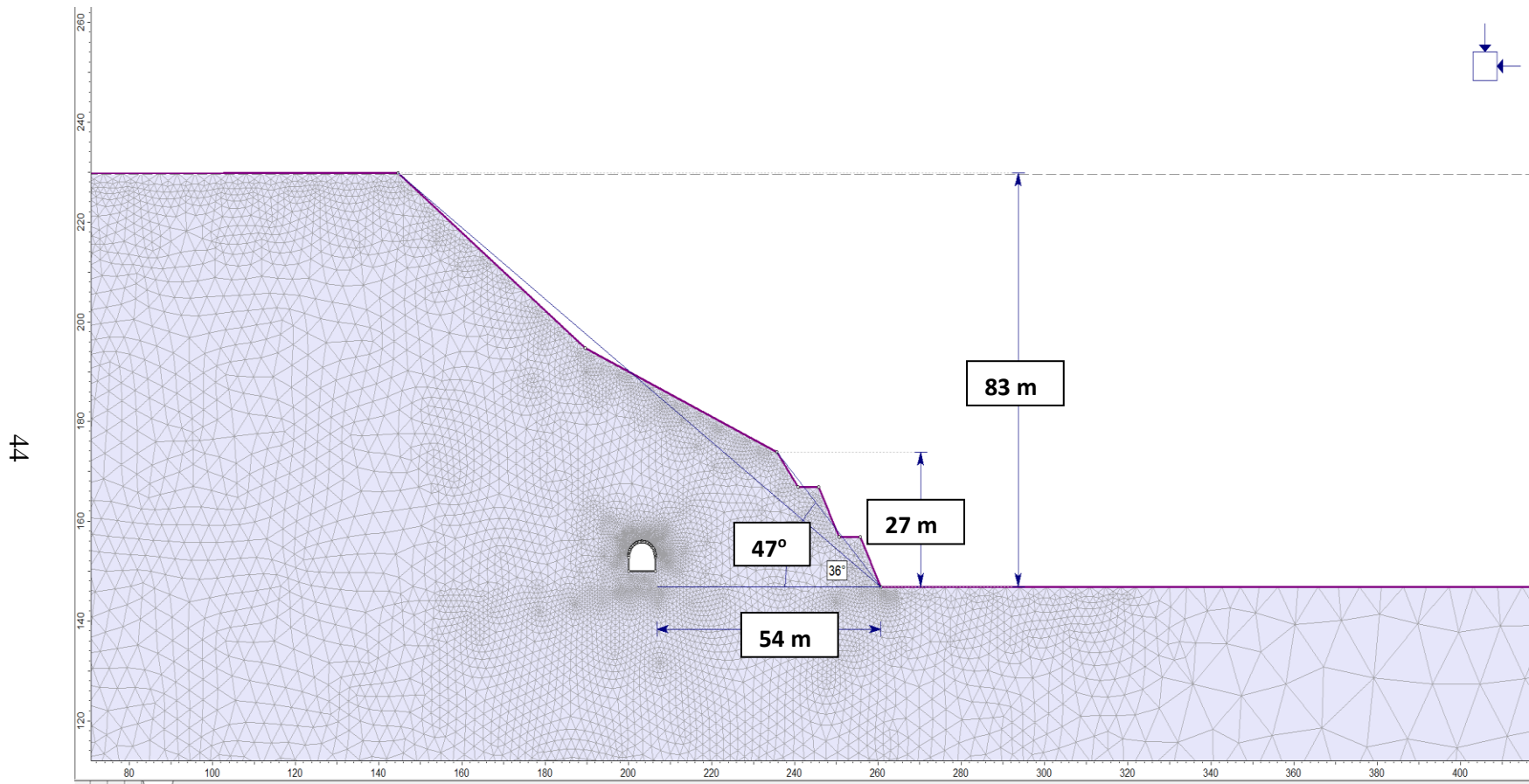
Figure 20. Slope dimensions and finite element model of the planned slope profile, section A-A', Km 26+600
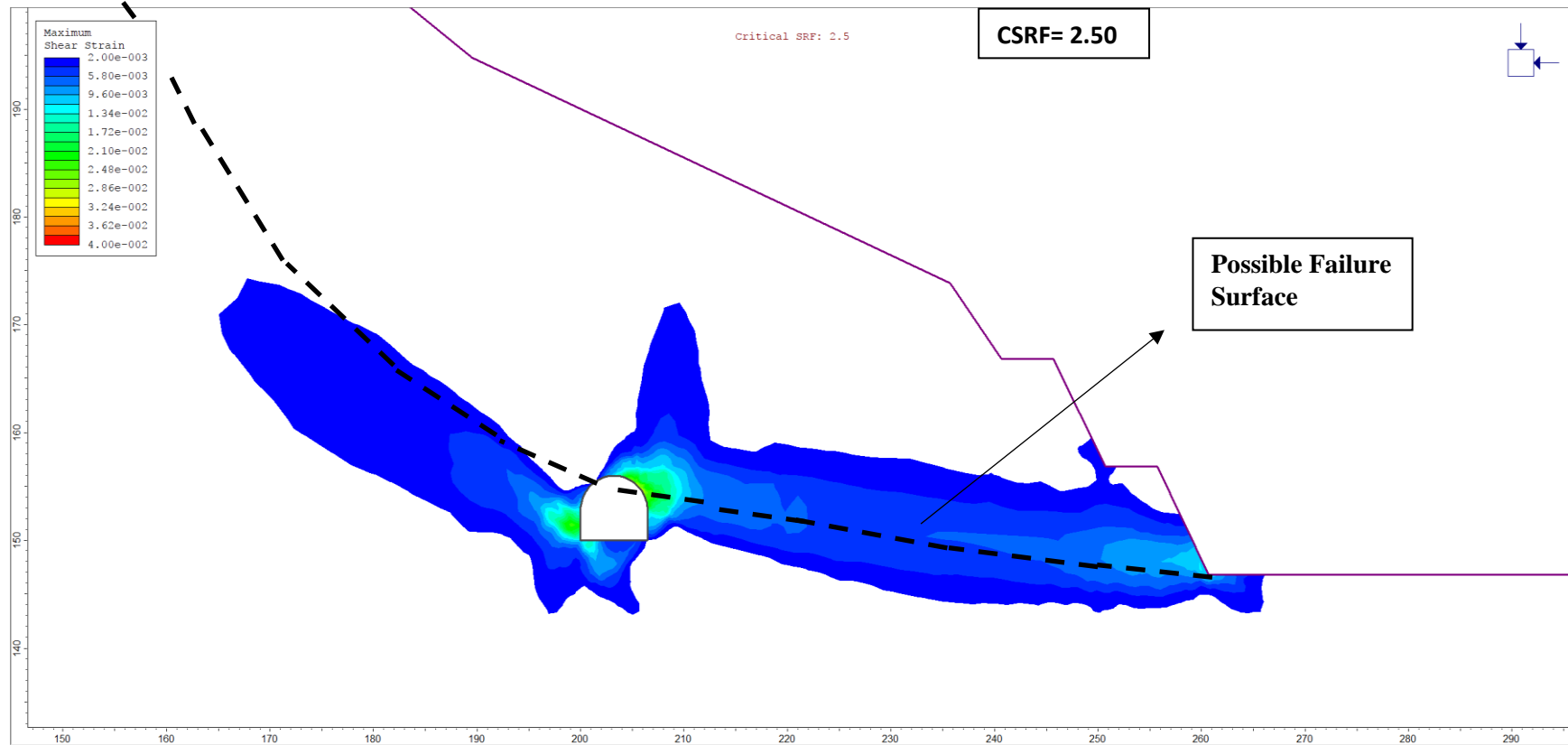
Figure 21. Maximum shear strain distribution and possible failure surface after planned slope cut at the CSRF=2.50 at Km 26+600
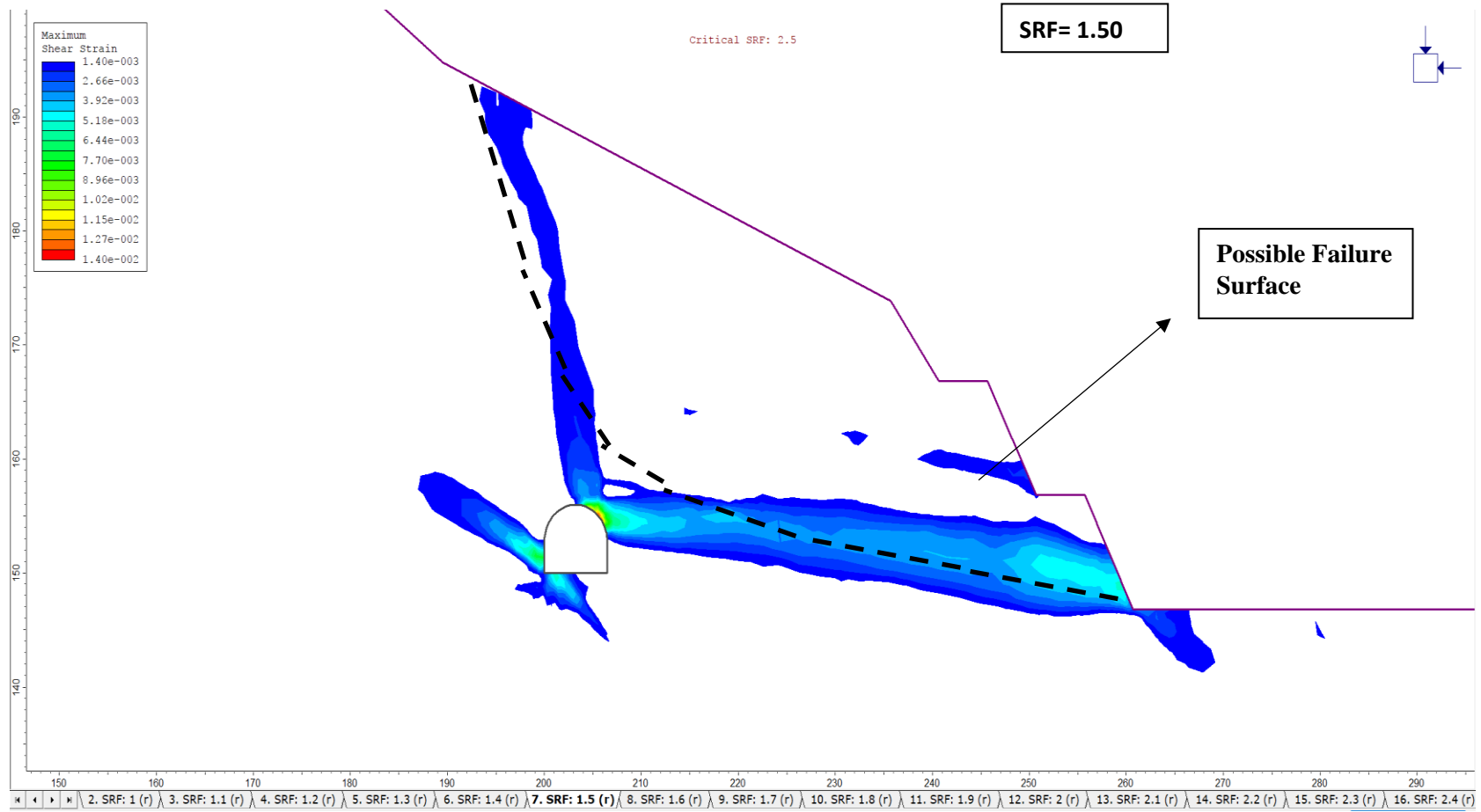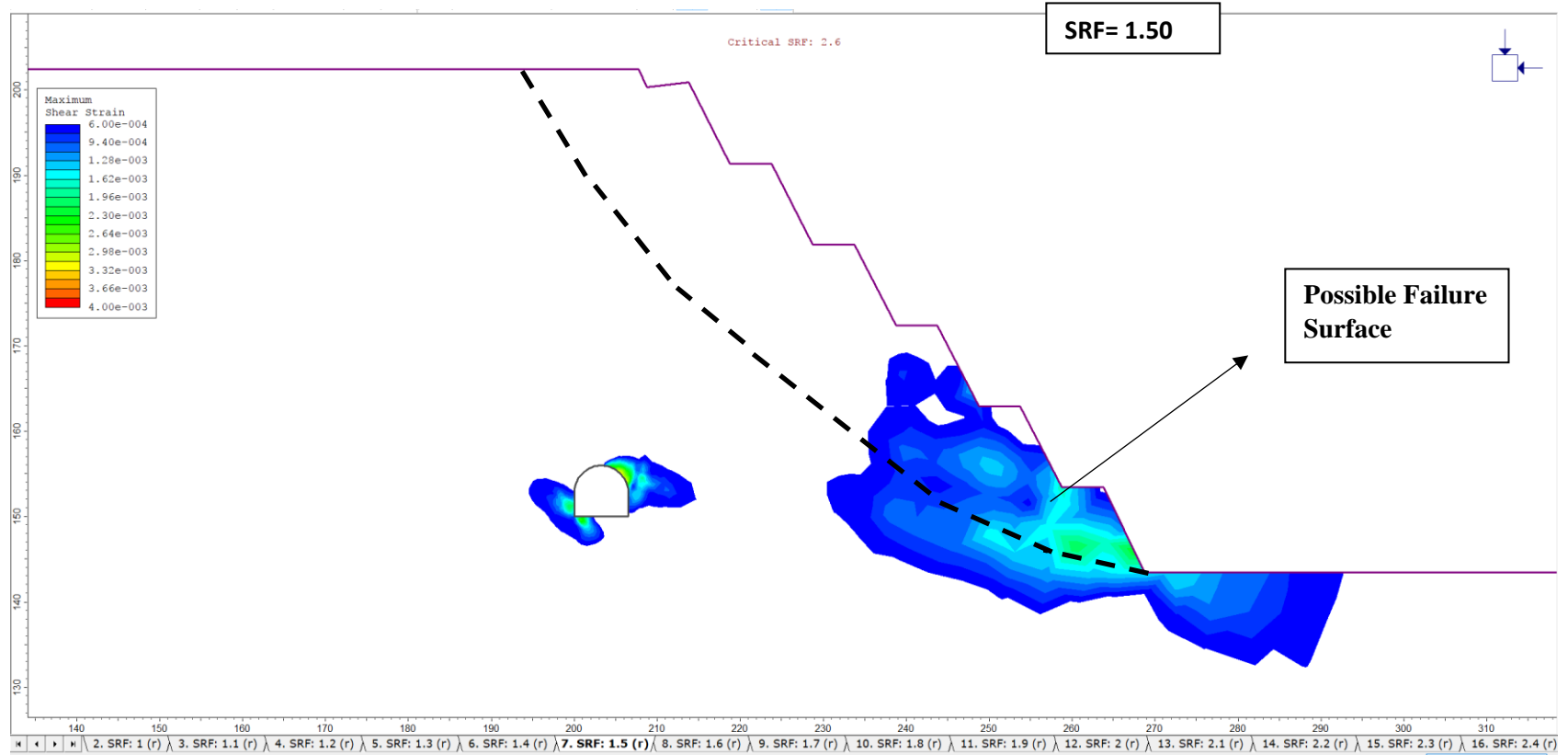
Figure 22. Maximum shear strain distribution and possible failure surface after planned slope cut at the SRF=1.50 at Km 26+600
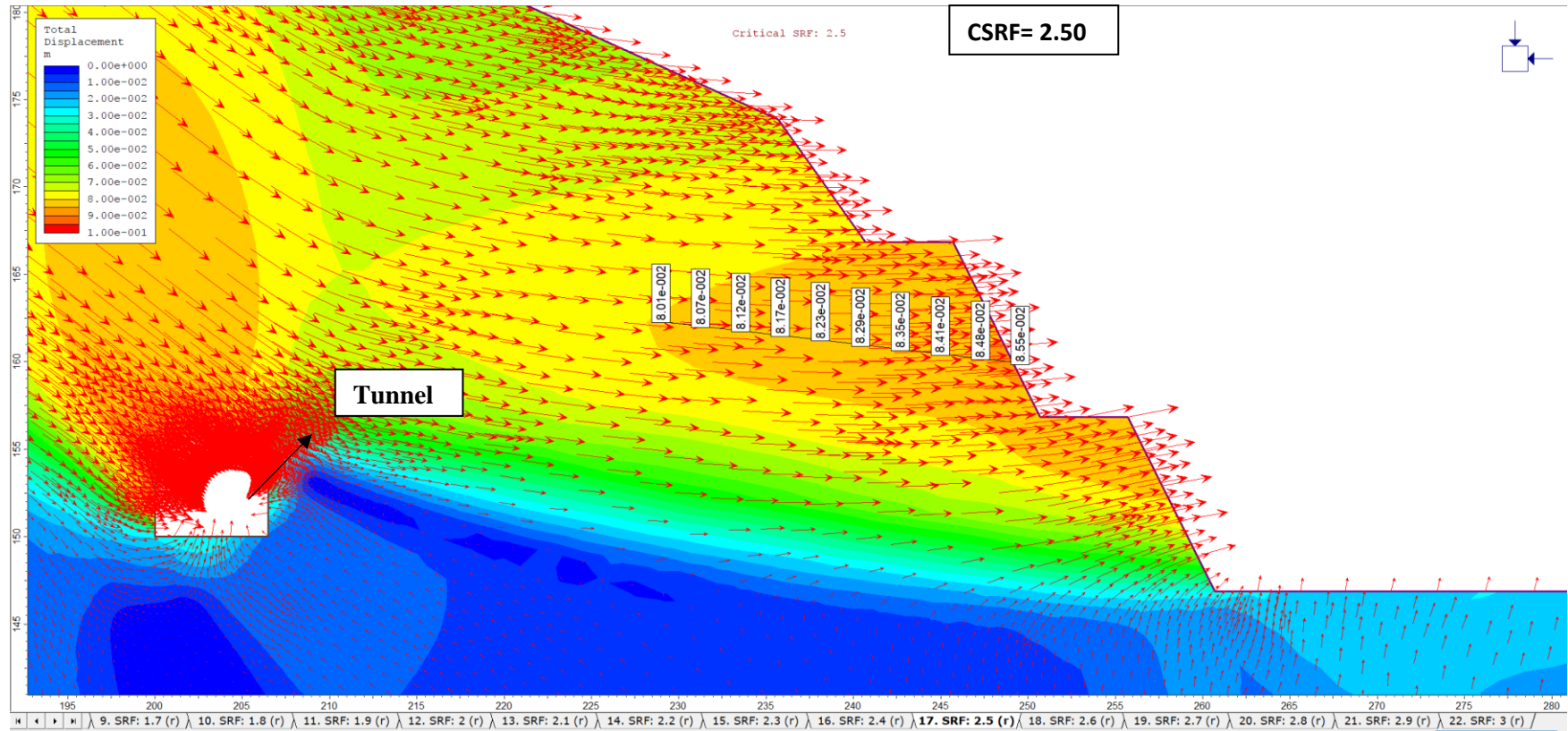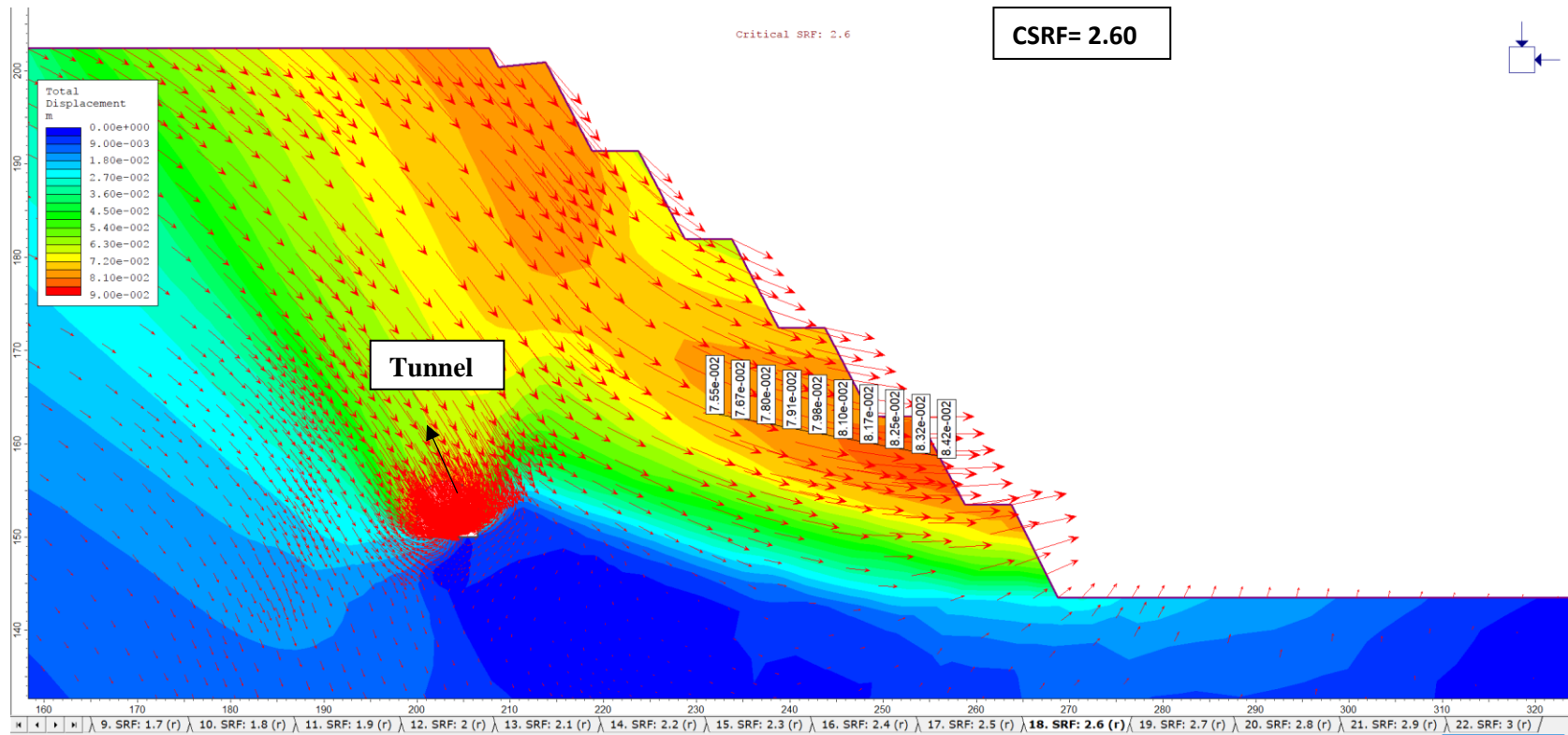
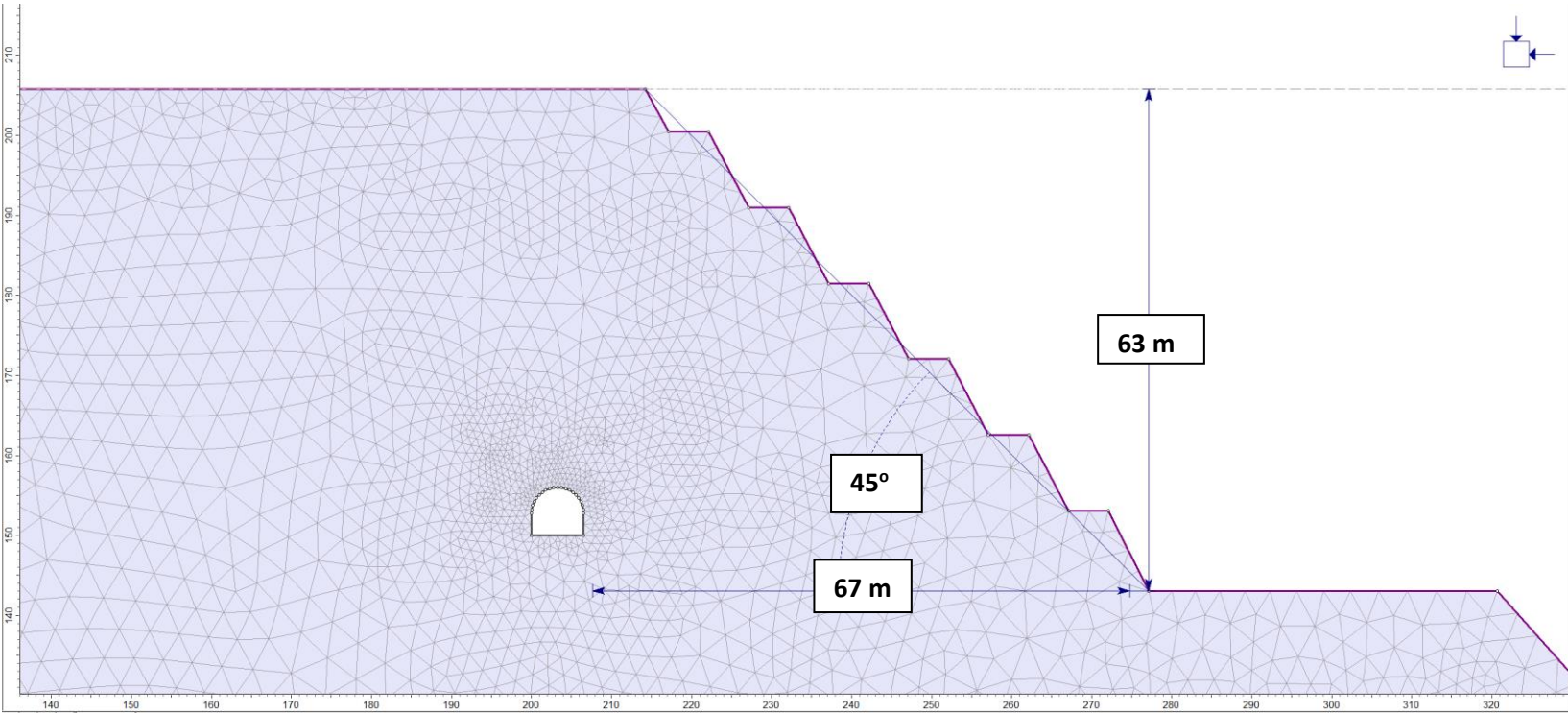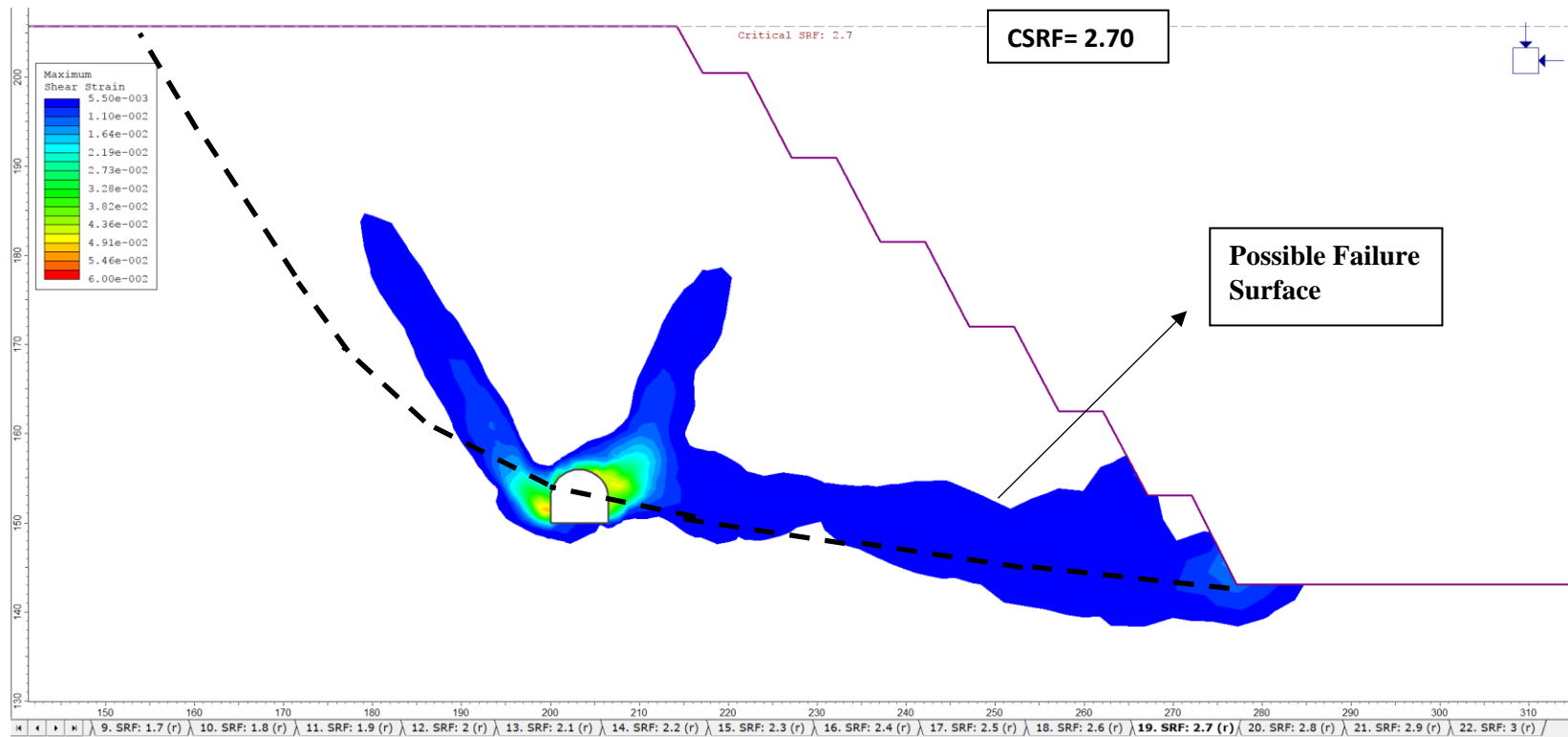*Figure 23. Displacement vectors and displacement magnitudes within planned slope cut at the CSRF=2.50 at Km 26+600*
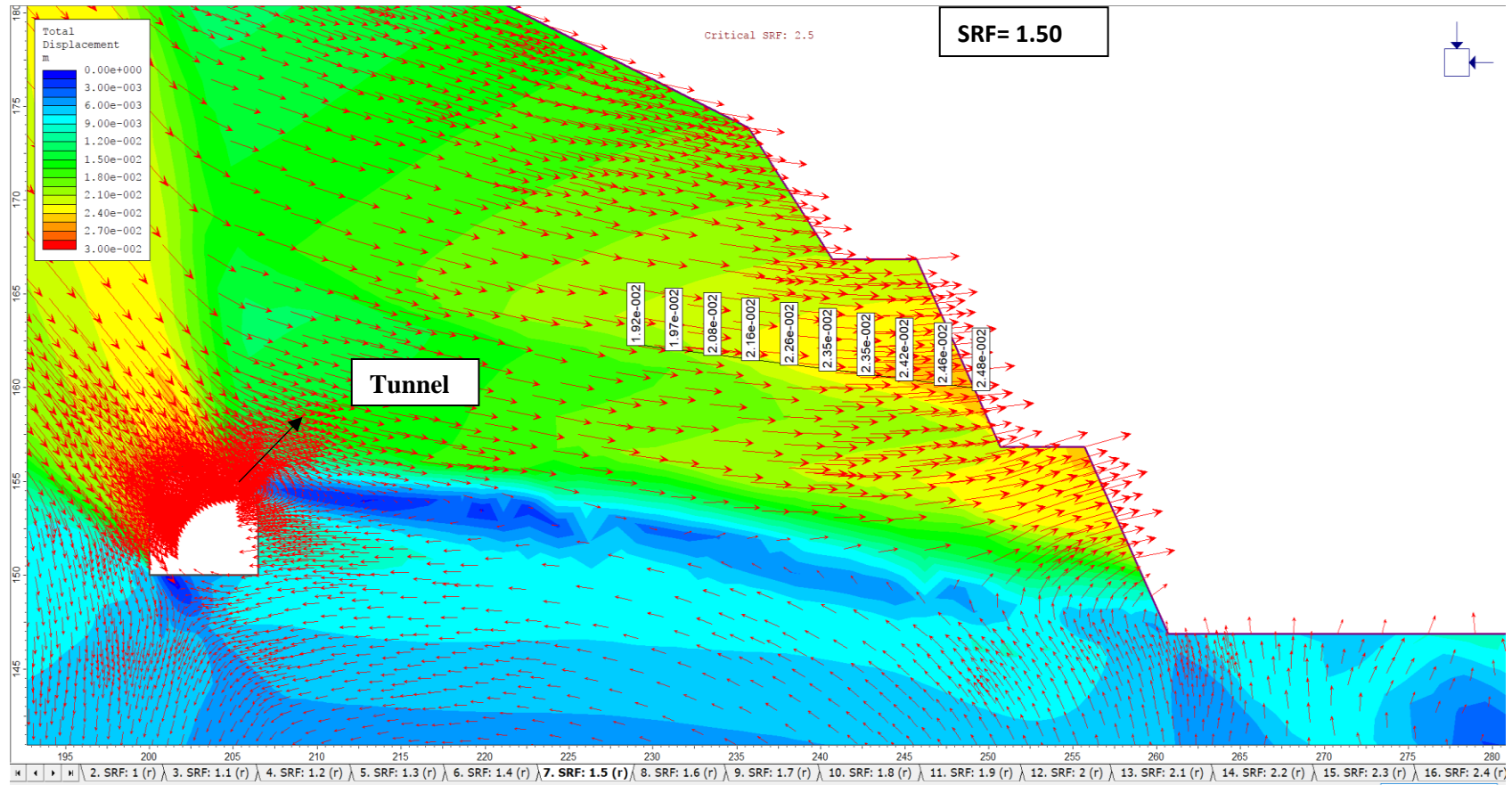
Figure 24. Displacement vectors and displacement magnitudes within planned slope cut at the SRF=1.50 at Km 26+600
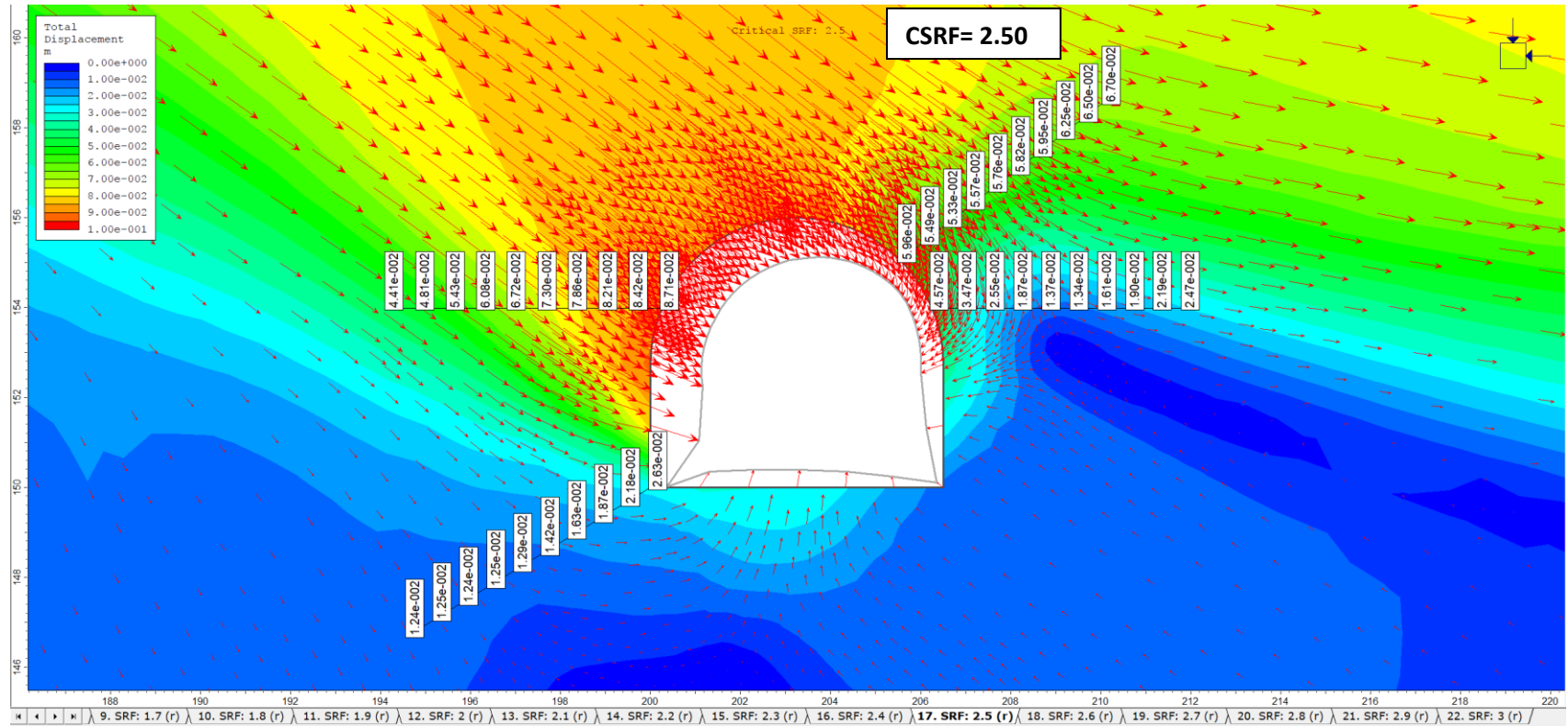
Figure 25. Deformations around the tunnel at the CSRF=2.50 at Km 26+600
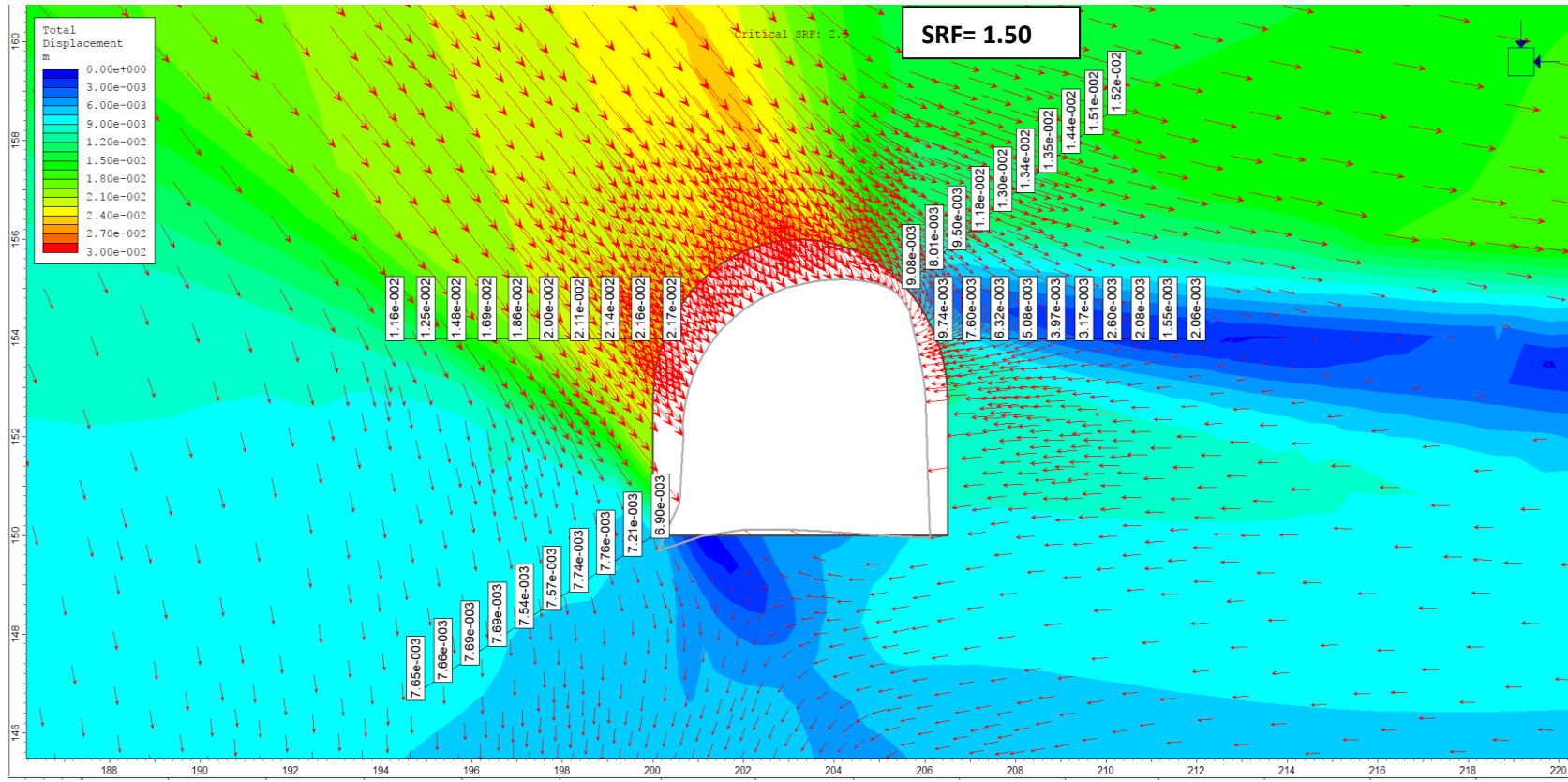
Figure 26. Deformations around the tunnel at the SRF=1.50 at Km 26+600
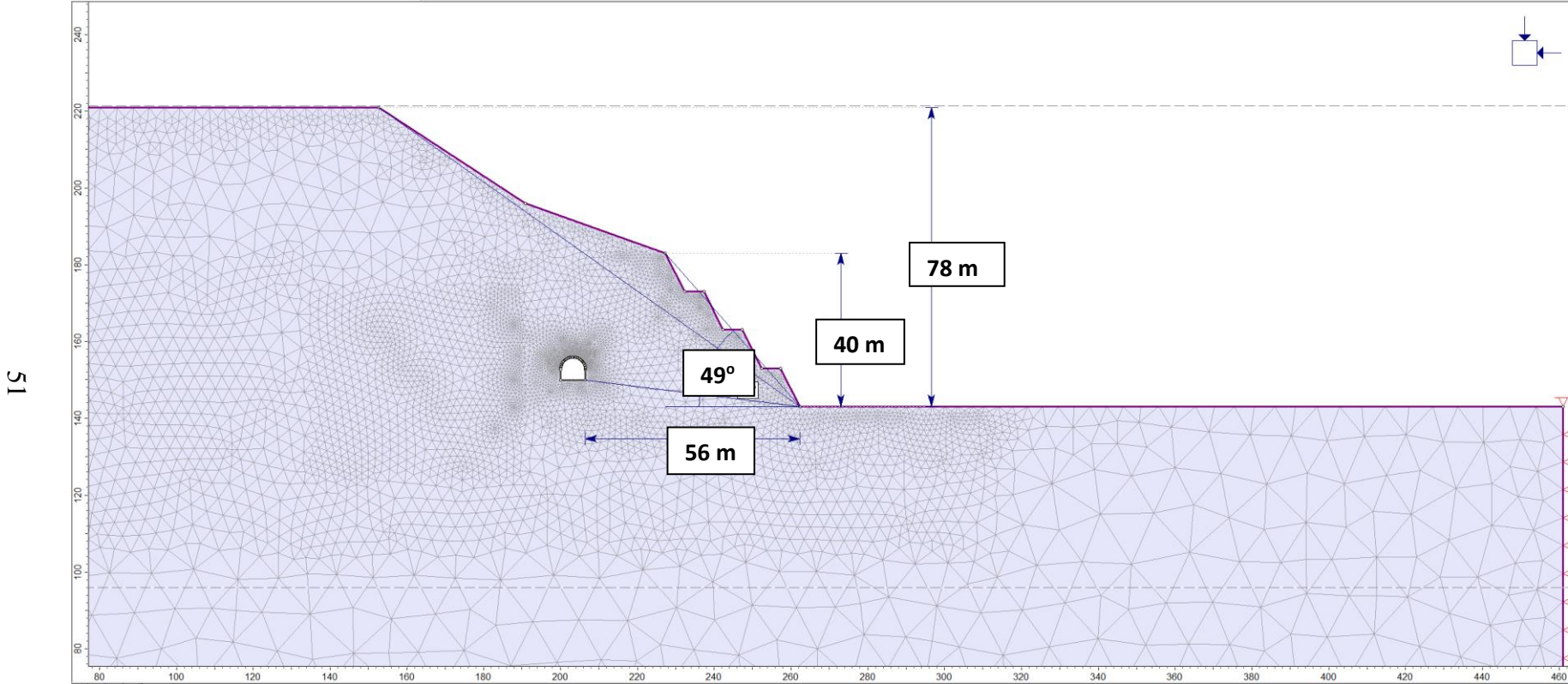
Figure 27. Slope dimensions and finite element model of the planned slope profile, section A-A', Km 26+610
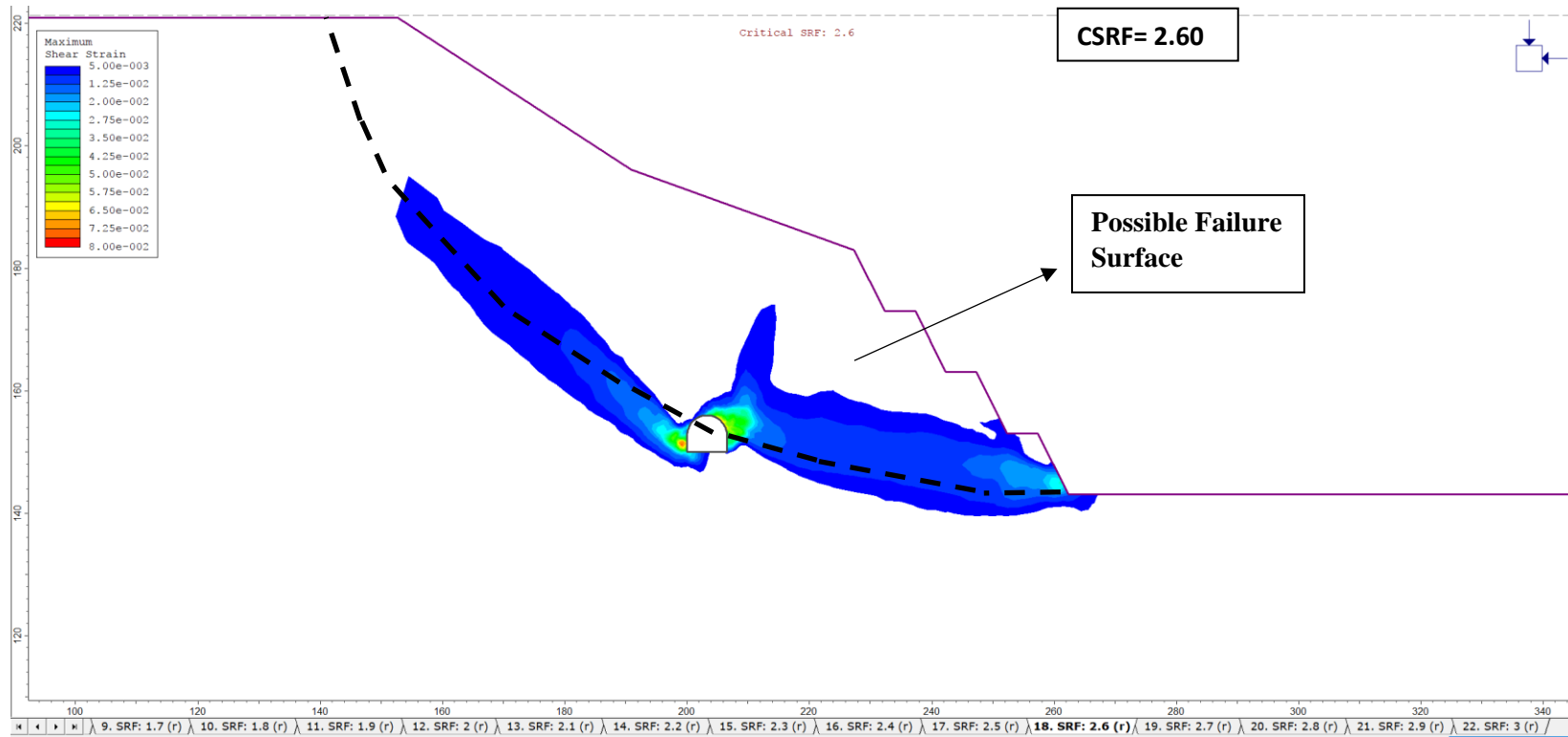
Figure 28. Maximum shear strain distribution and possible failure surface after planned slope cut at the CSRF=2.60 at Km 26+610
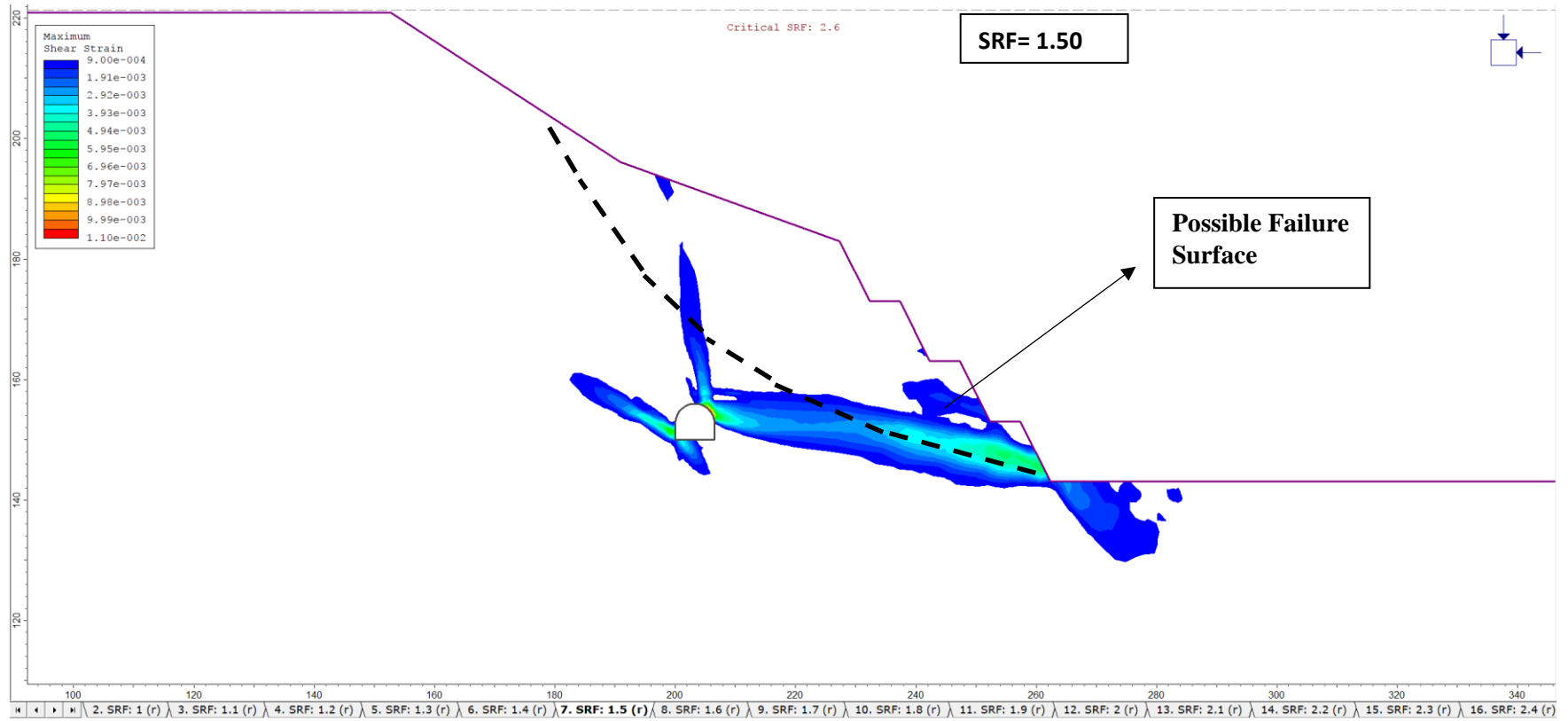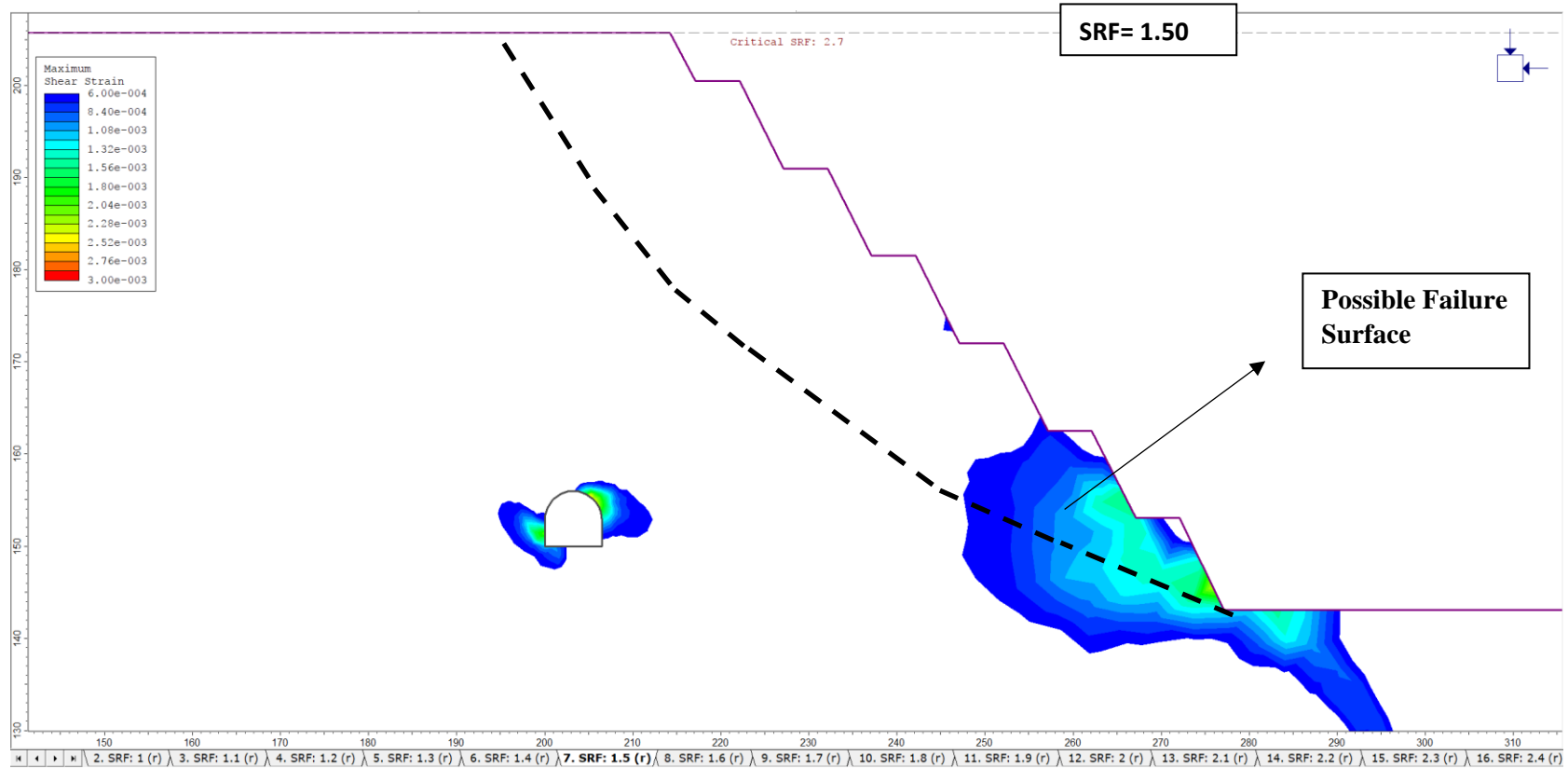
Figure 29. Maximum shear strain distribution and possible failure surface after planned slope cut at the SRF=1.50 at Km 26+610
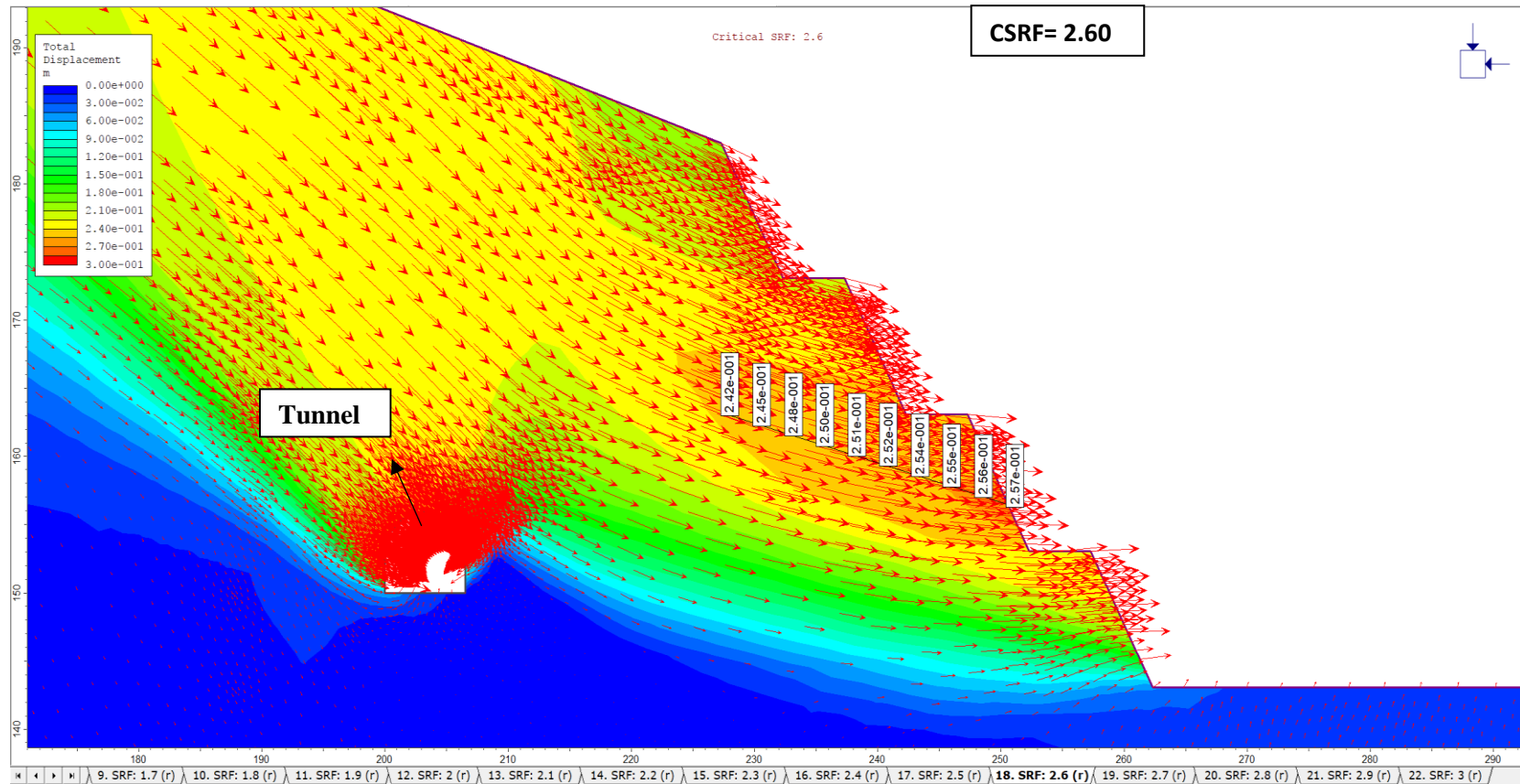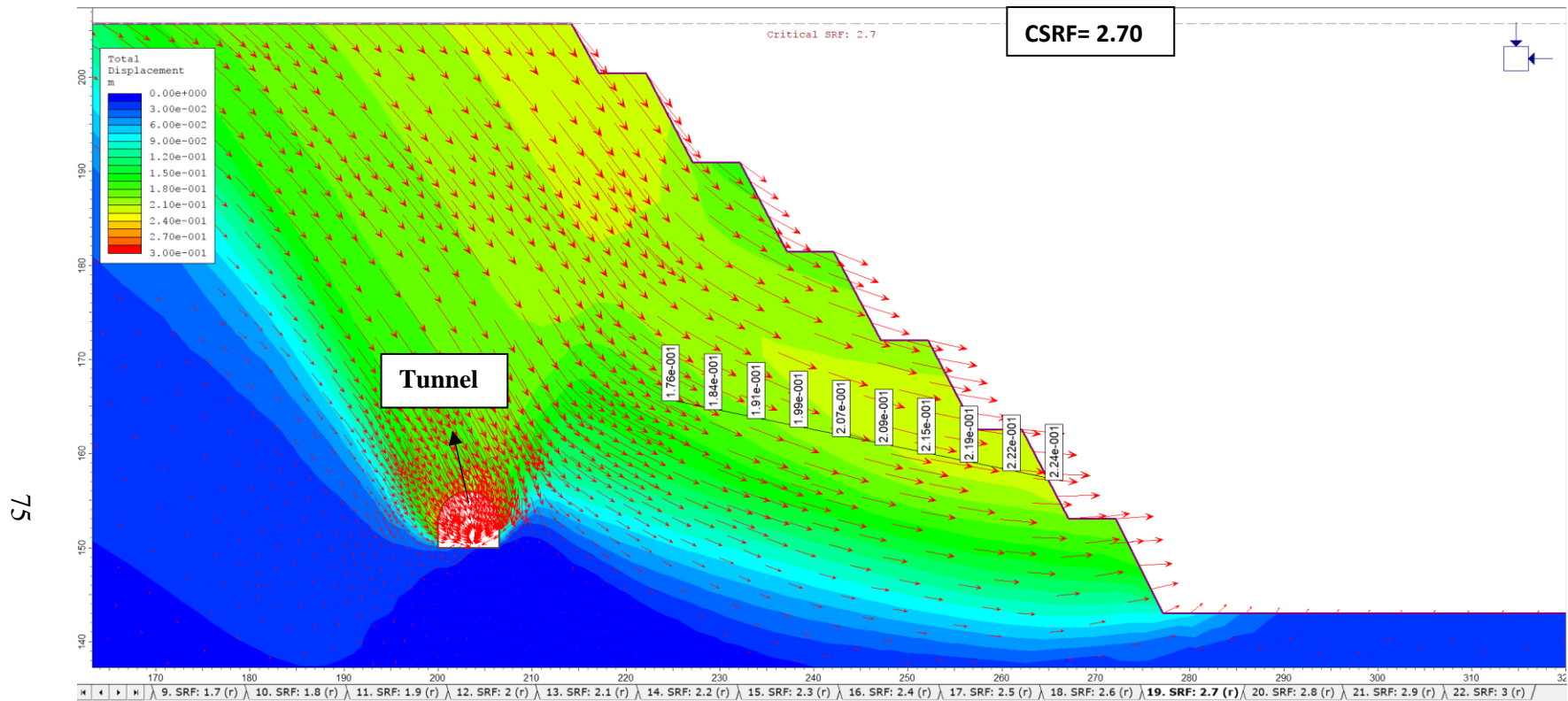
Figure 30. Displacement vectors and displacement magnitudes within planned slope cut at the CSRF=2.60 at Km 26+610
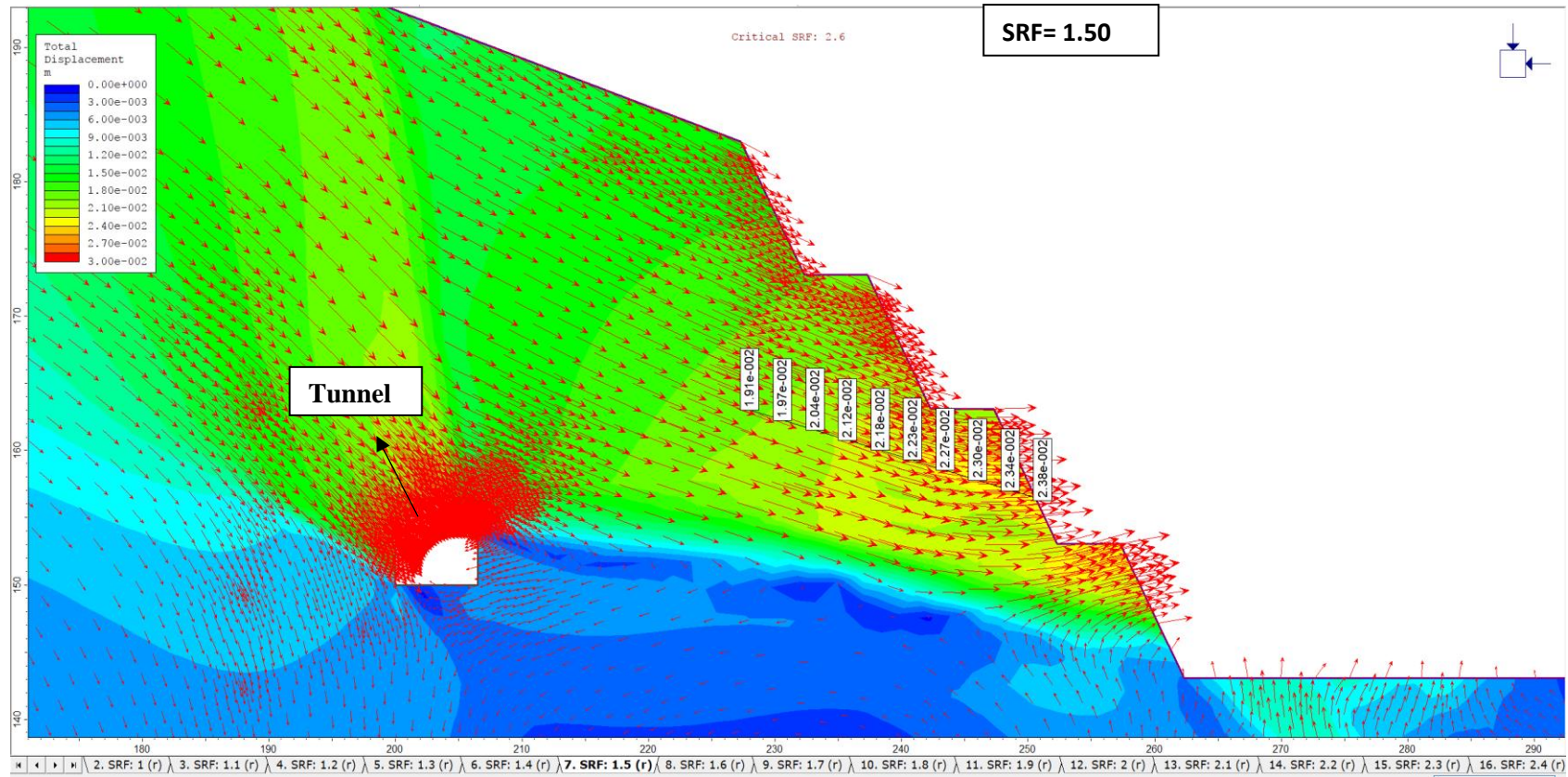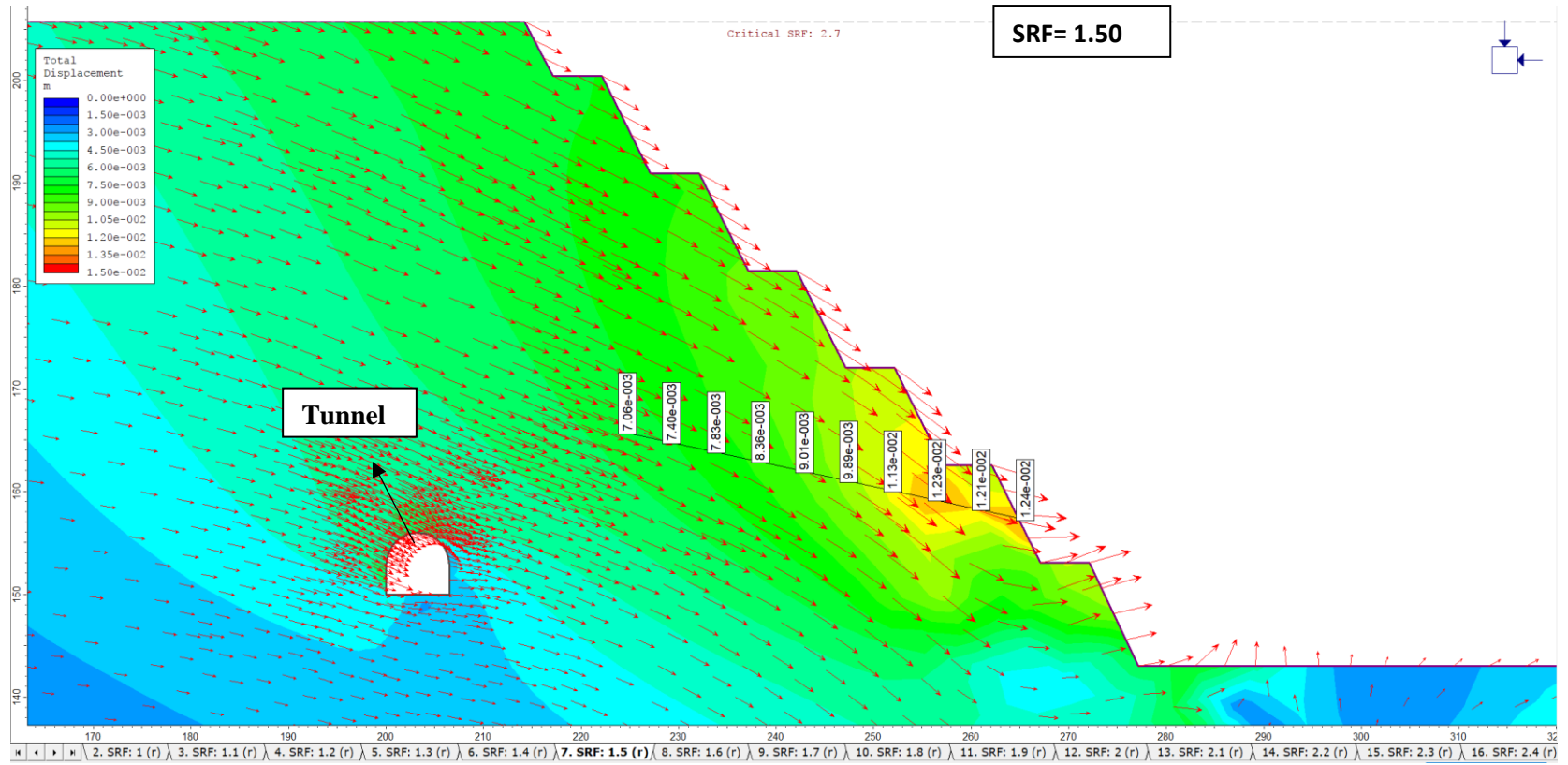
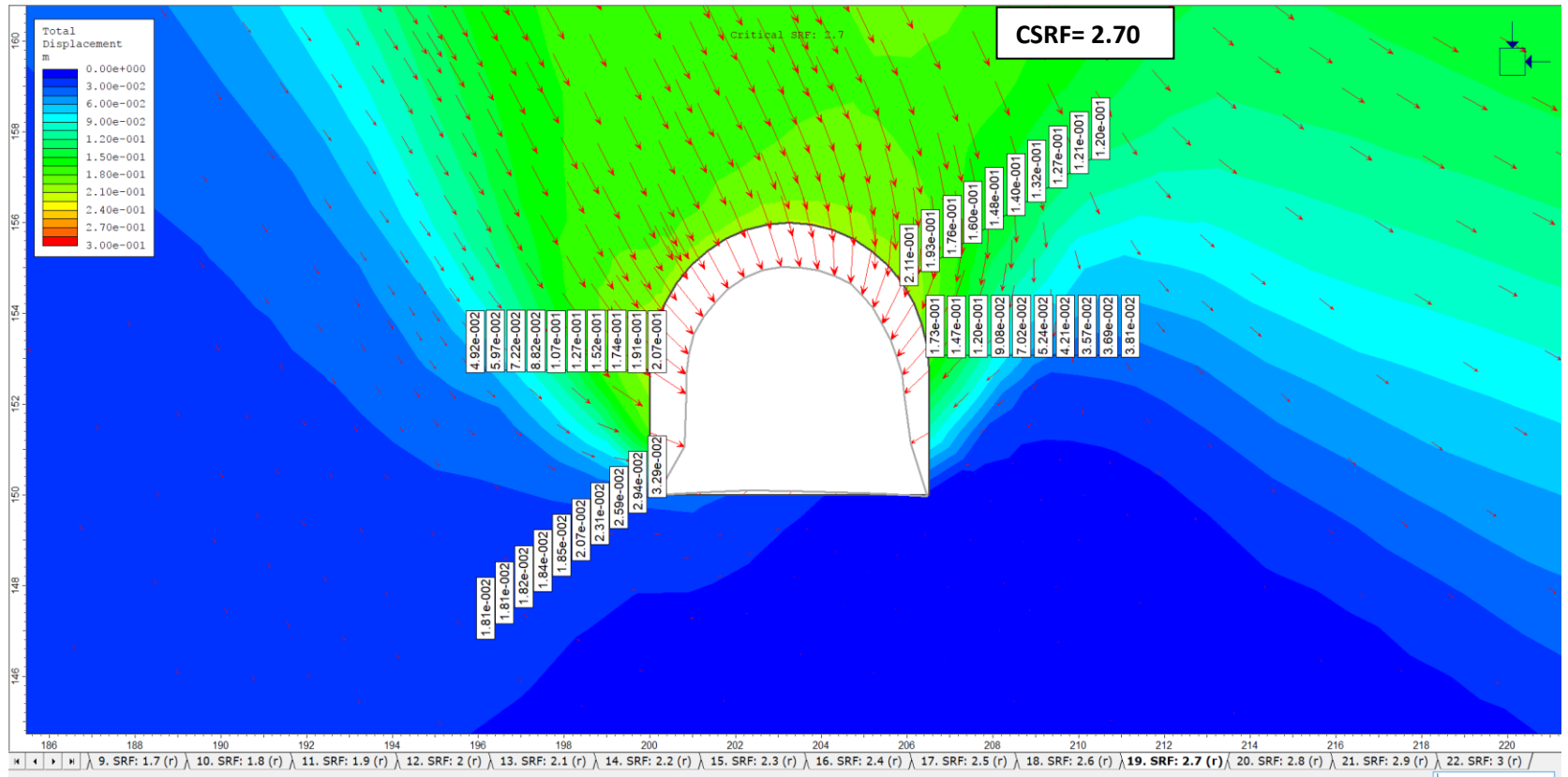*Figure 31. Displacement vectors and displacement magnitudes within planned slope cut at the SRF=1.50 at Km 26+610*
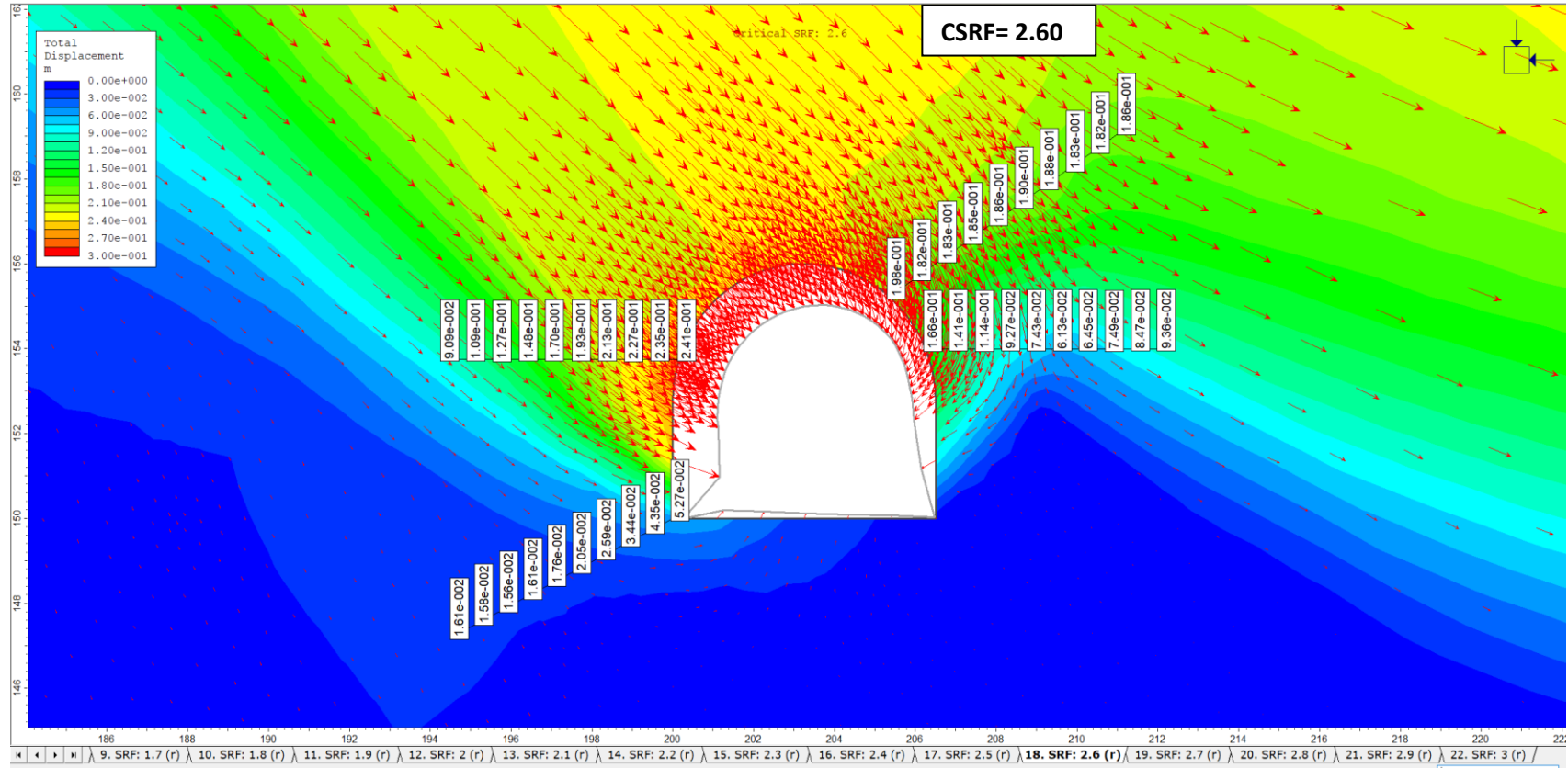
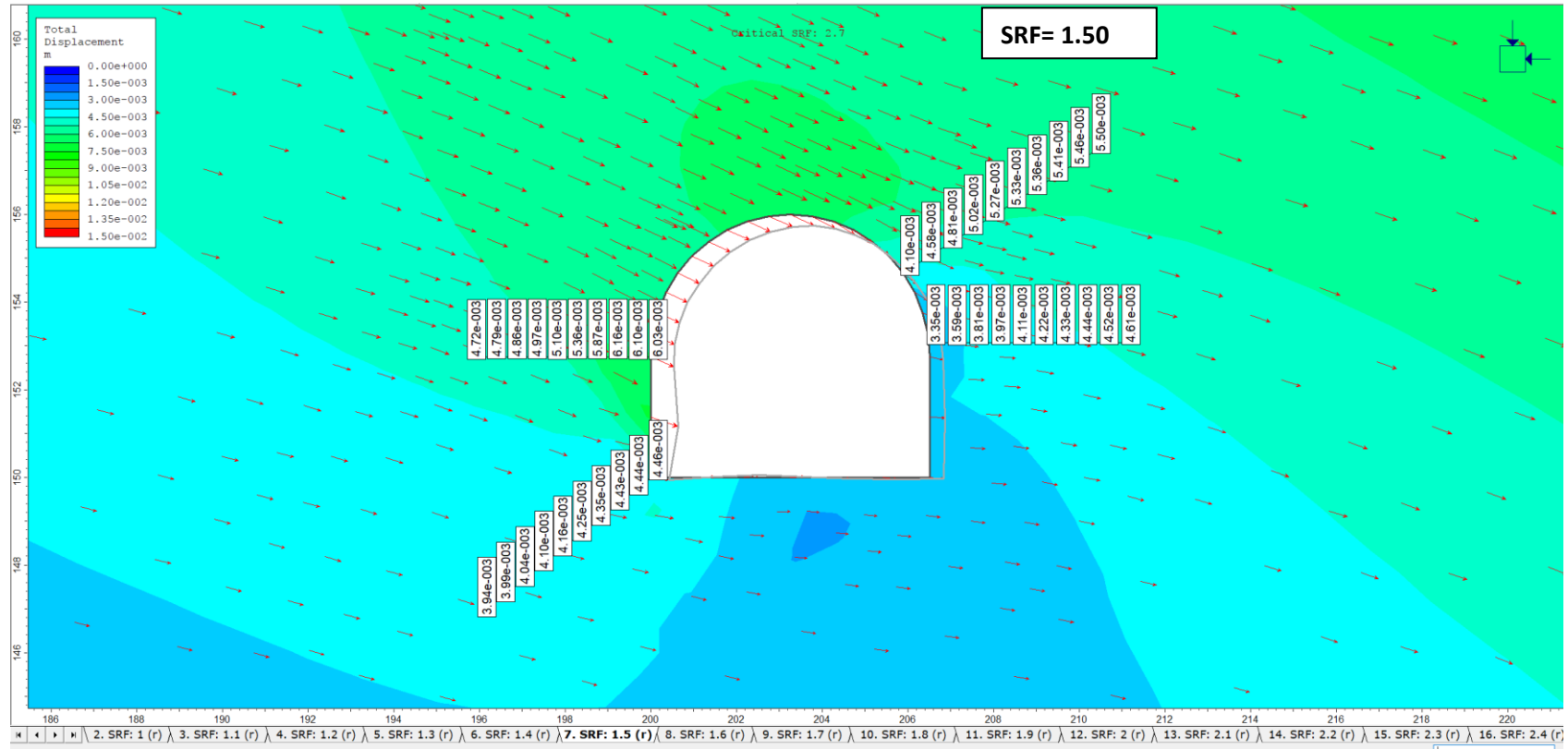*Figure 32. Deformations around the tunnel at the CSRF=2.60 at Km 26+610*
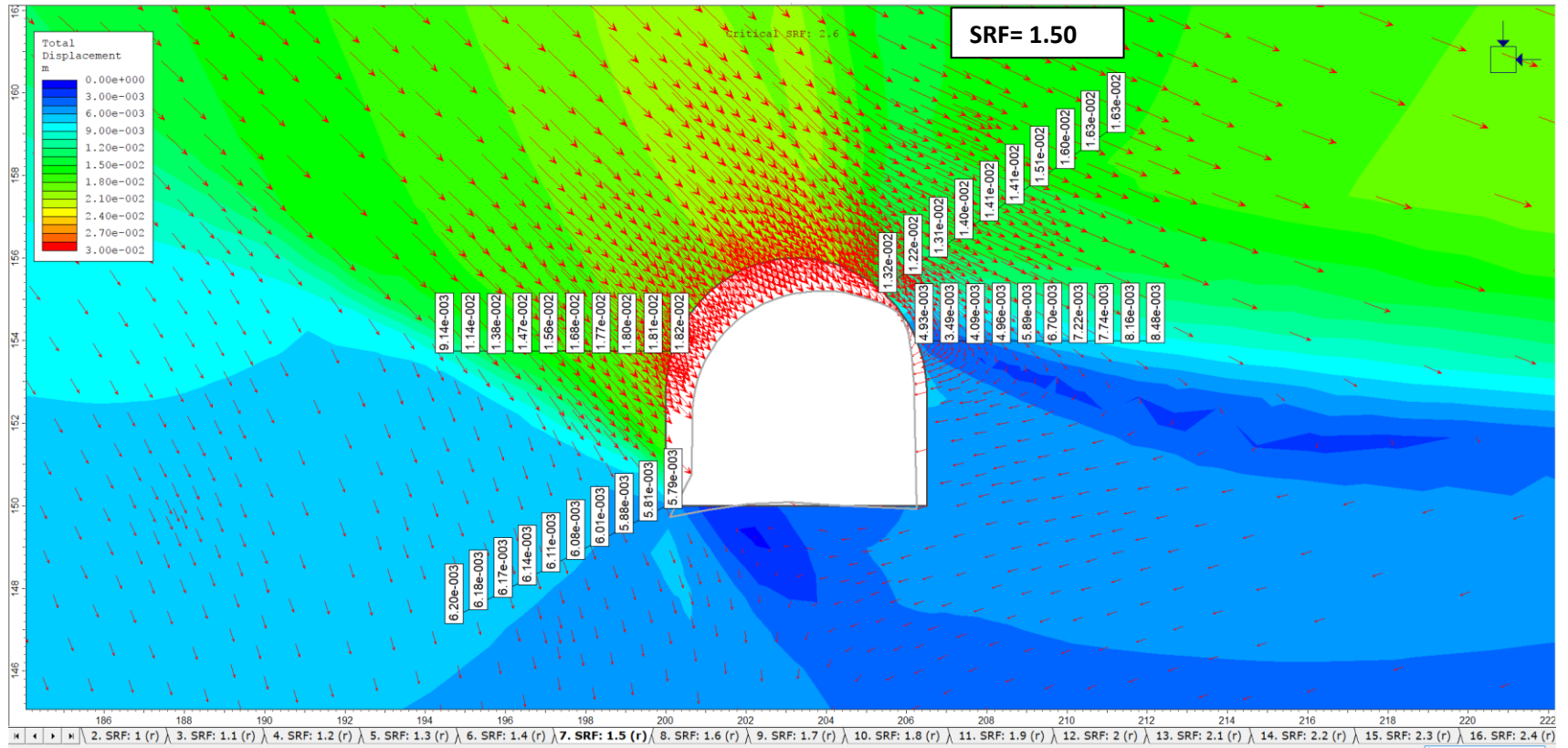
Figure 33. Deformations around the tunnel at the SRF=1.50 at Km 26+610

79 m
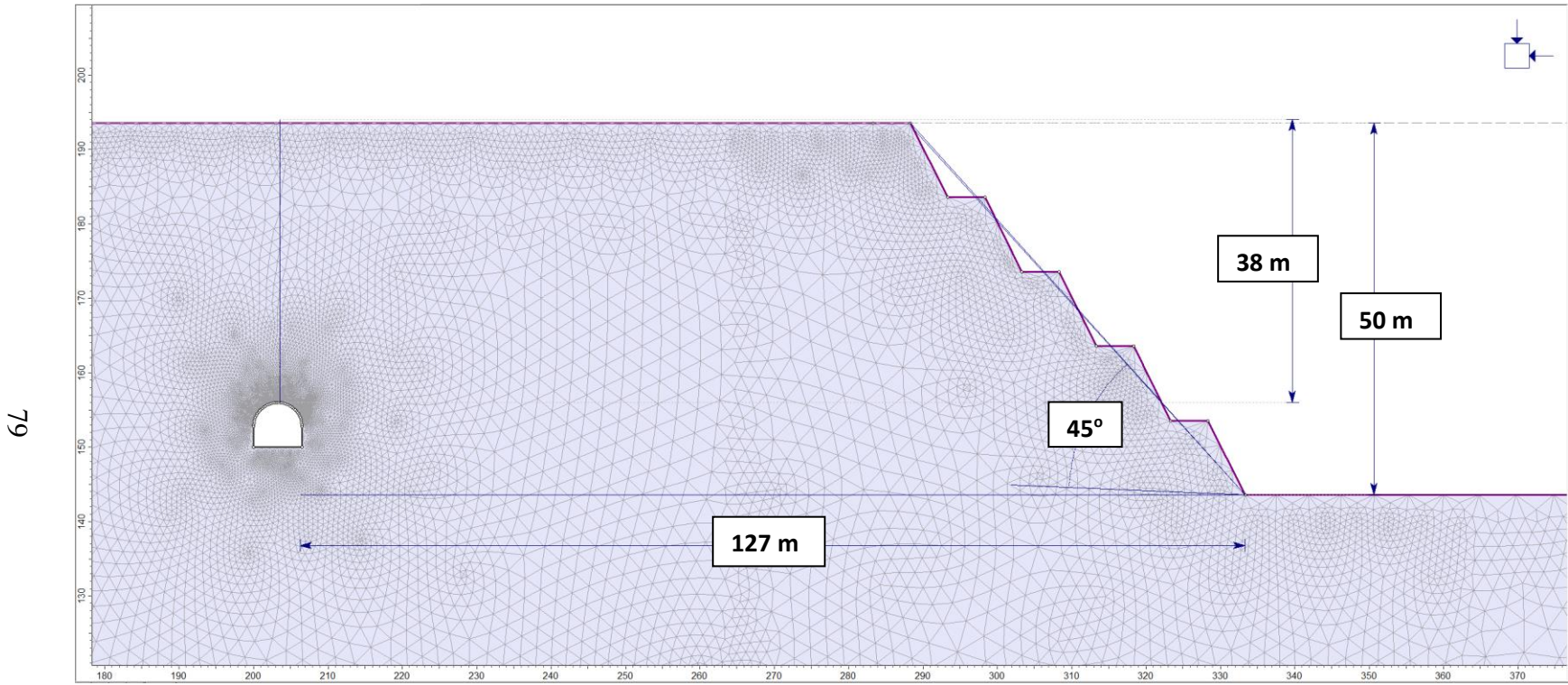
50 m

45°

58 m
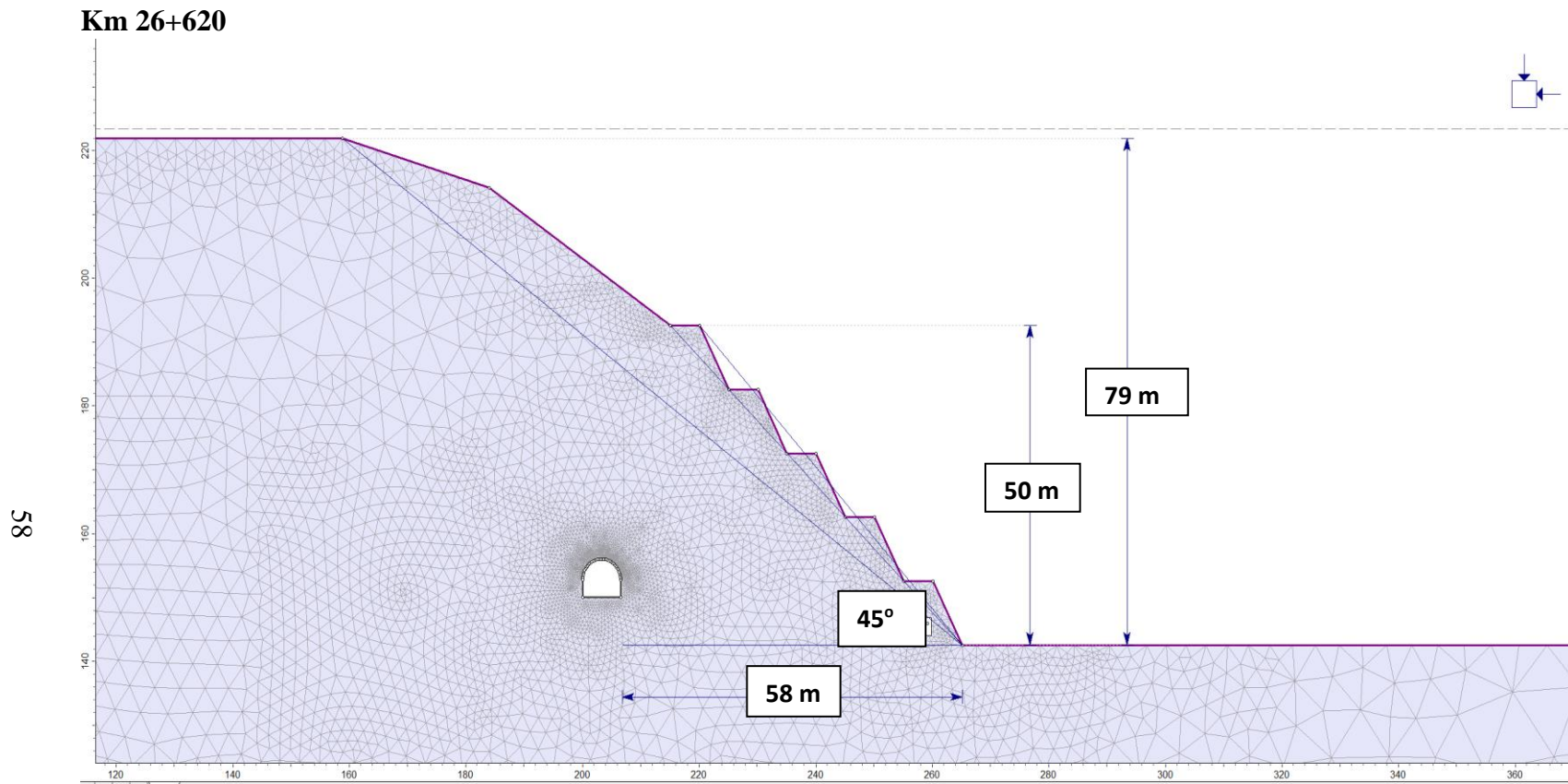
Figure 34. Slope dimensions and finite element model of the planned slope profile, section A-A', Km 26+620
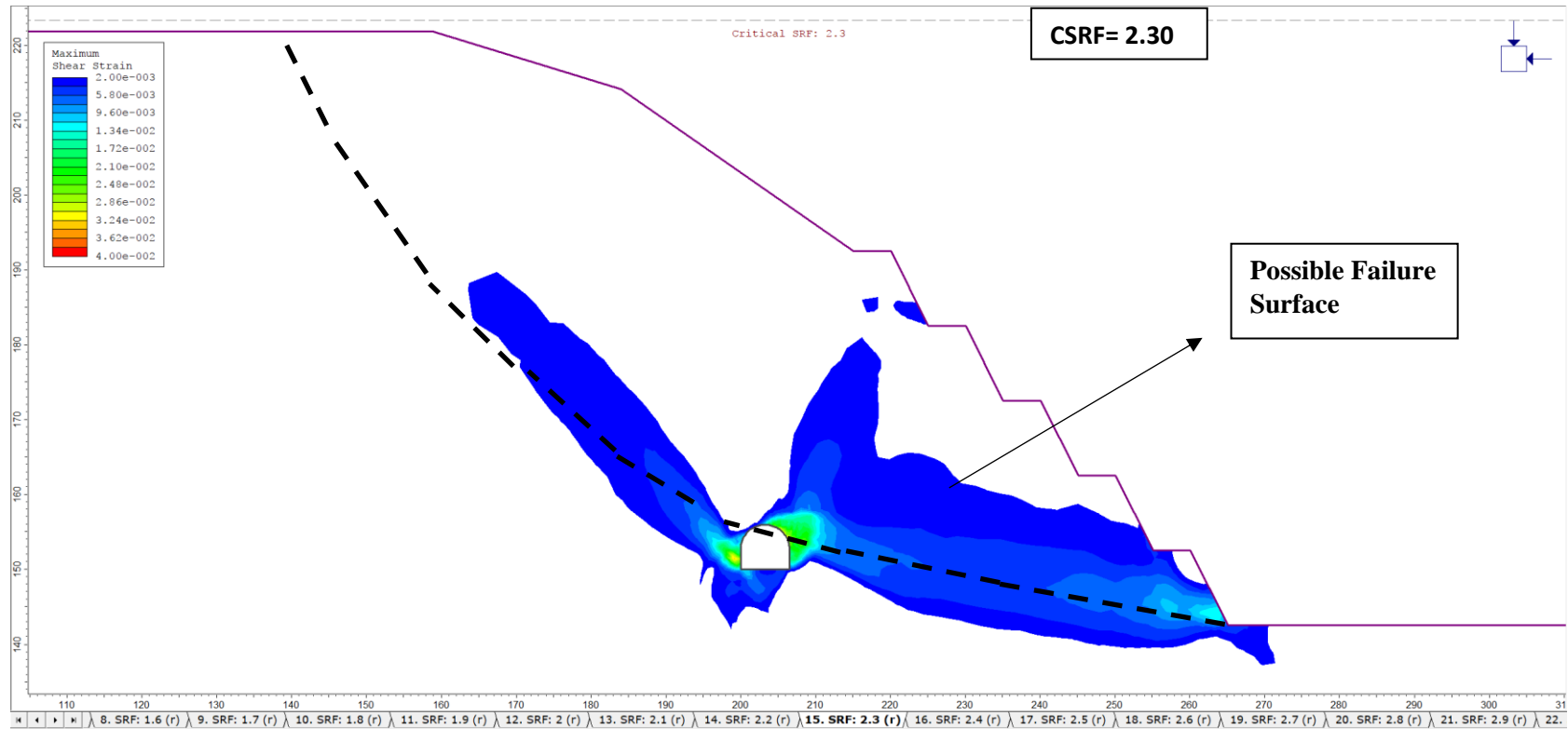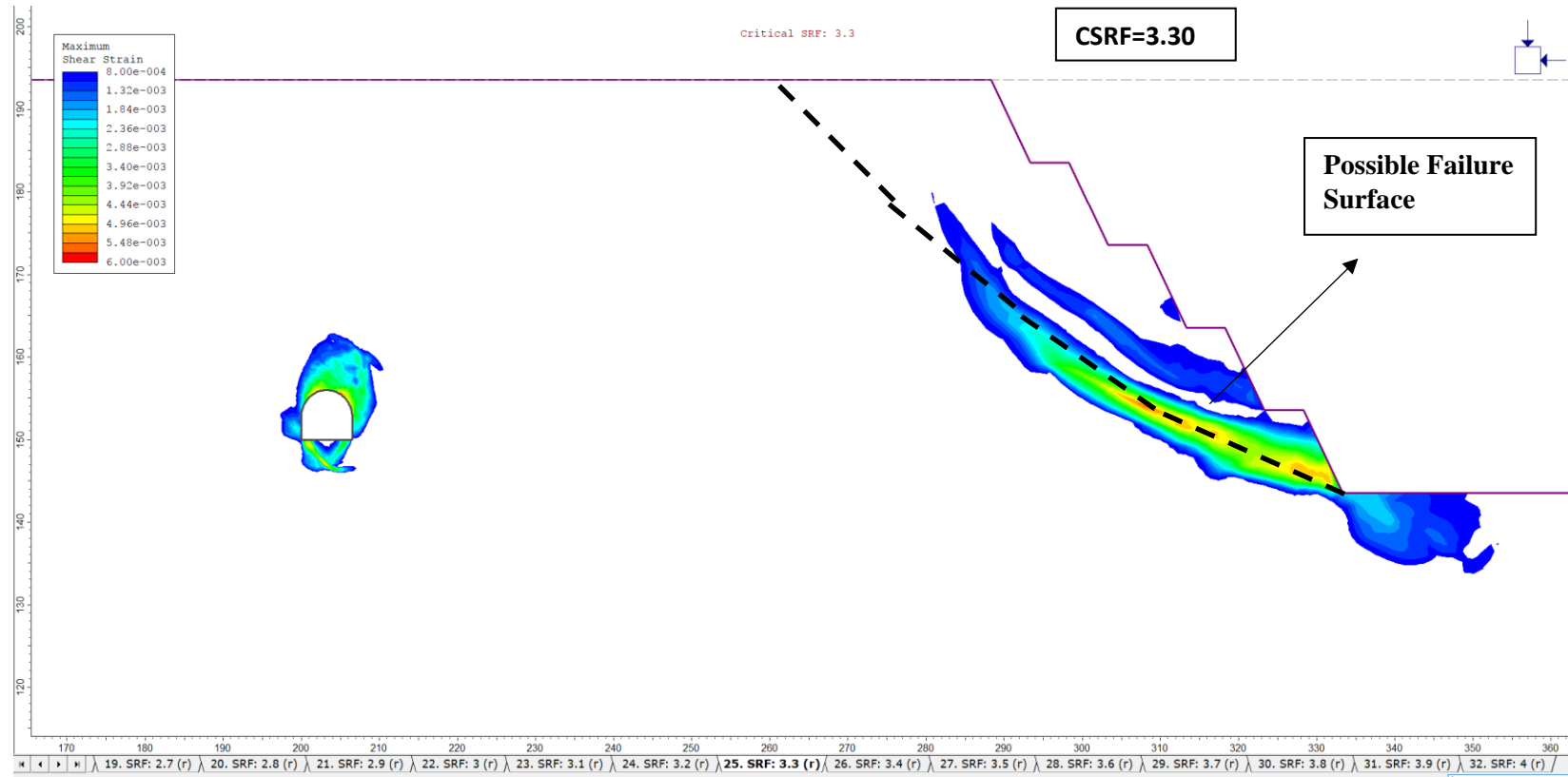
Figure 35. Maximum shear strain distribution and possible failure surface after planned slope cut at the CSRF=2.30 at Km 26+620
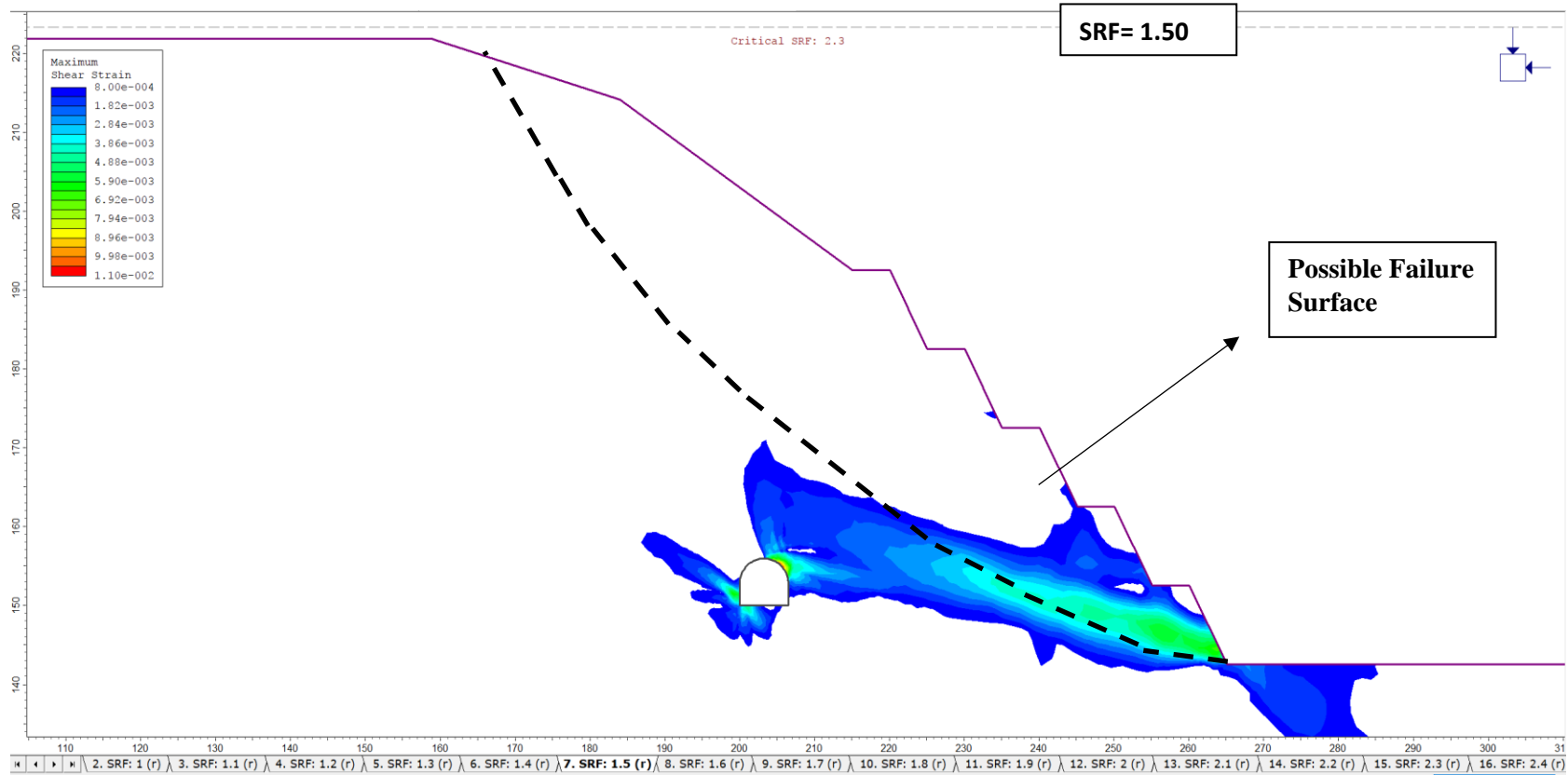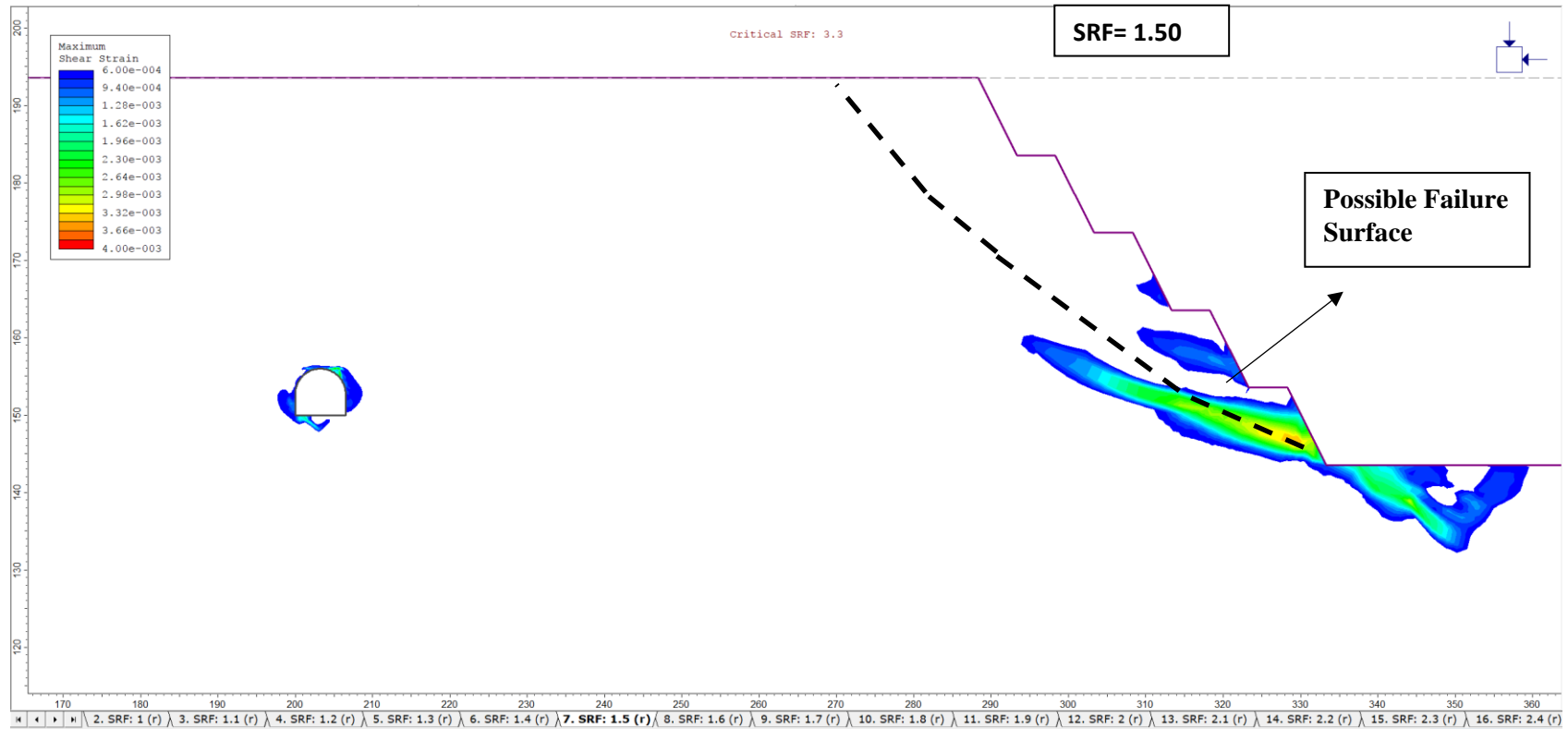
Figure 36. Maximum shear strain distribution and possible failure surface after planned slope cut at the SRF=1.50 at Km 26+620
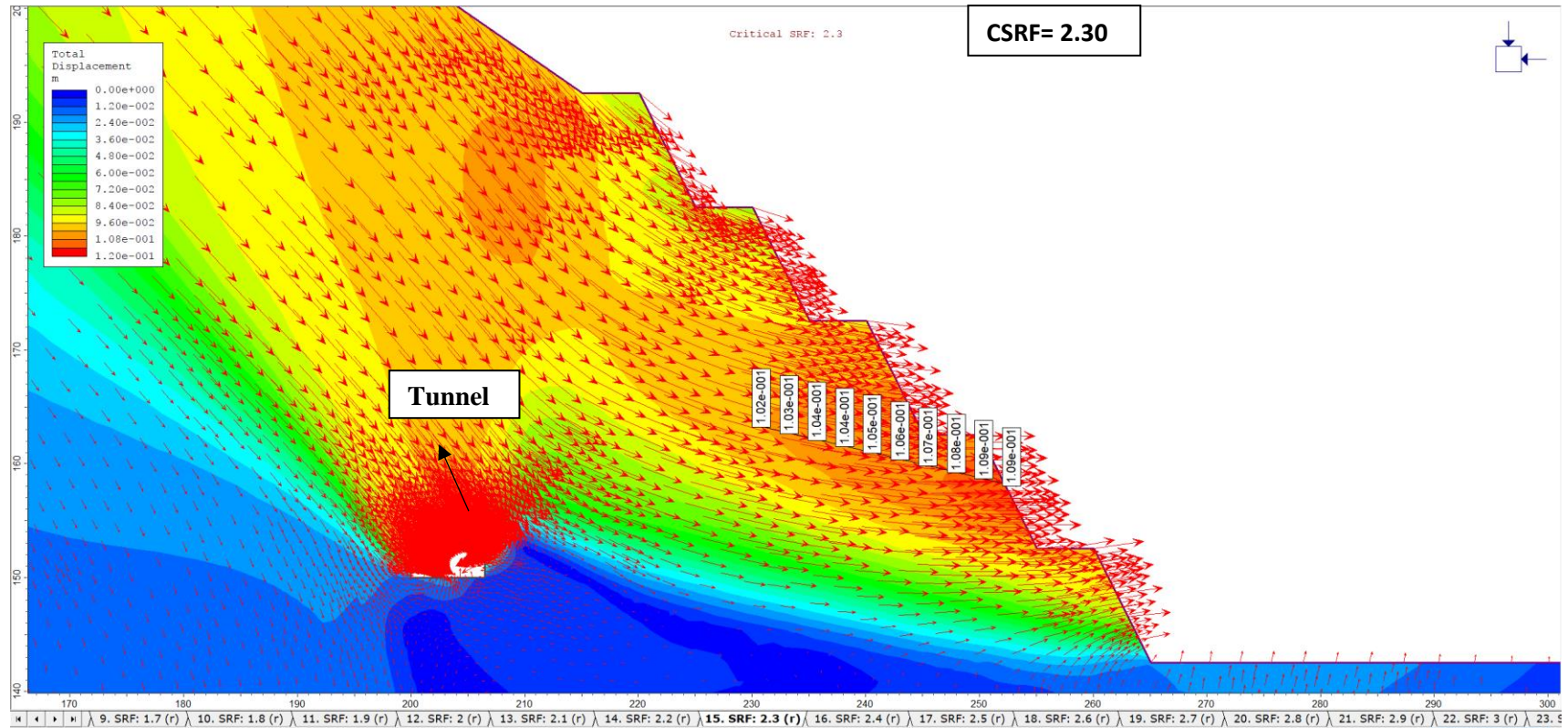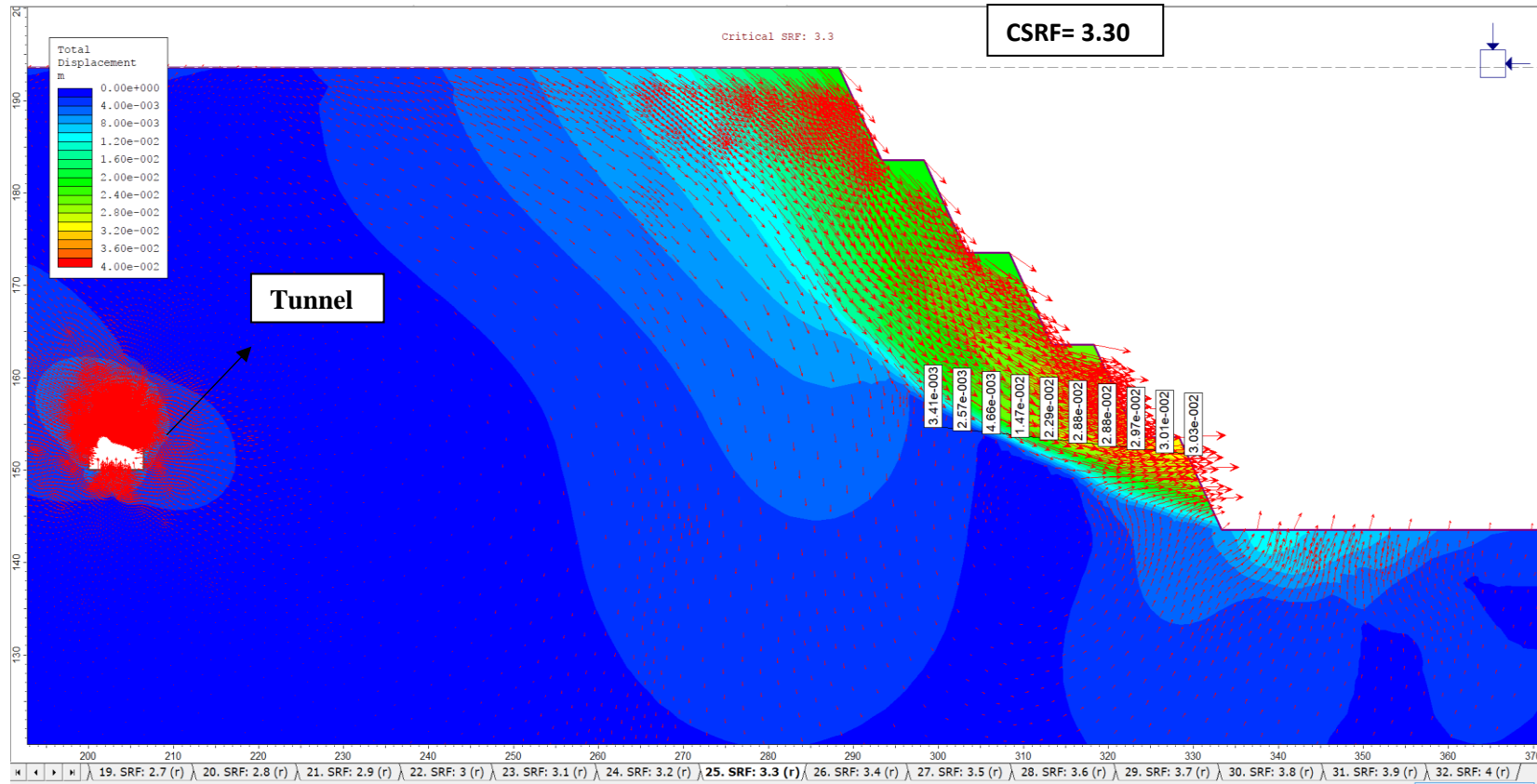
Figure 37. Displacement vectors and displacement magnitudes within planned slope cut at the CSRF=2.30 at Km 26+620
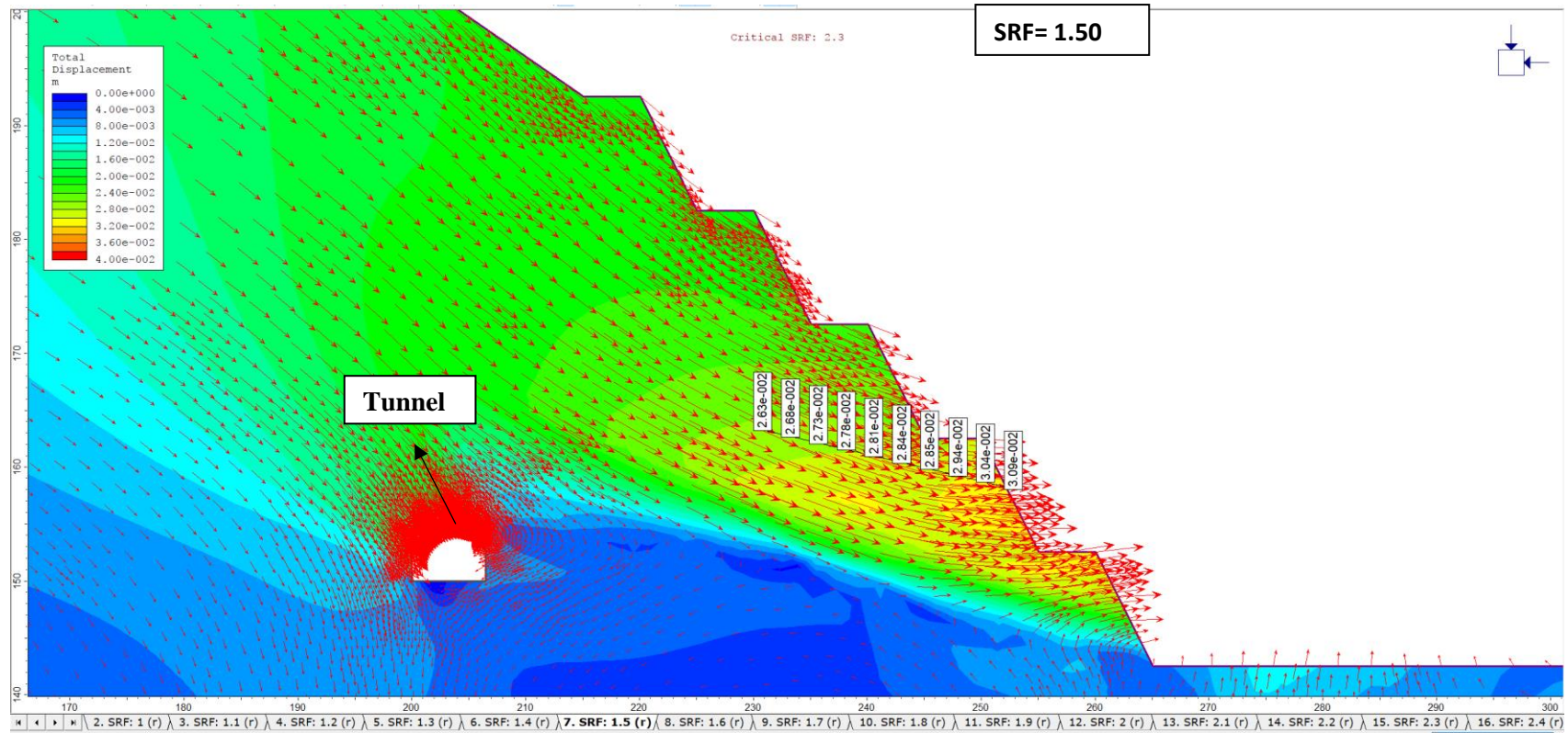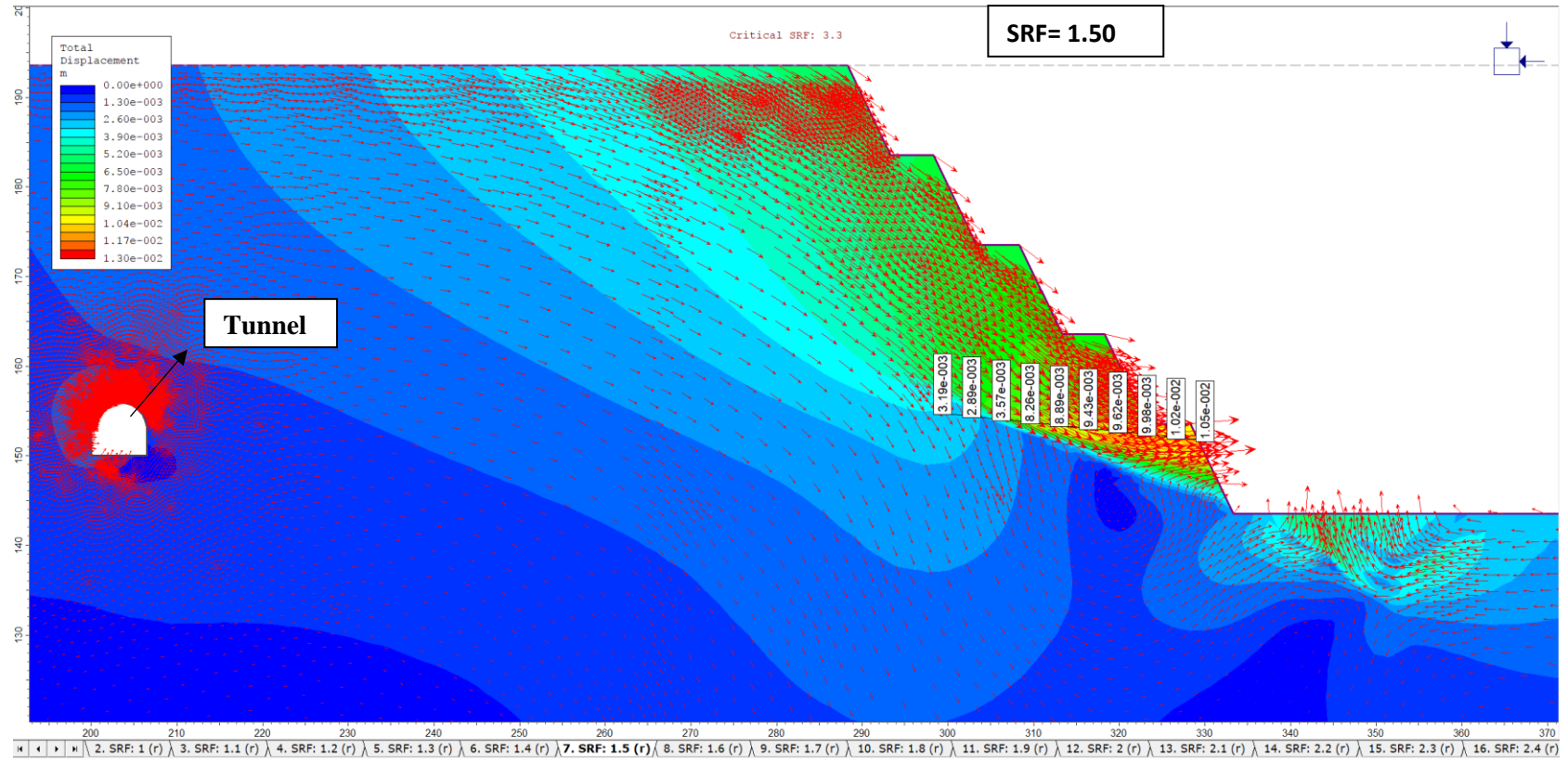
Figure 38. Displacement vectors and displacement magnitudes within planned slope cut at the SRF=1.50 at Km 26+620
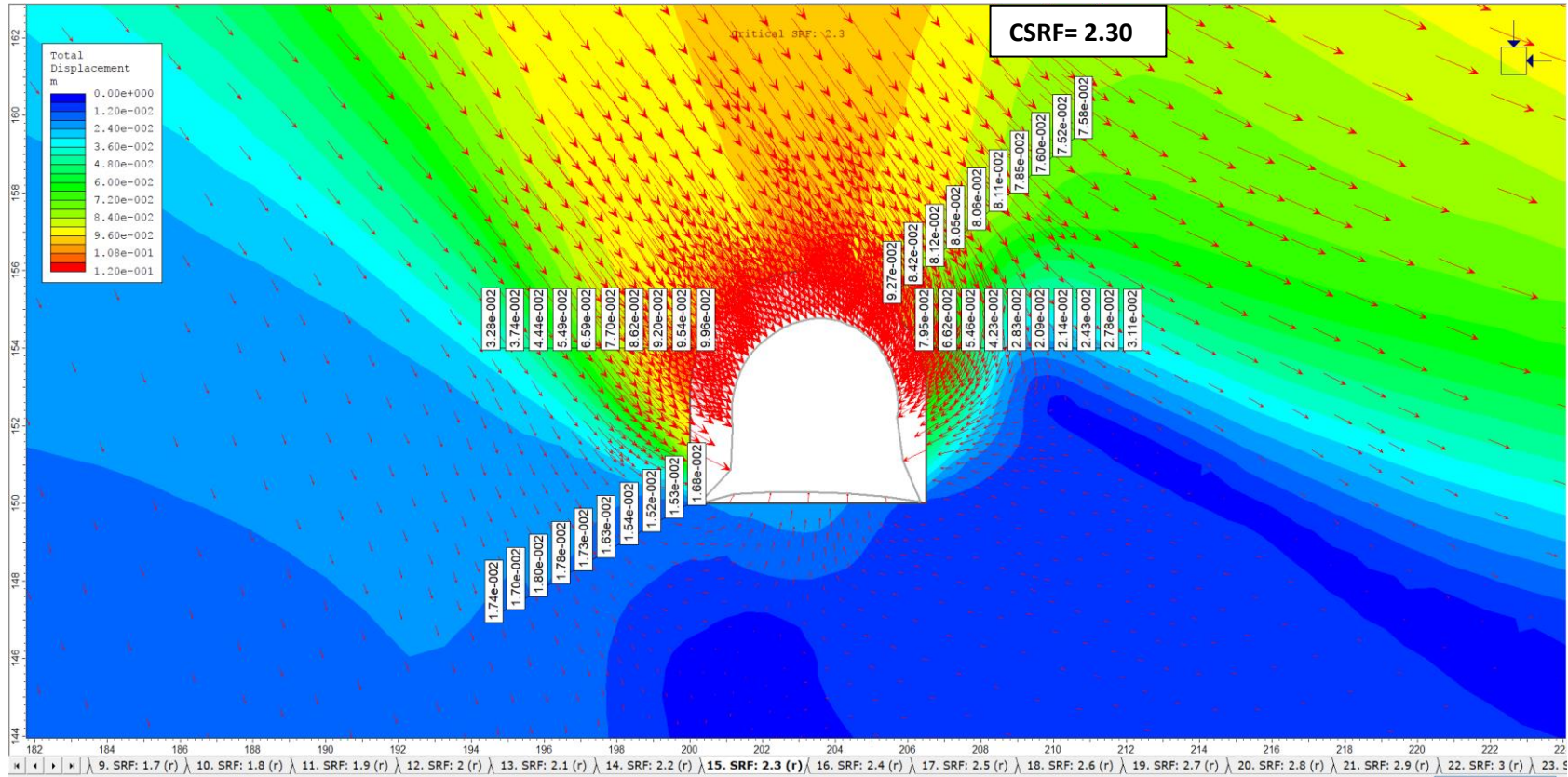
Figure 39. Deformations around the tunnel at the CSRF=2.30 at Km 26+620
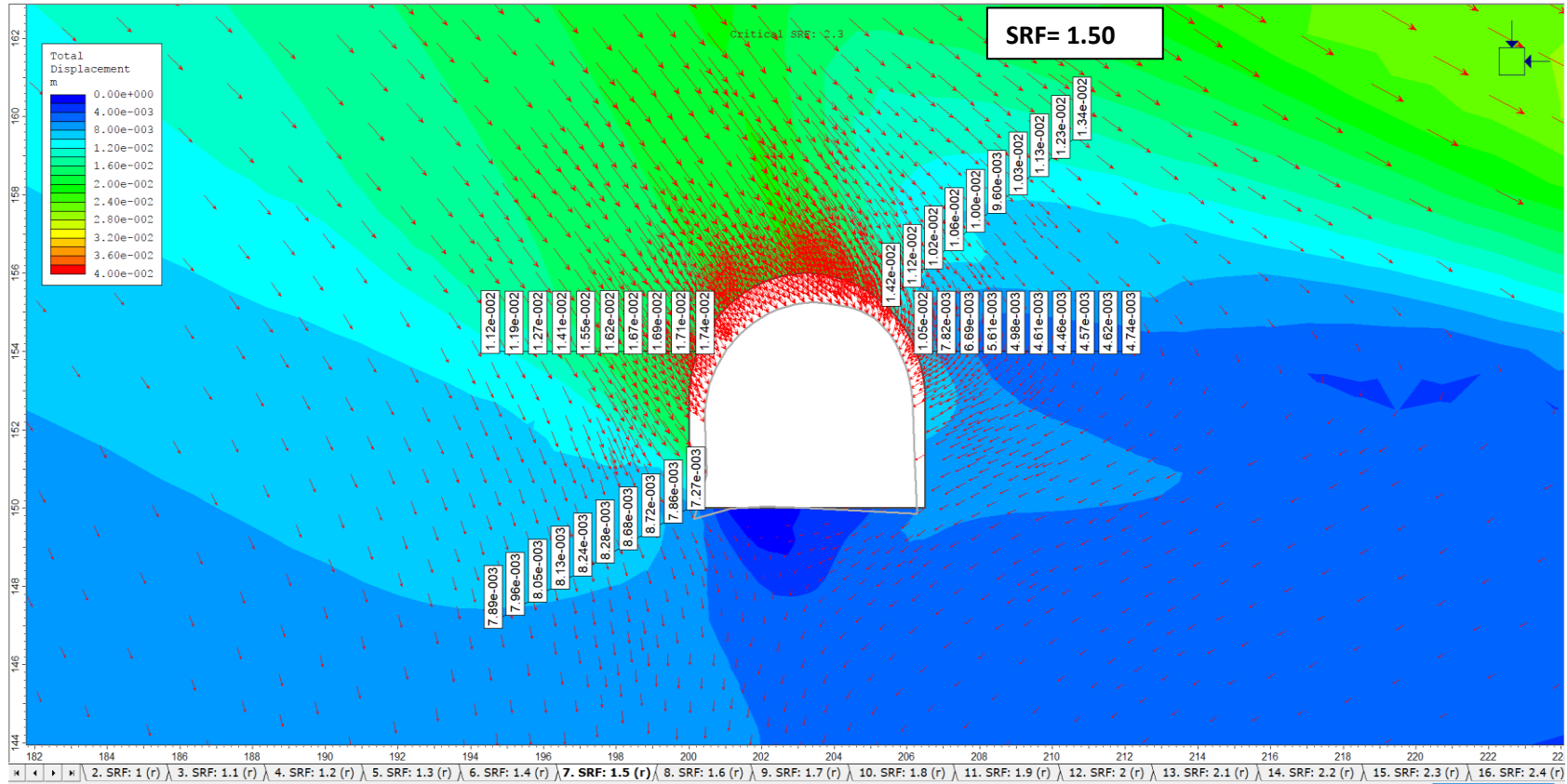
Figure 40. Deformations around the tunnel at the SRF=1.50 at Km 26+620
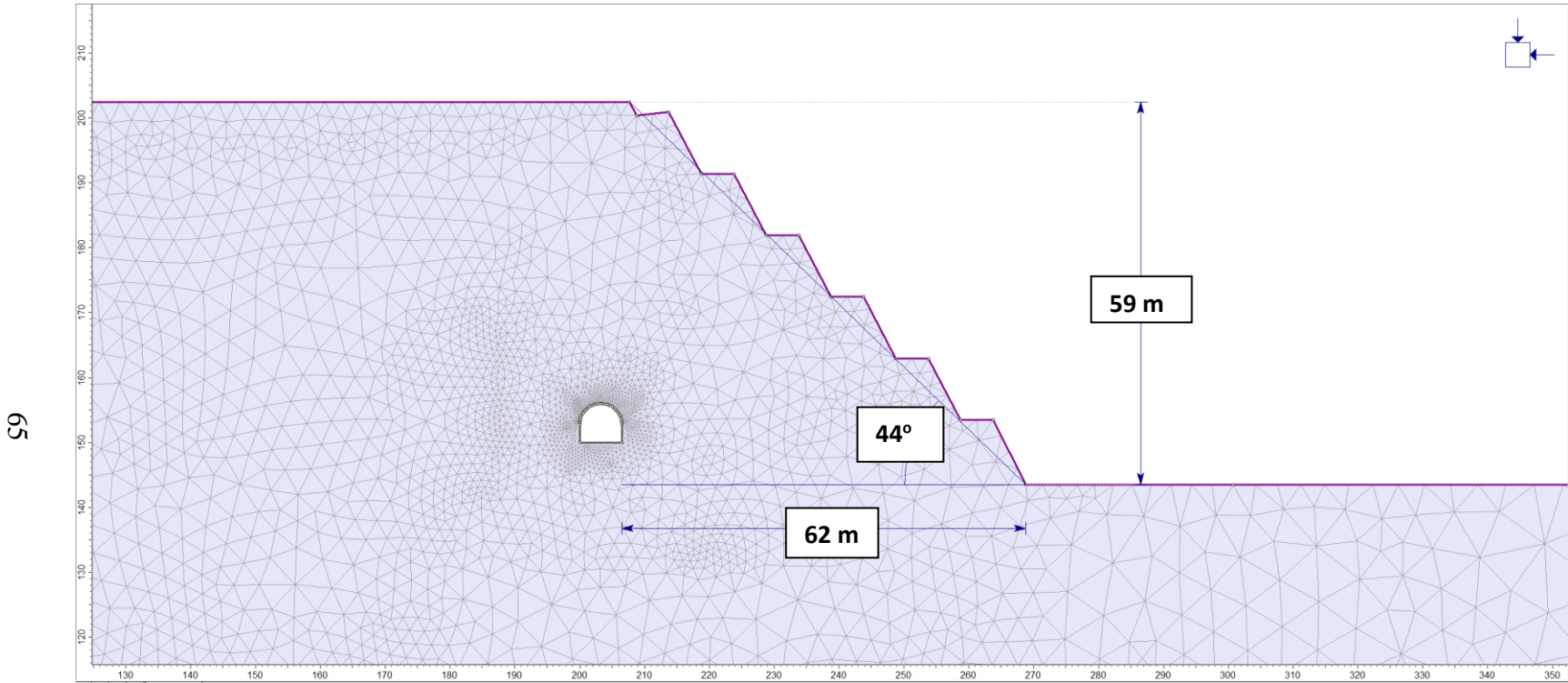
Figure 41. Slope dimensions and finite element model of the planned slope profile, section A-A', Km 26+630
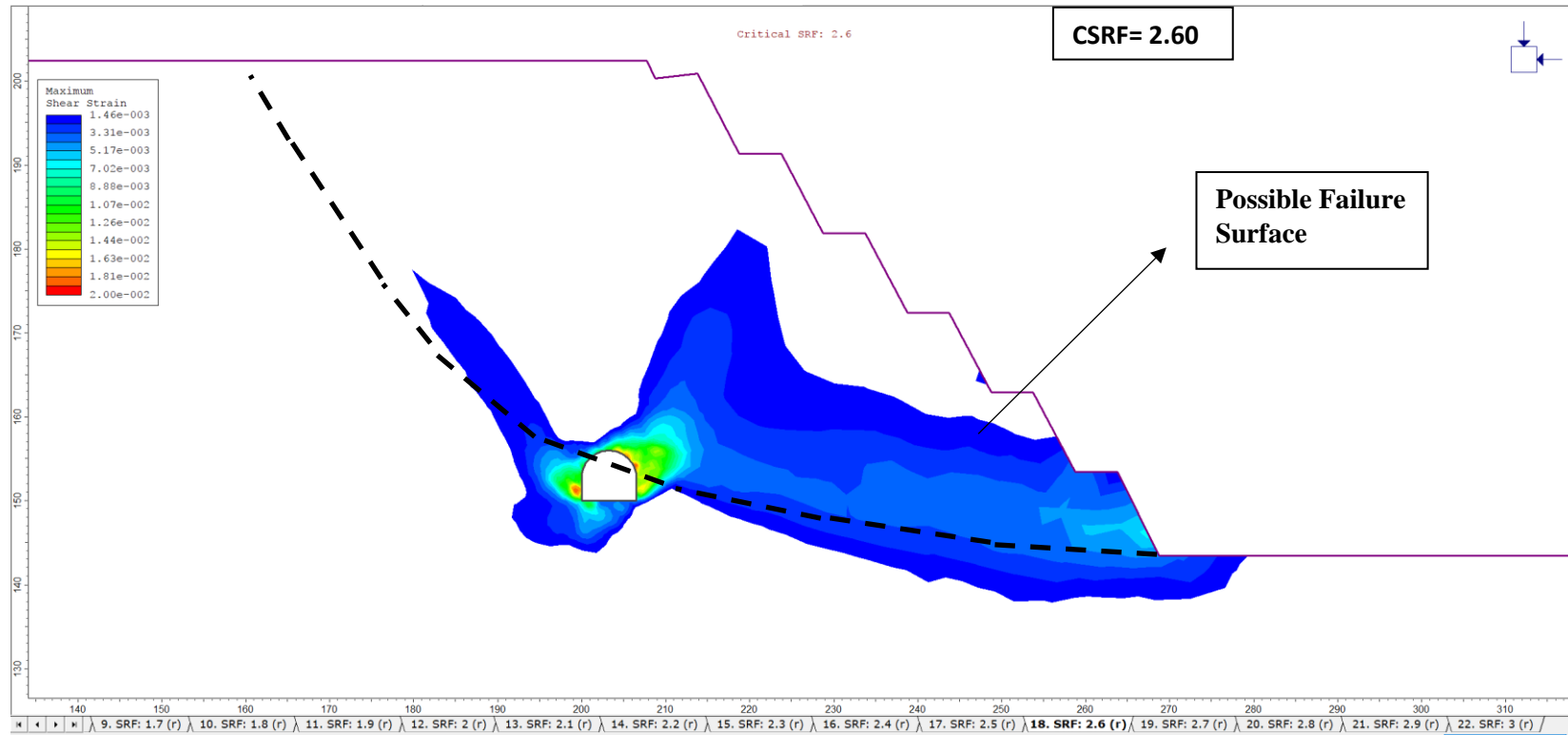
Figure 42. Maximum shear strain distribution and possible failure surface after planned slope cut at the CSRF=2.60 at Km 26+630

Figure 43. Maximum shear strain distribution and possible failure surface after planned slope cut at the SRF=1.50 at Km 26+630

Figure 44. Displacement vectors and displacement magnitudes within planned slope cut at the CSRF=2.60 at Km 26+630
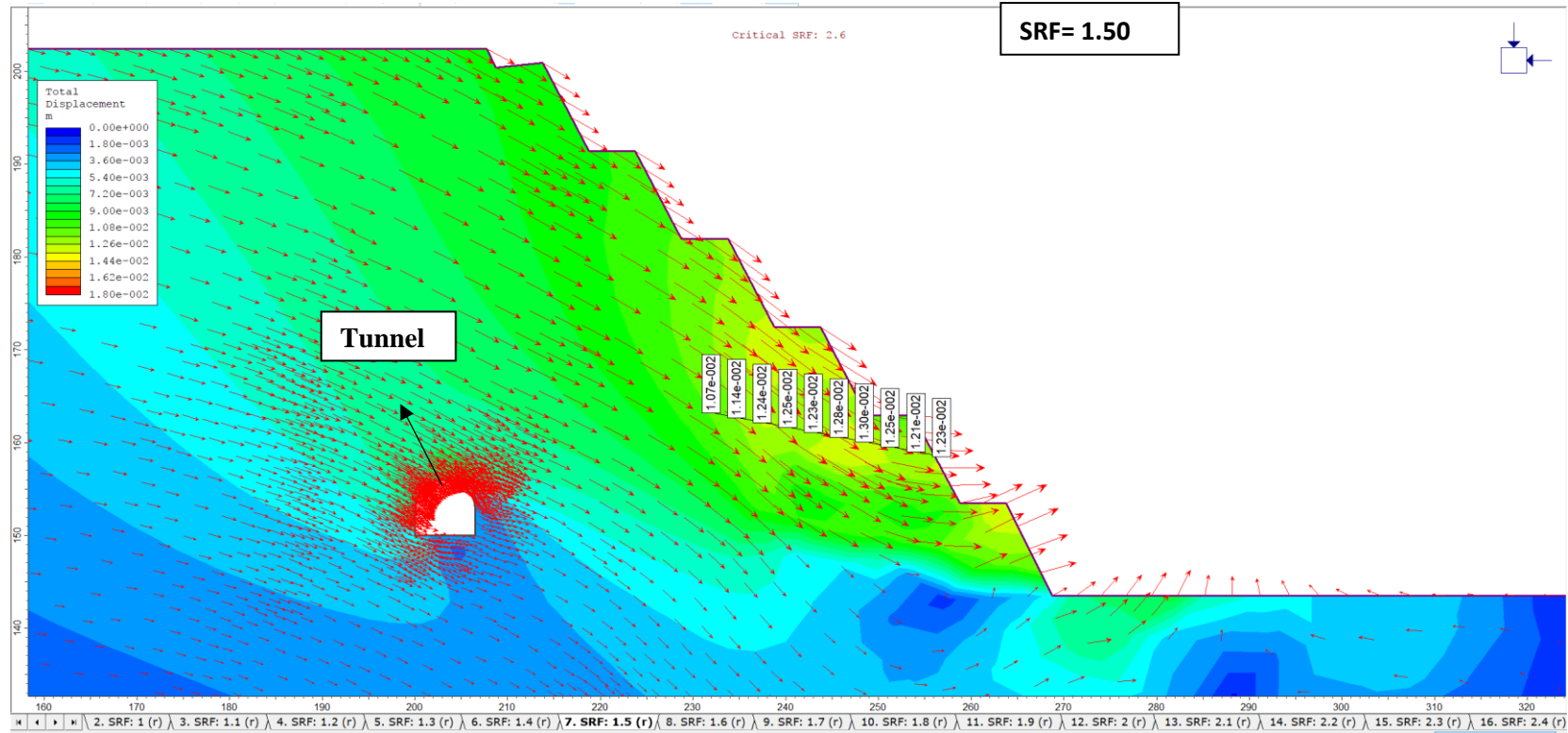
Figure 45. Displacement vectors and displacement magnitudes within planned slope cut at the SRF=1.50 at Km 26+630
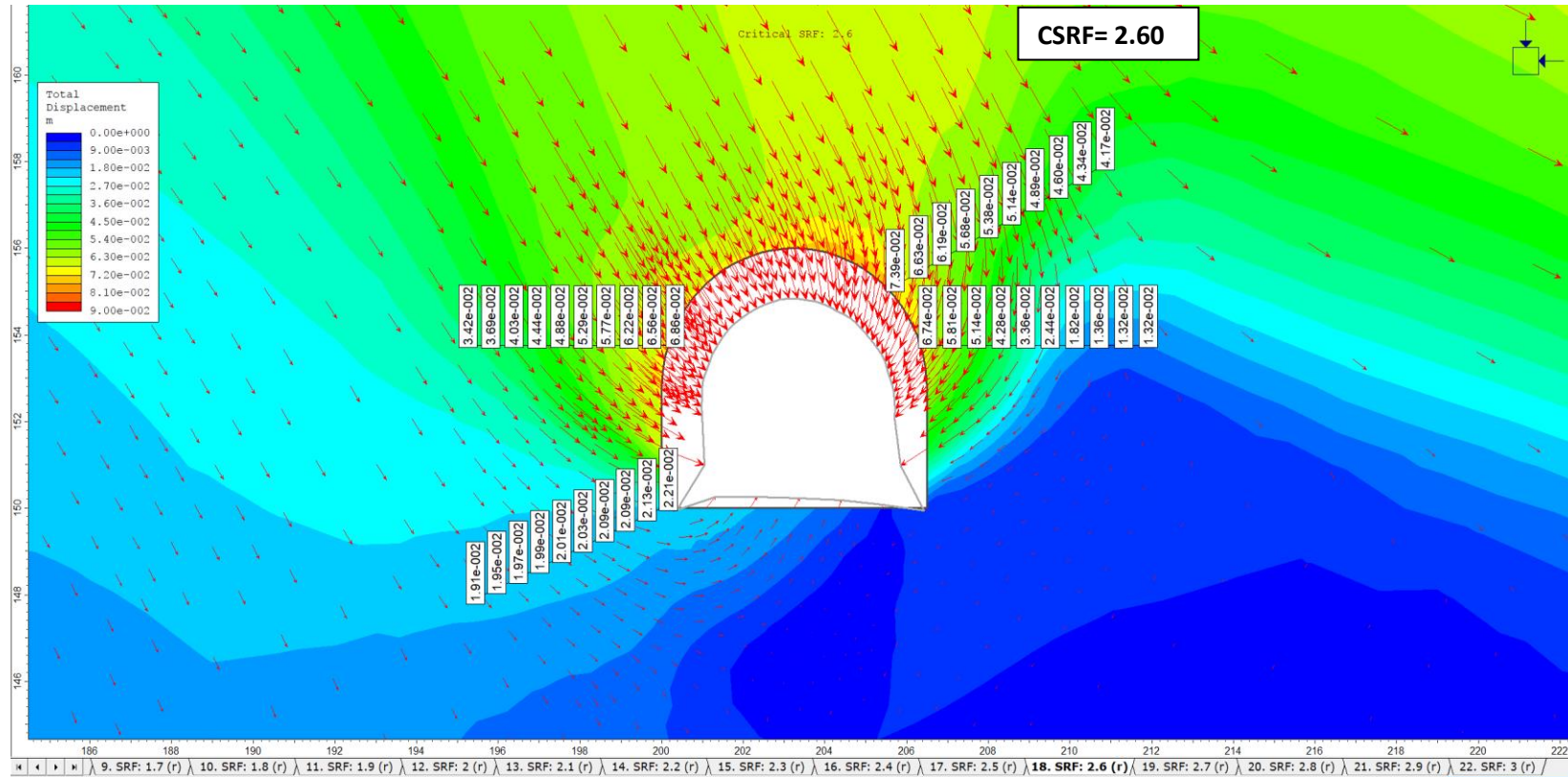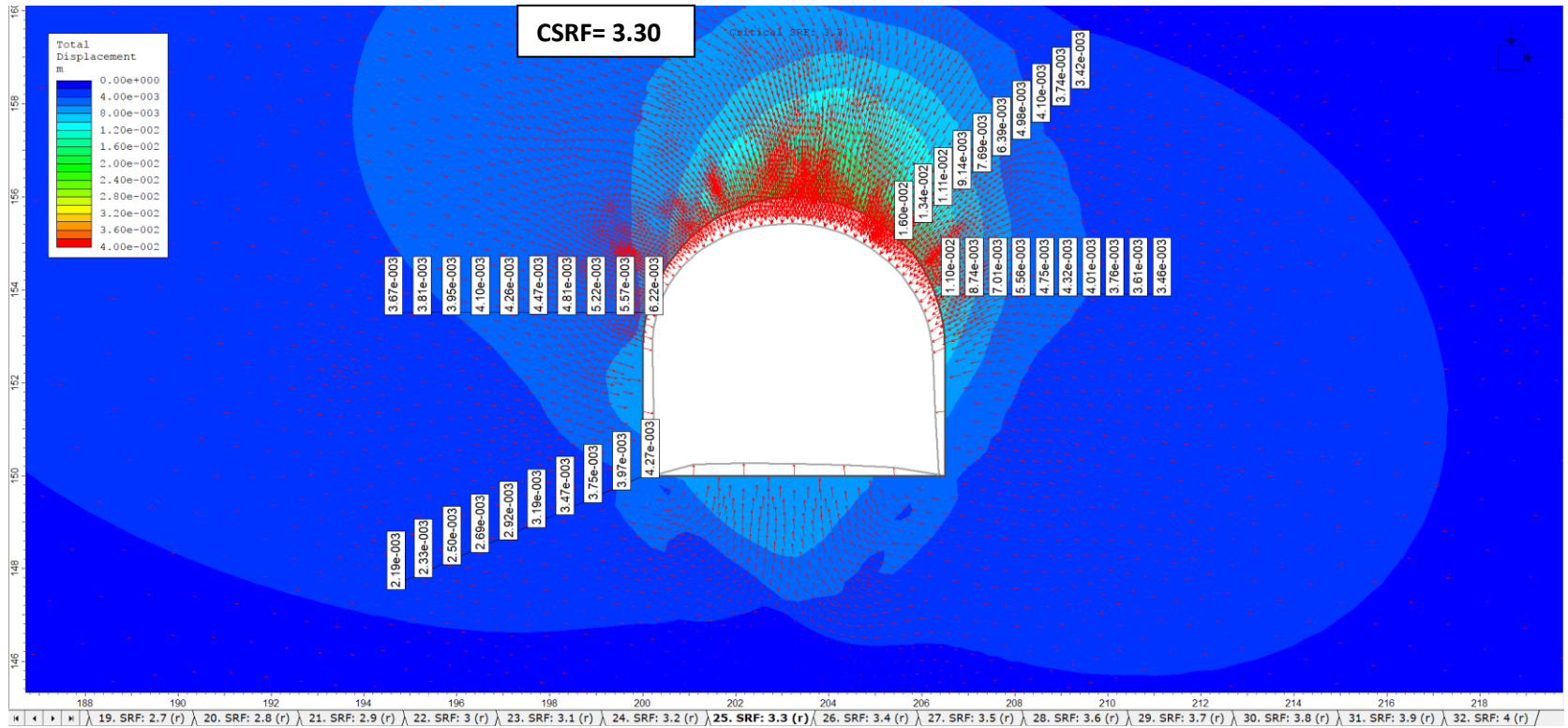
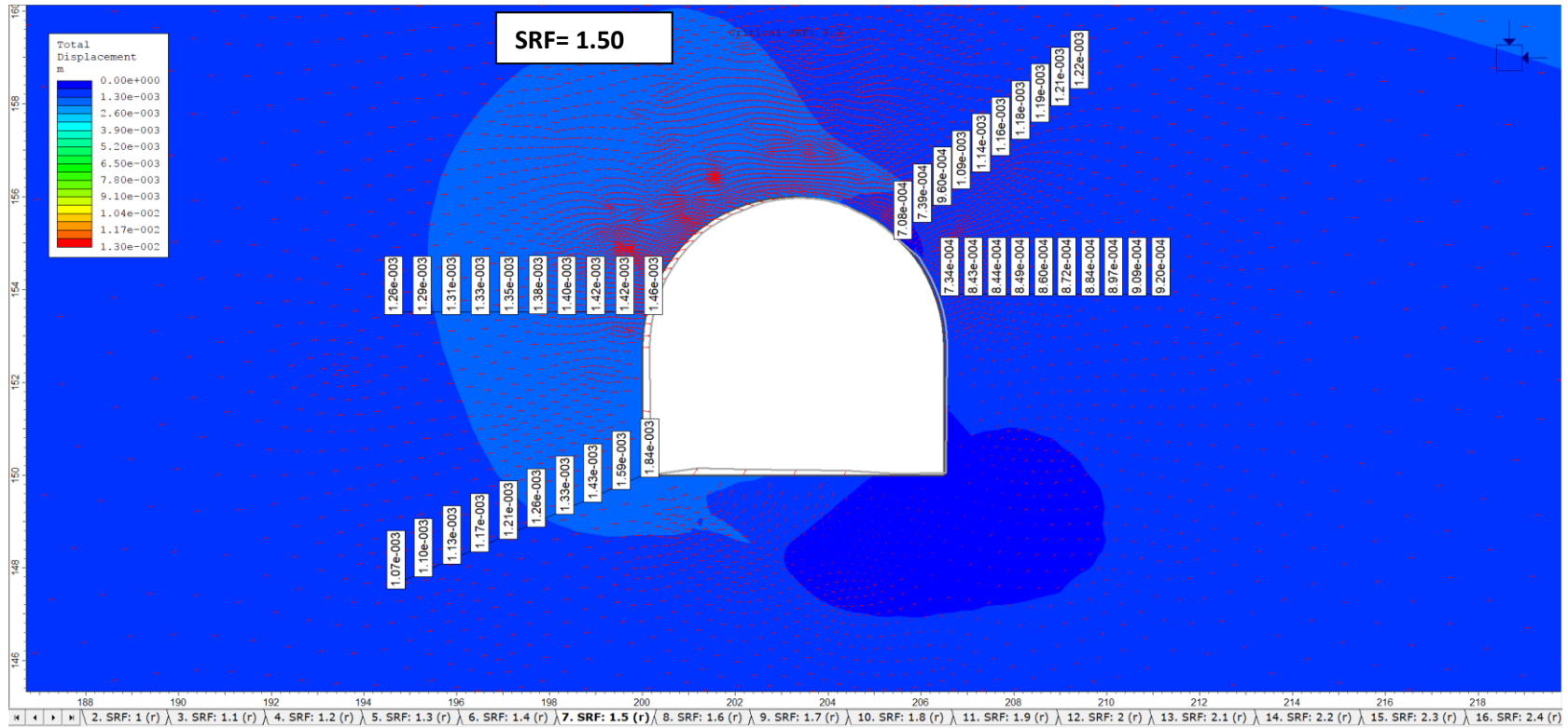*Figure 46. Deformations around the tunnel at the CSRF=2.60 at Km 26+630*
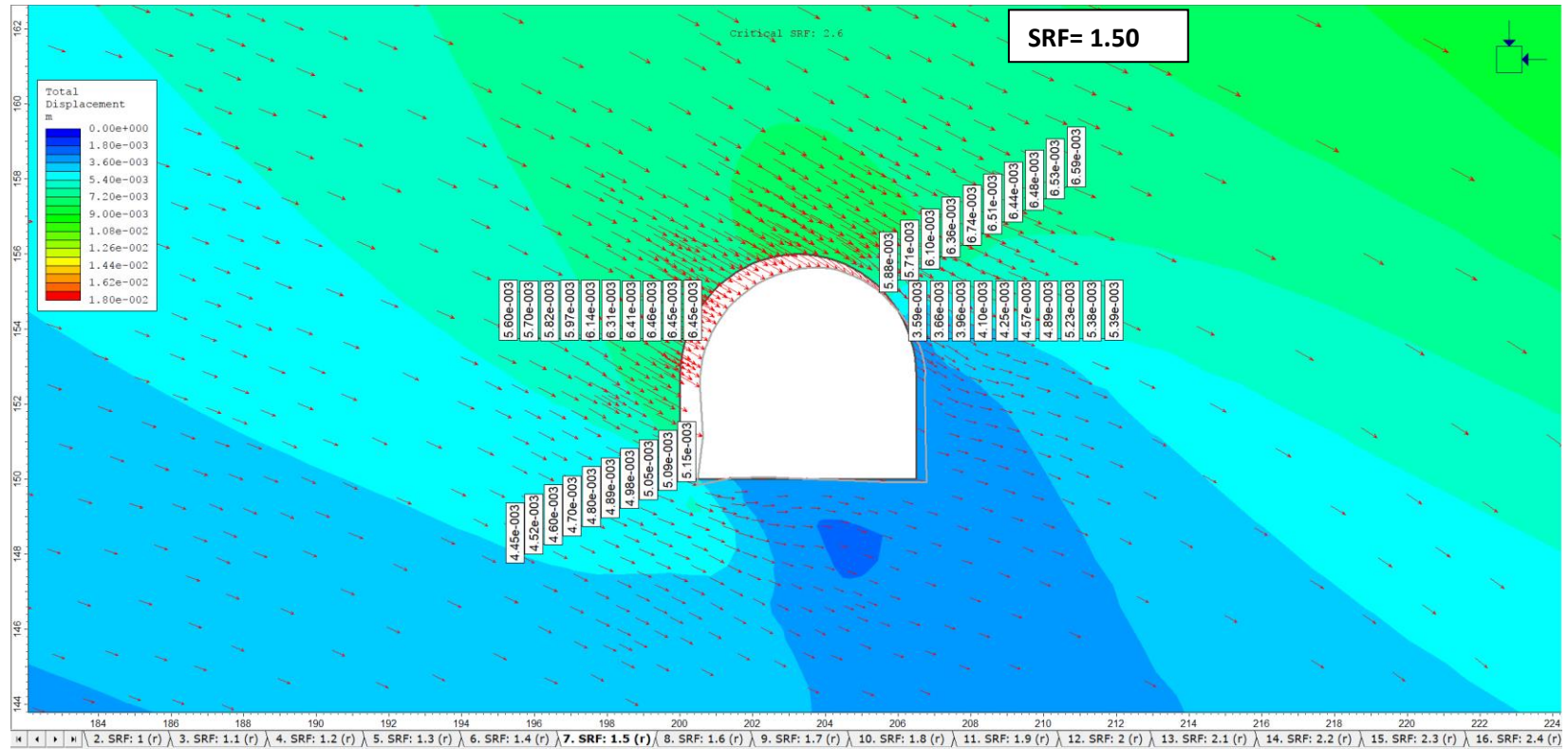
Figure 47. Deformations around the tunnel at the SRF=1.50 at Km 26+630
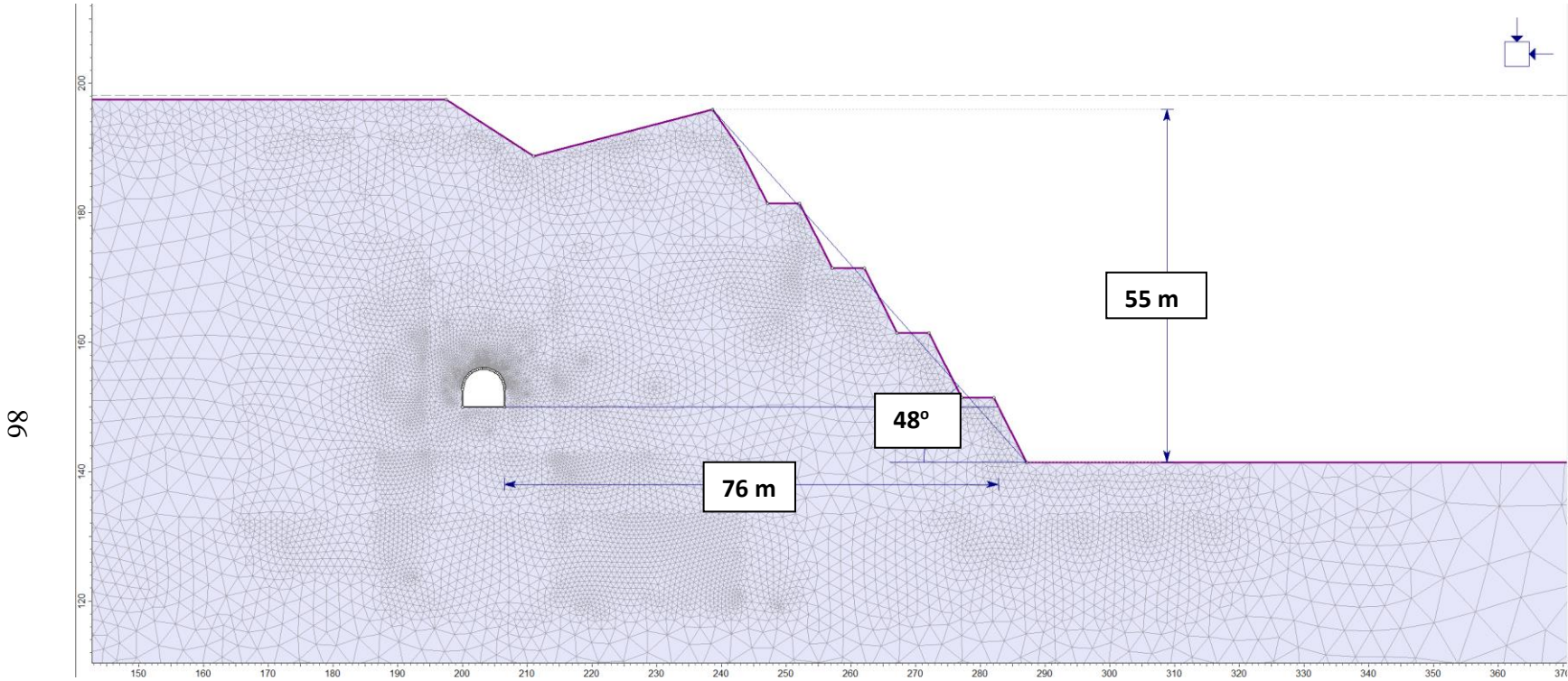
Figure 48. Slope dimensions and finite element model of the planned slope profile, section A-A', Km 26+650
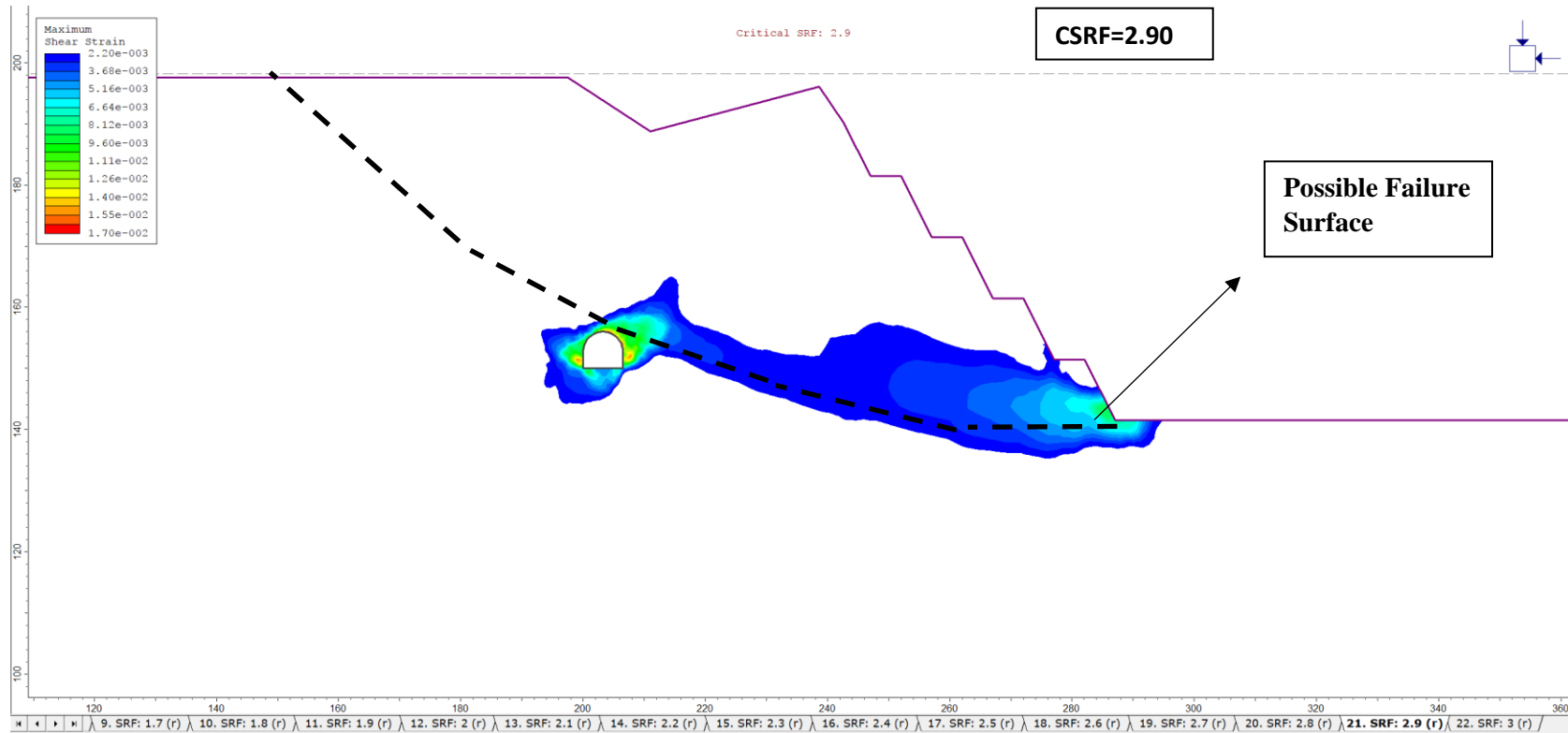
Figure 49. Maximum shear strain distribution and possible failure surface after planned slope cut at the CSRF=2.70 at Km 26+650
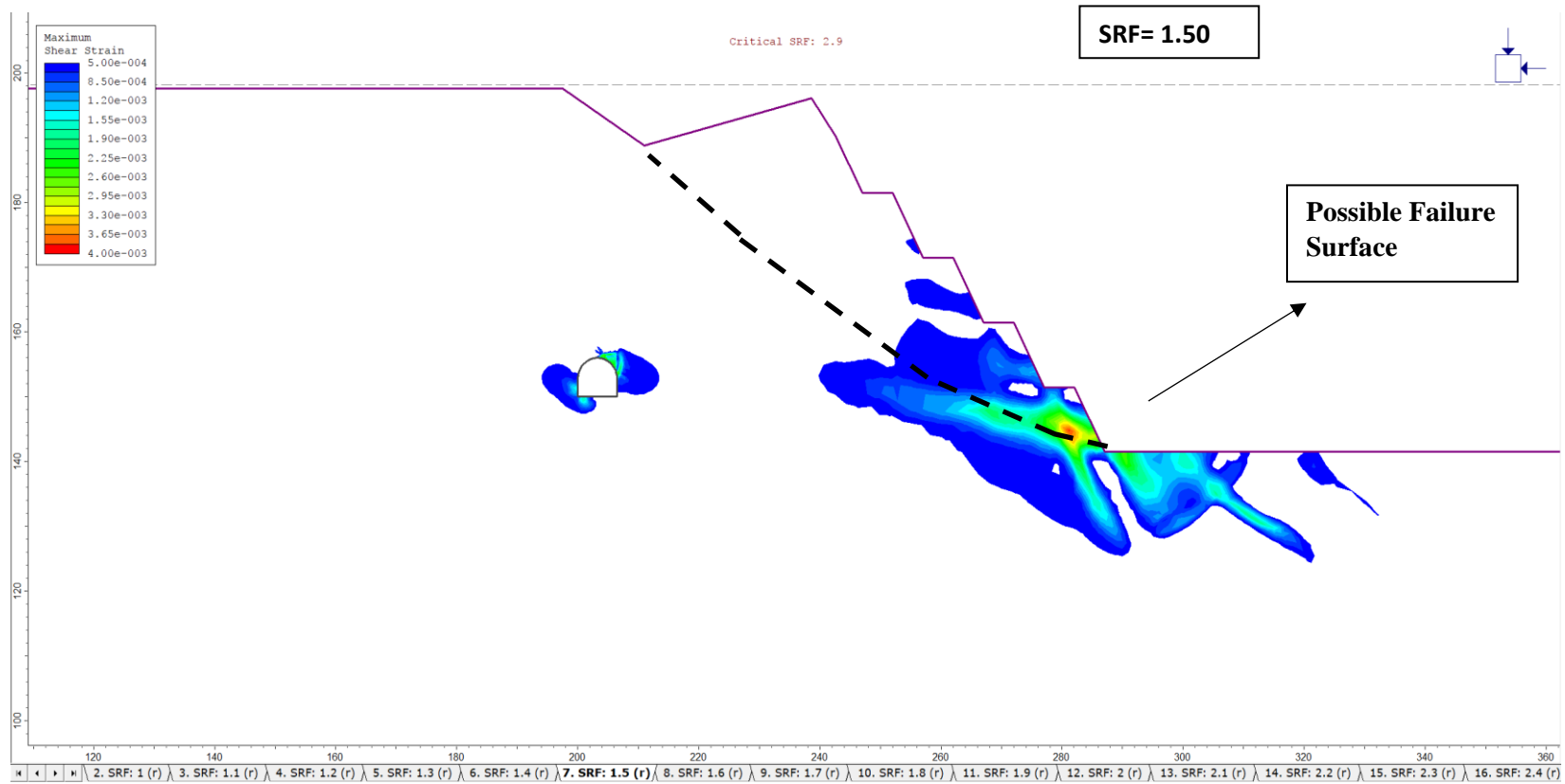
Figure 50. Maximum shear strain distribution and possible failure surface after planned slope cut at the SRF=1.50 at Km 26+650
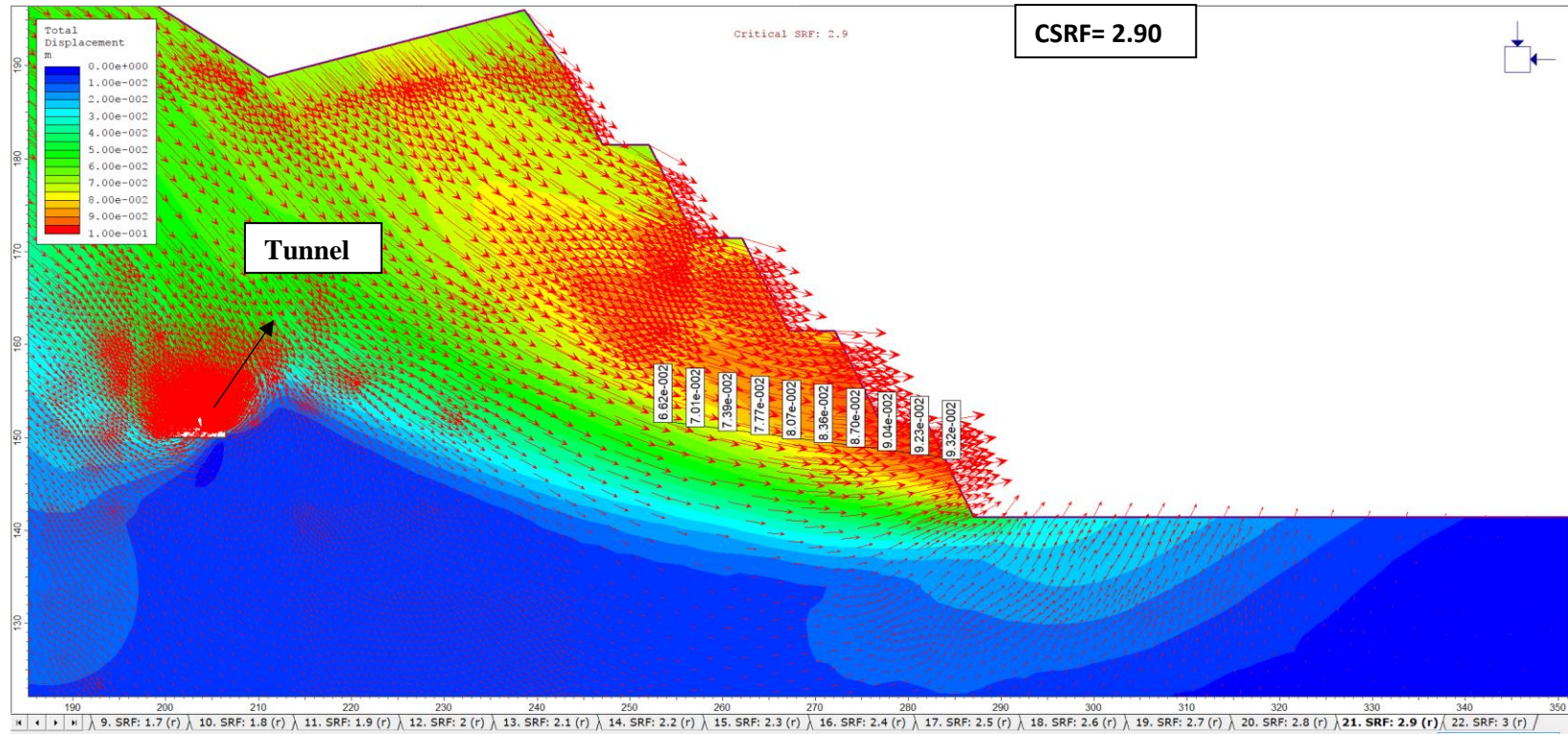
Figure 51. Displacement vectors and displacement magnitudes within planned slope cut at the CSRF=2.70 at Km 26+650
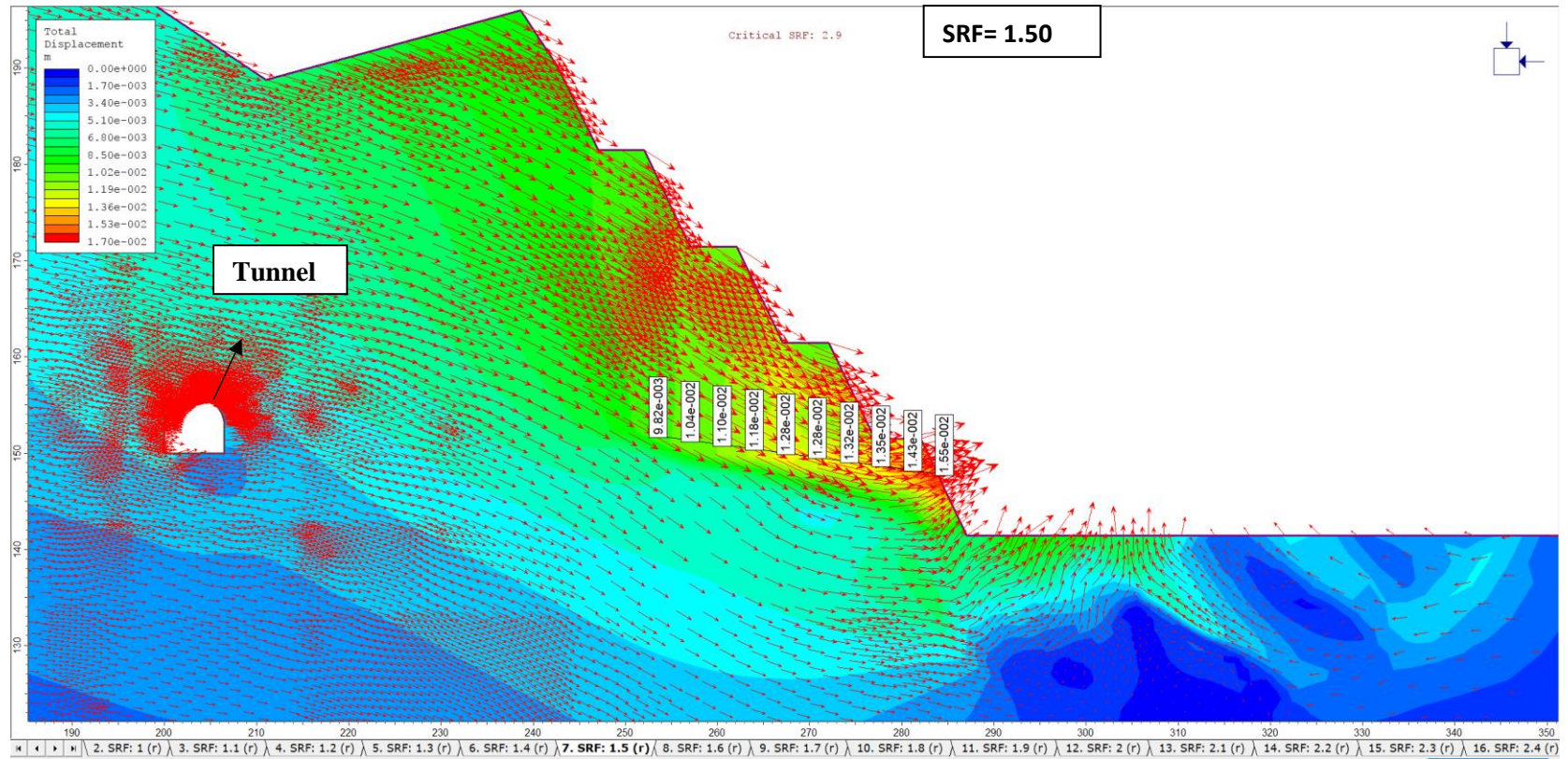
Figure 52. Displacement vectors and displacement magnitudes within planned slope cut at the SRF=1.50 at Km 26+650

Figure 53. Deformations around the tunnel at the CSRF=2.70 at Km 26+650

Figure 54. Deformations around the tunnel at the SRF=1.50 at Km 26+650

Figure 55. Slope dimensions and finite element model of the planned slope profile, section A-A', Km 26+660

Figure 56. Maximum shear strain distribution and possible failure surface after planned slope cut at the CSRF=3.30 at Km 26+660

Figure 57. Maximum shear strain distribution and possible failure surface after planned slope cut at the SRF=1.50 at Km 26+660

Figure 58. Displacement vectors and displacement magnitudes within planned slope cut at the CSRF=3.30 at Km 26+660
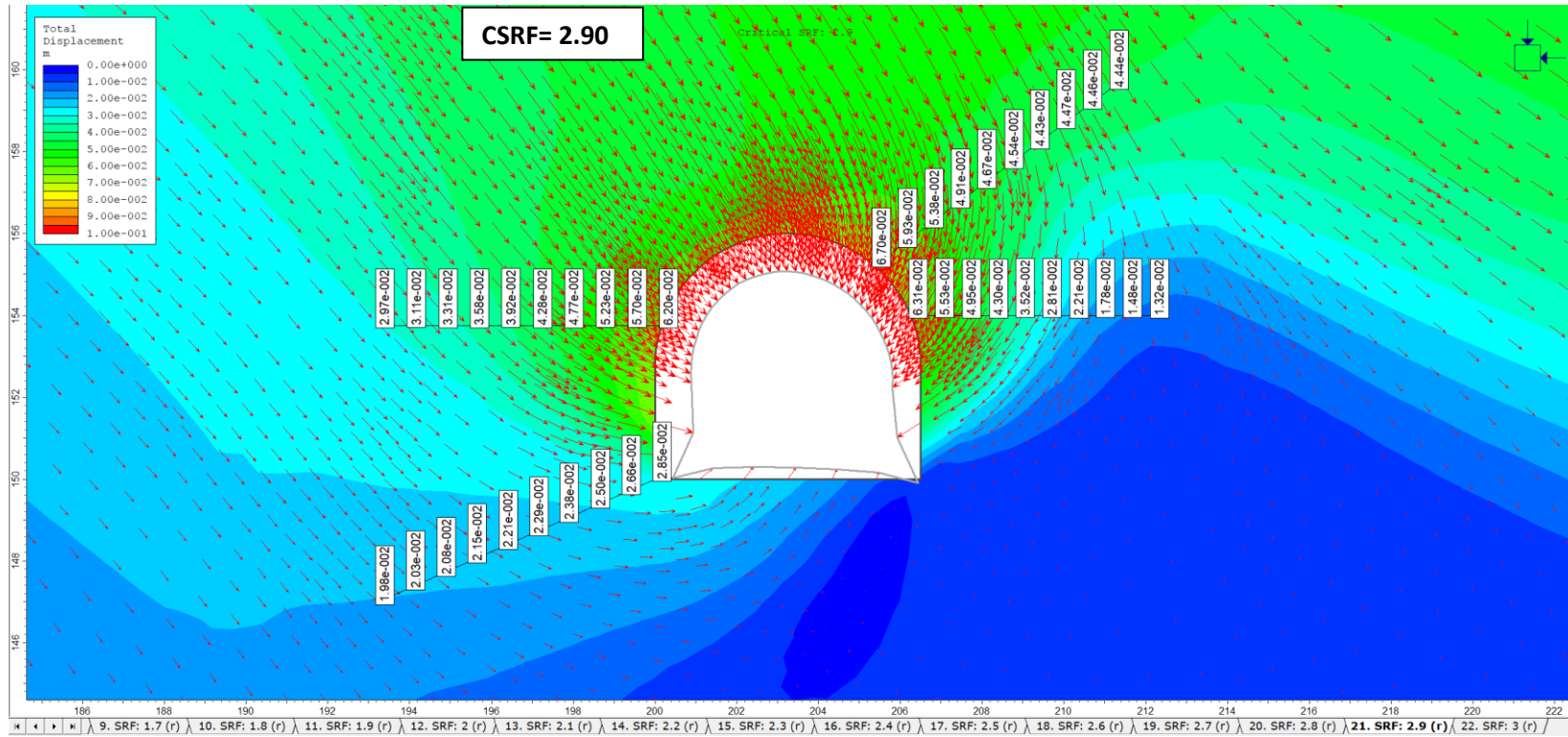
Figure 59. Displacement vectors and displacement magnitudes within planned slope cut at the SRF=1.50 at Km 26+660

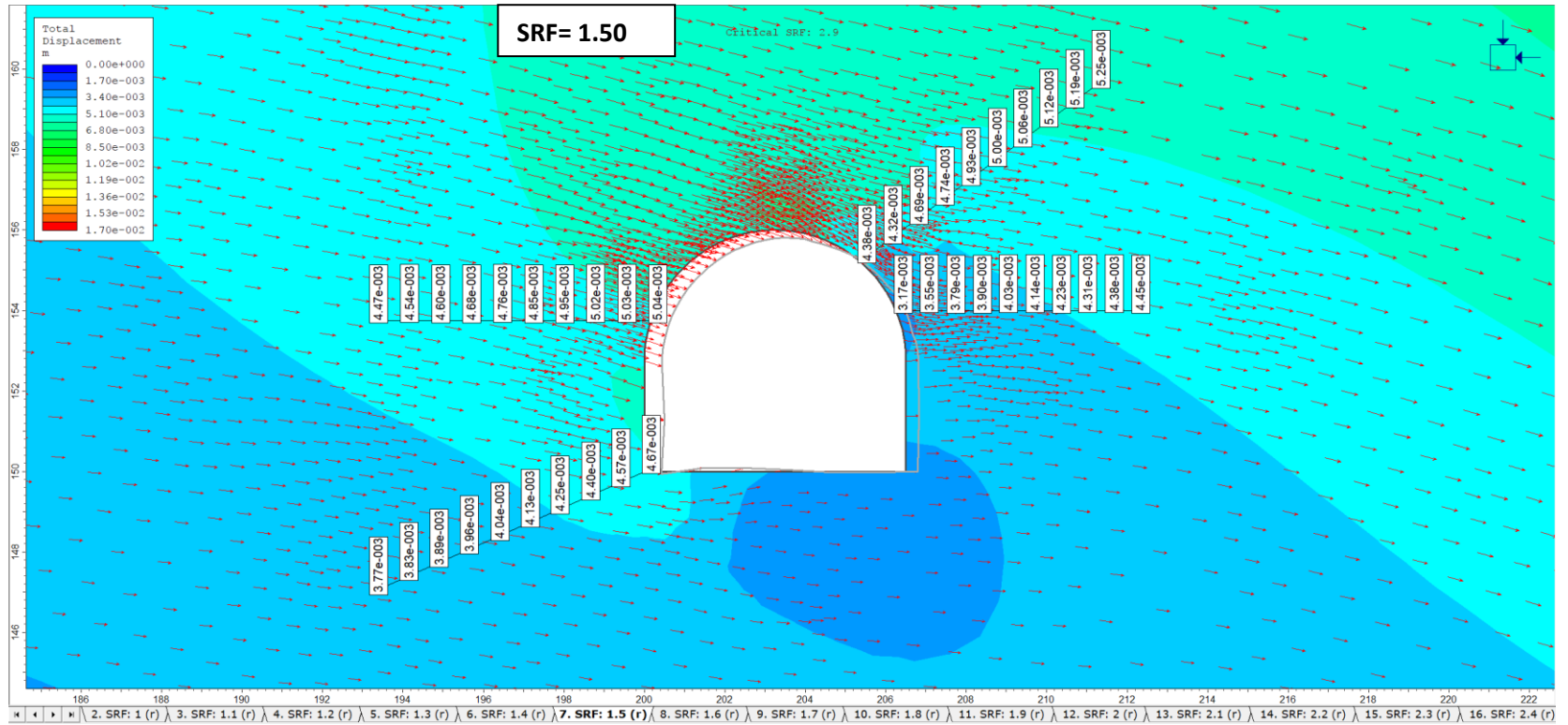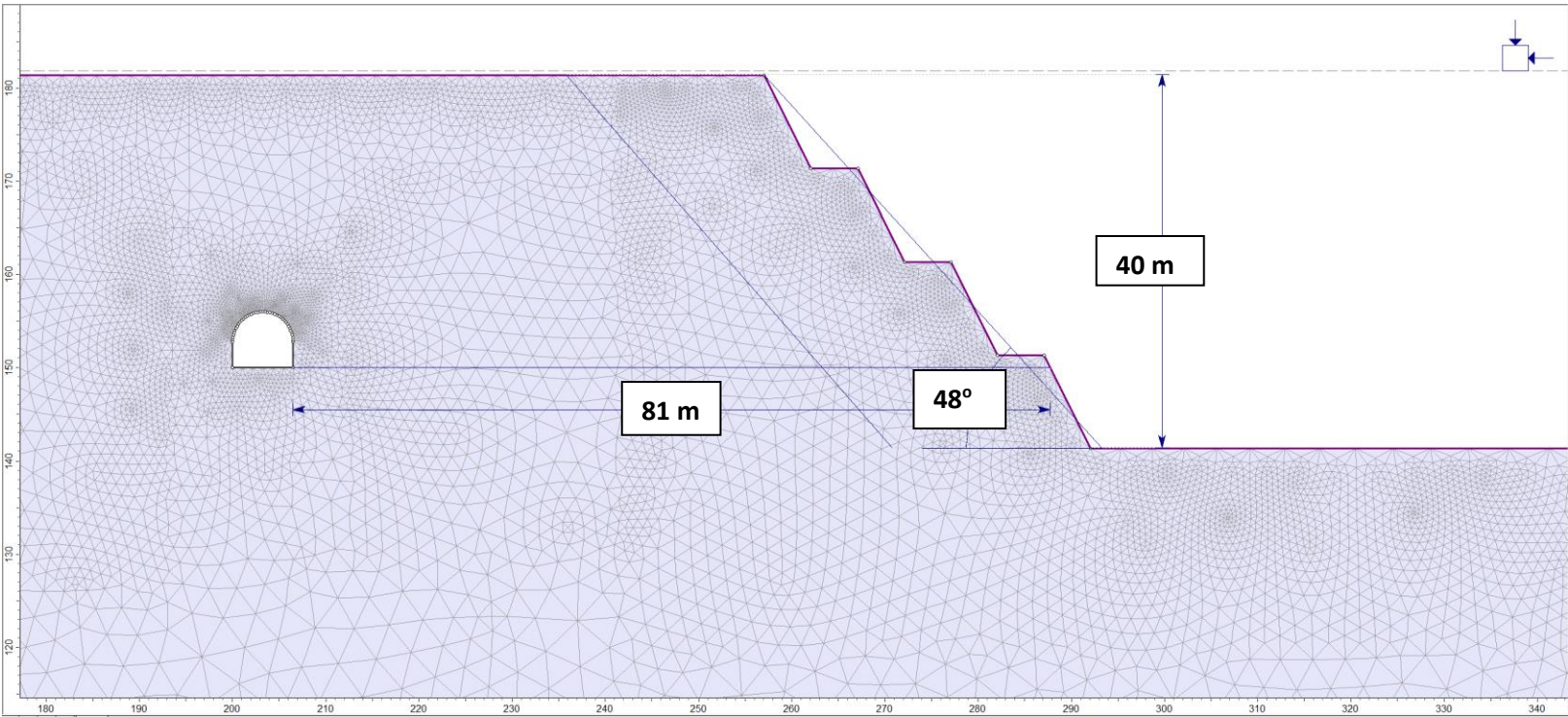*Figure 60. Deformations around the tunnel at the CSRF=3.30 at Km 26+660*

Figure 61. Deformations around the tunnel at the SRF=1.50 at Km 26+660

Km 26+670

Figure 62. Slope dimensions and finite element model of the planned slope profile, section A-A', Km 26+670
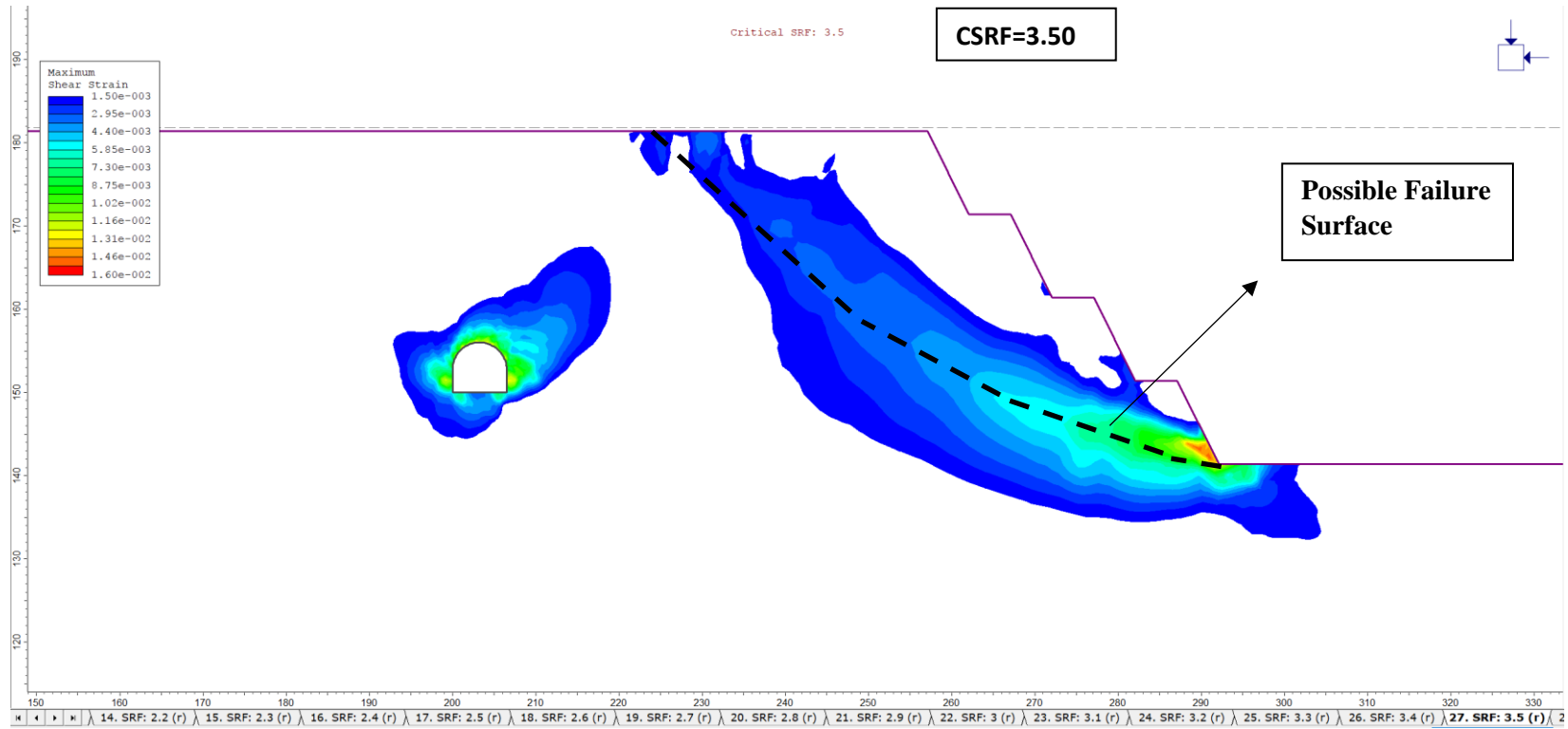
Figure 63. Maximum shear strain distribution and possible failure surface after planned slope cut at the CSRF=2.90 at Km 26+670
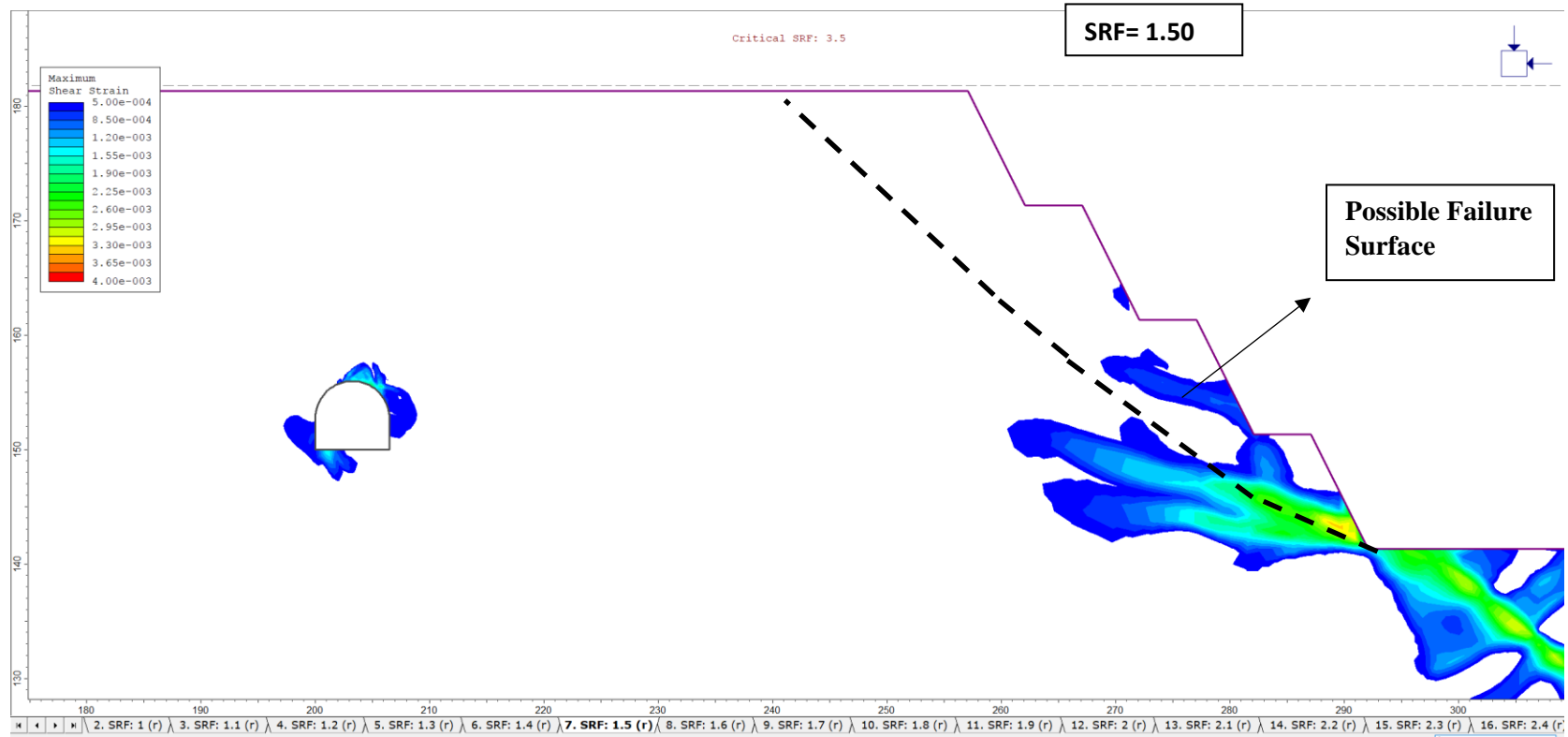
Figure 64. Maximum shear strain distribution and possible failure surface after planned slope cut at the SRF=1.50 at Km 26+670
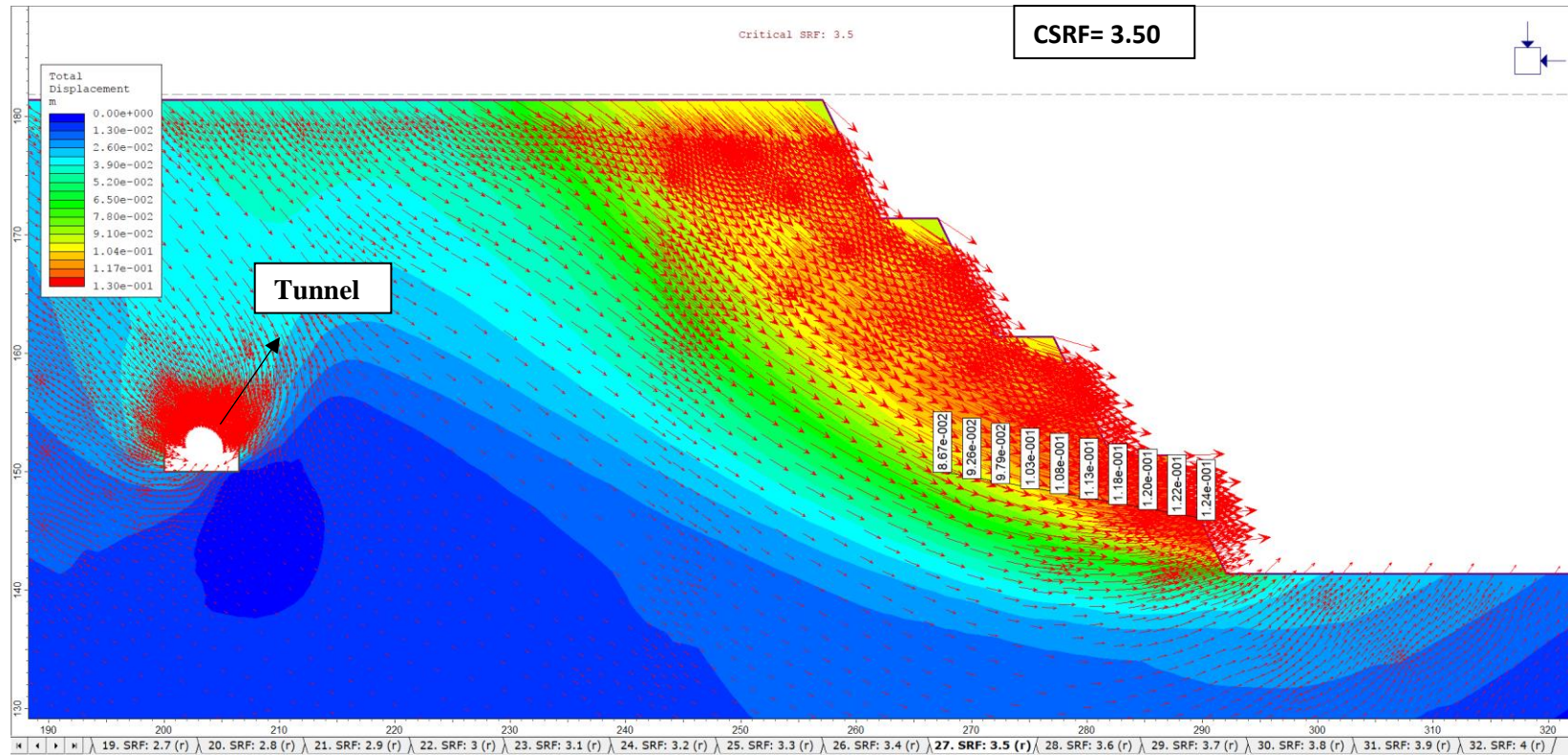
Figure 65. Displacement vectors and displacement magnitudes within planned slope cut at the CSRF=2.90 at Km 26+670
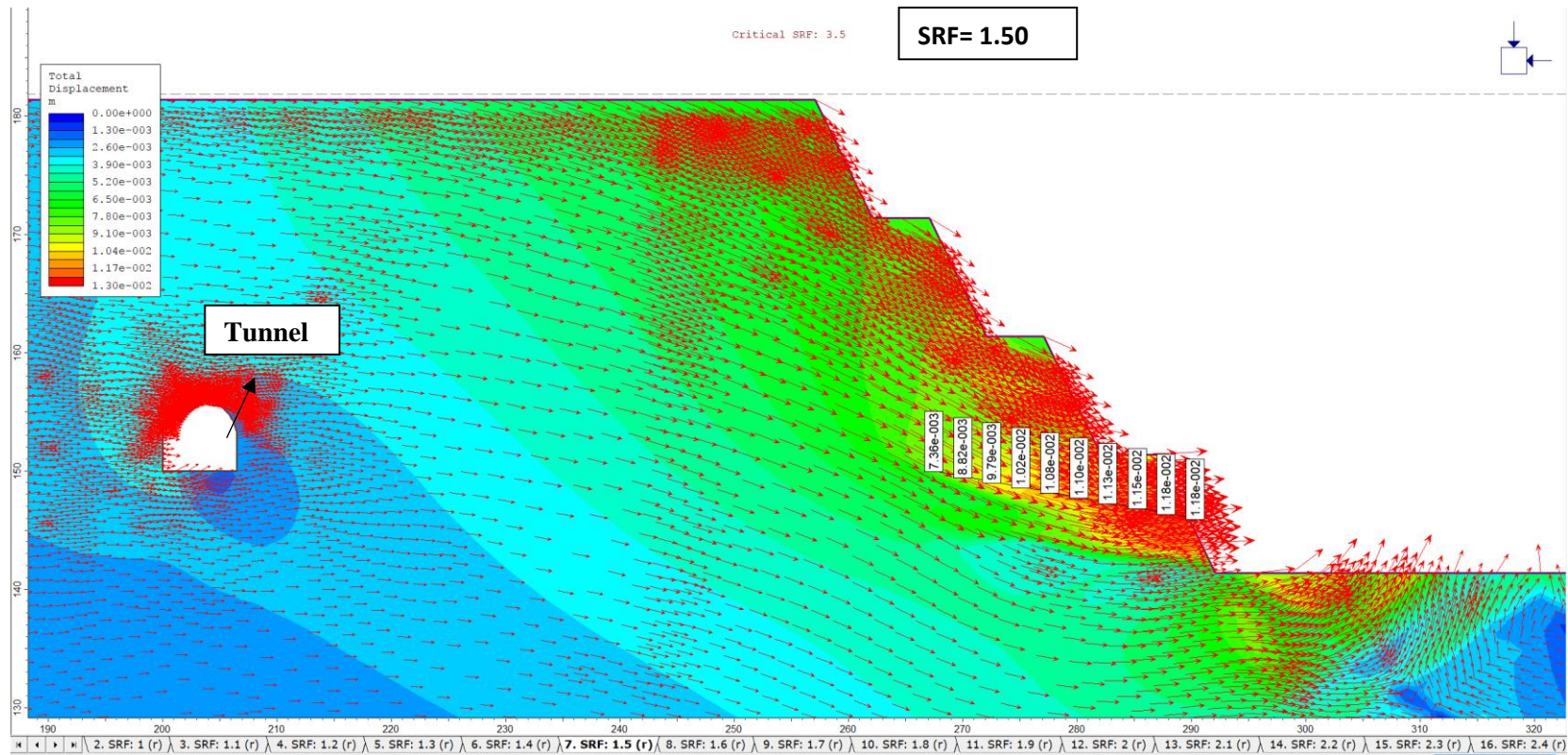
Figure 66. Displacement vectors and displacement magnitudes within planned slope cut at the SRF=1.50 at Km 26+670
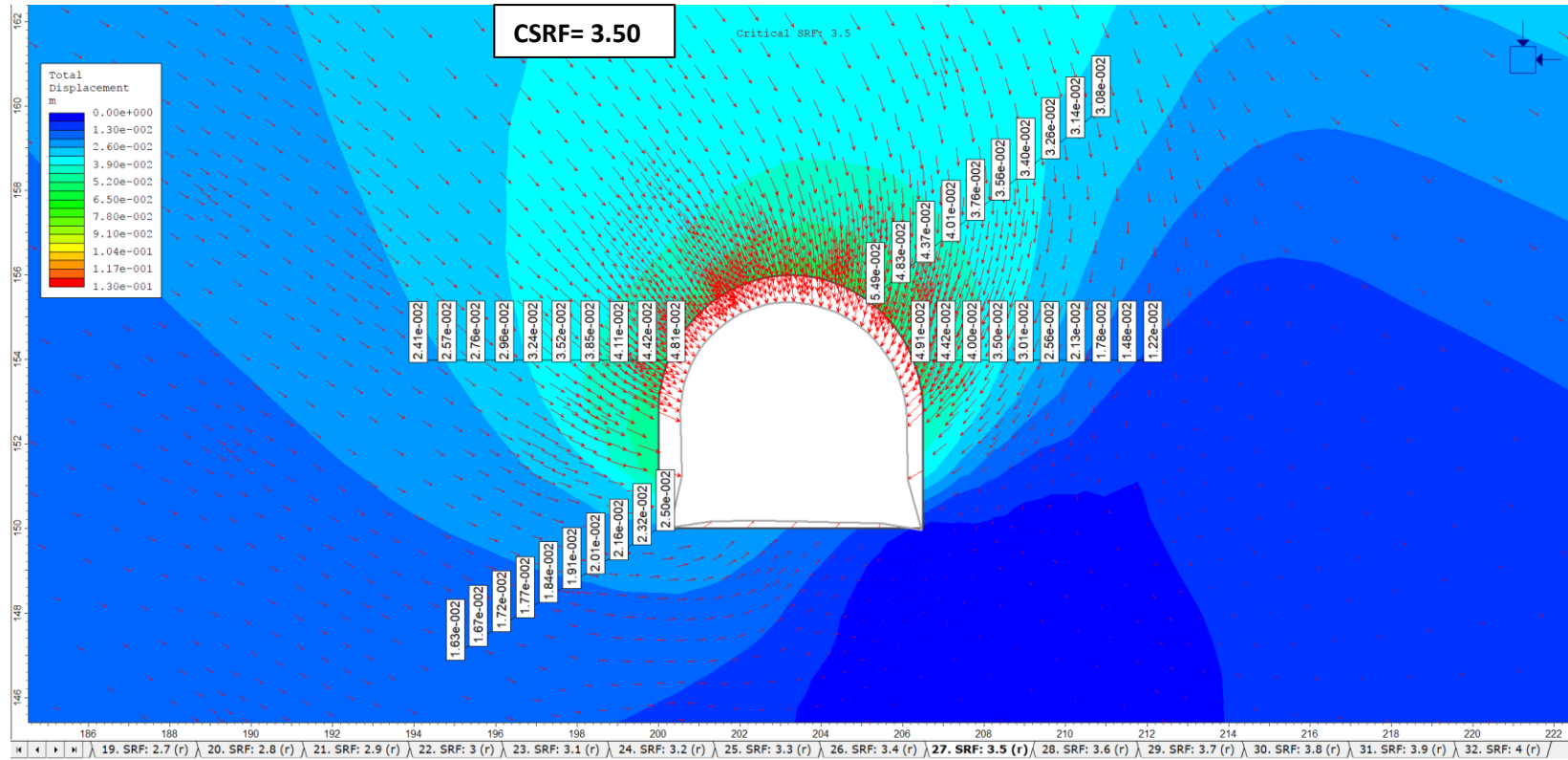
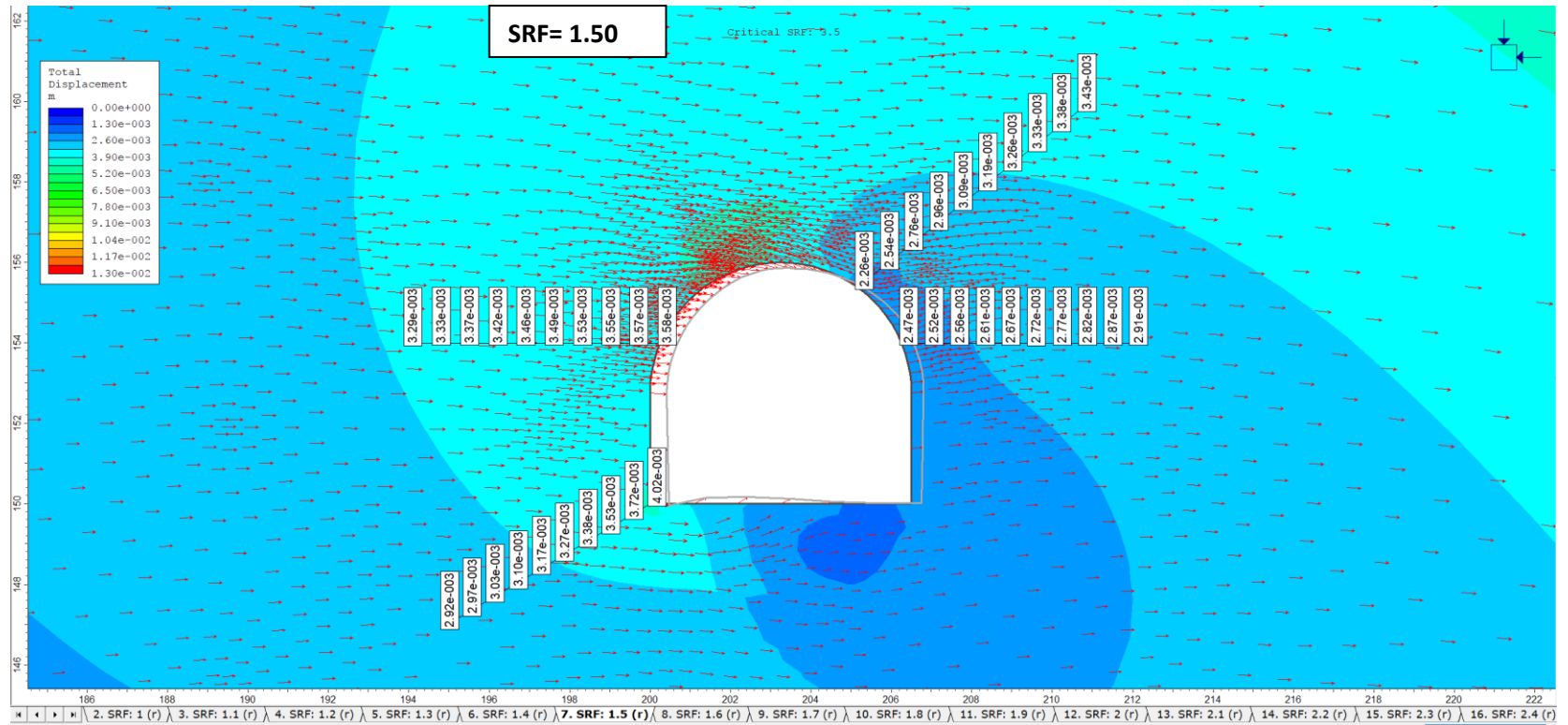*Figure 67. Deformations around the tunnel at the CSRF=2.90 at Km 26+670*

Figure 68. Deformations around the tunnel at the SRF=1.50 at Km 26+670
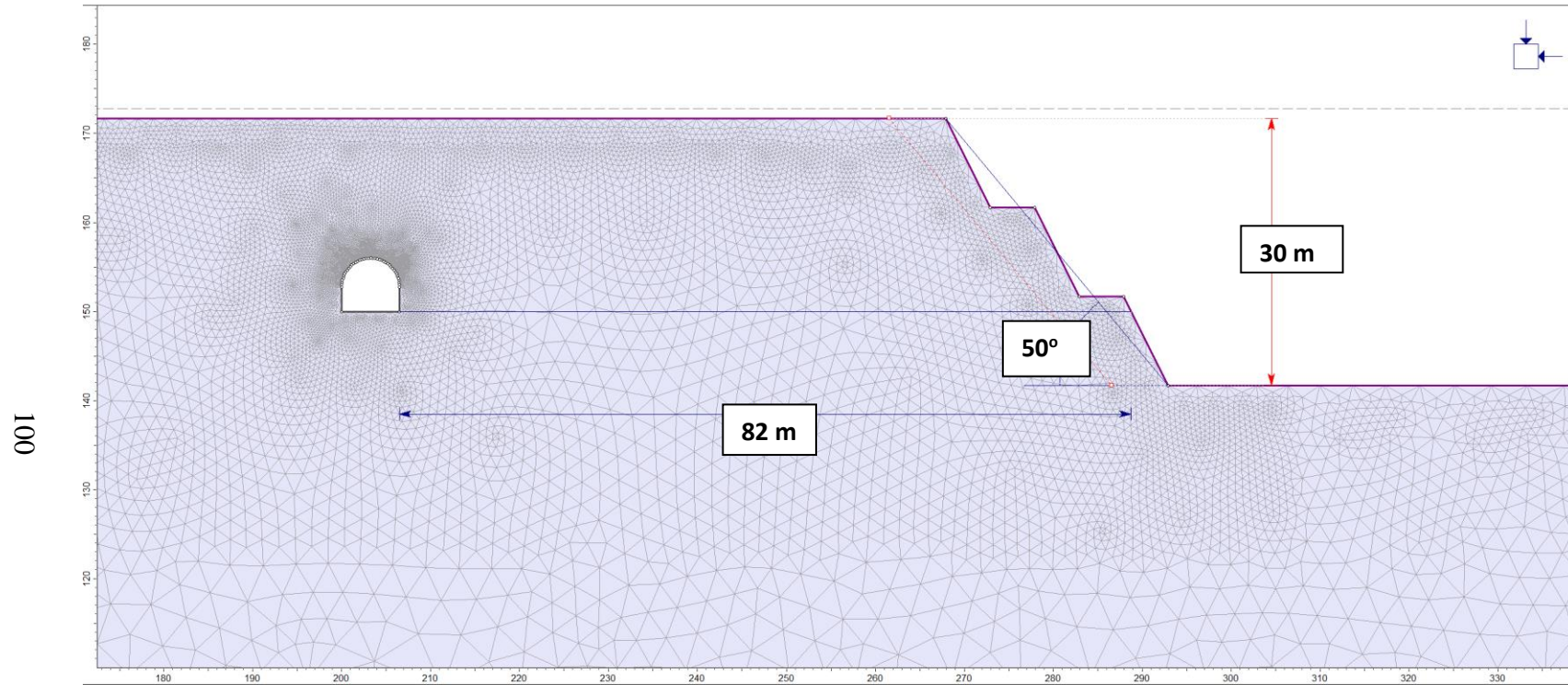
Km 26+680

Figure 69. Slope dimensions and finite element model of the planned slope profile, section A-A', Km 26+680
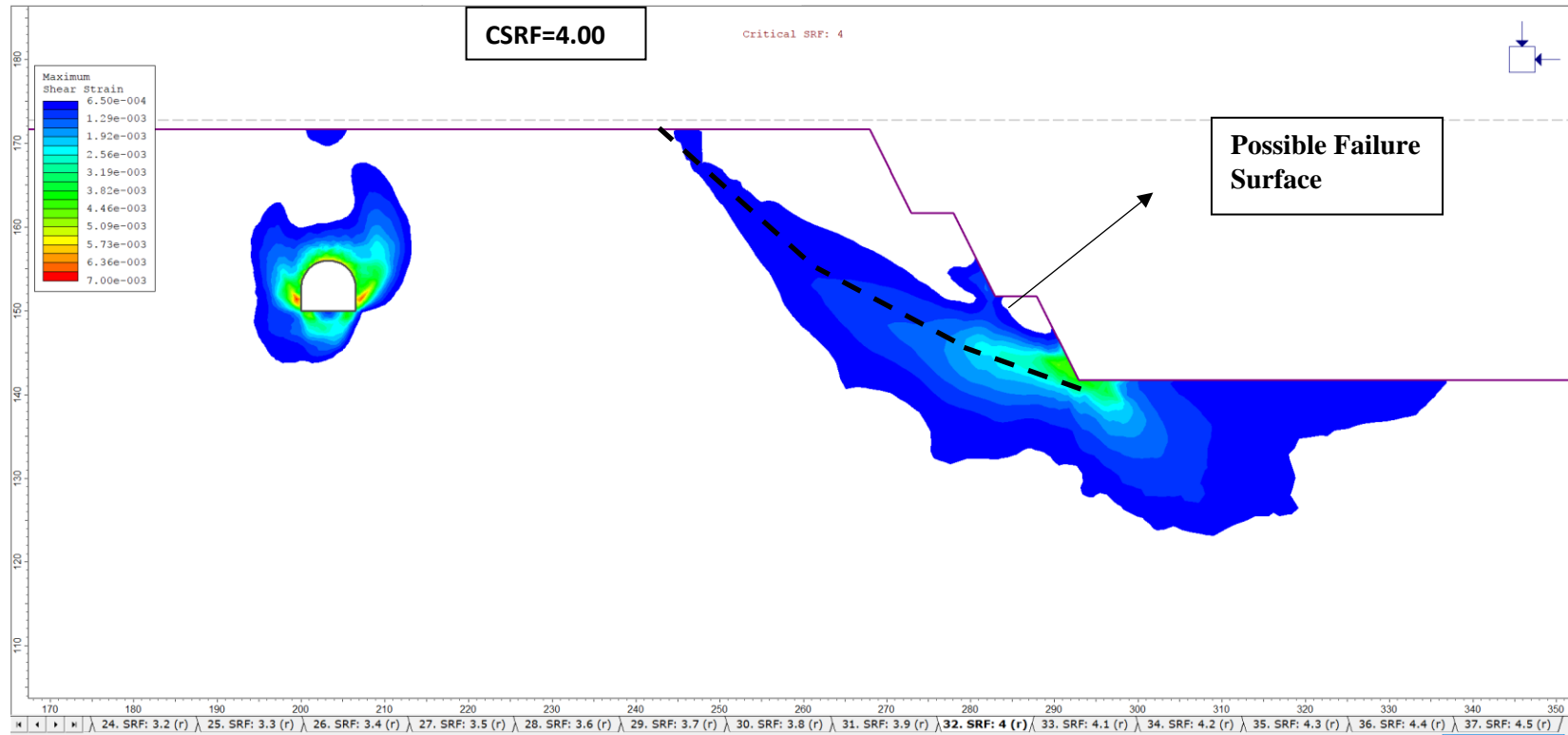
Figure 70. Maximum shear strain distribution and possible failure surface after planned slope cut at the CSRF=3.50 at Km 26+680

Figure 71. Maximum shear strain distribution and possible failure surface after planned slope cut at the SRF=1.50 at Km 26+680

Figure 72. Displacement vectors and displacement magnitudes within planned slope cut at the CSRF=3.50 at Km 26+680

Figure 73. Displacement vectors and displacement magnitudes within planned slope cut at the SRF=1.50 at Km 26+680

Figure 74. Deformations around the tunnel at the CSRF=3.50 at Km 26+680

Figure 75. Deformations around the tunnel at the SRF=1.50 at Km 26+680

Figure 76. Slope dimensions and finite element model of the planned slope profile, section A-A', Km 26+690

Figure 77. Maximum shear strain distribution and possible failure surface after planned slope cut at the CSRF=4.00 at Km 26+690
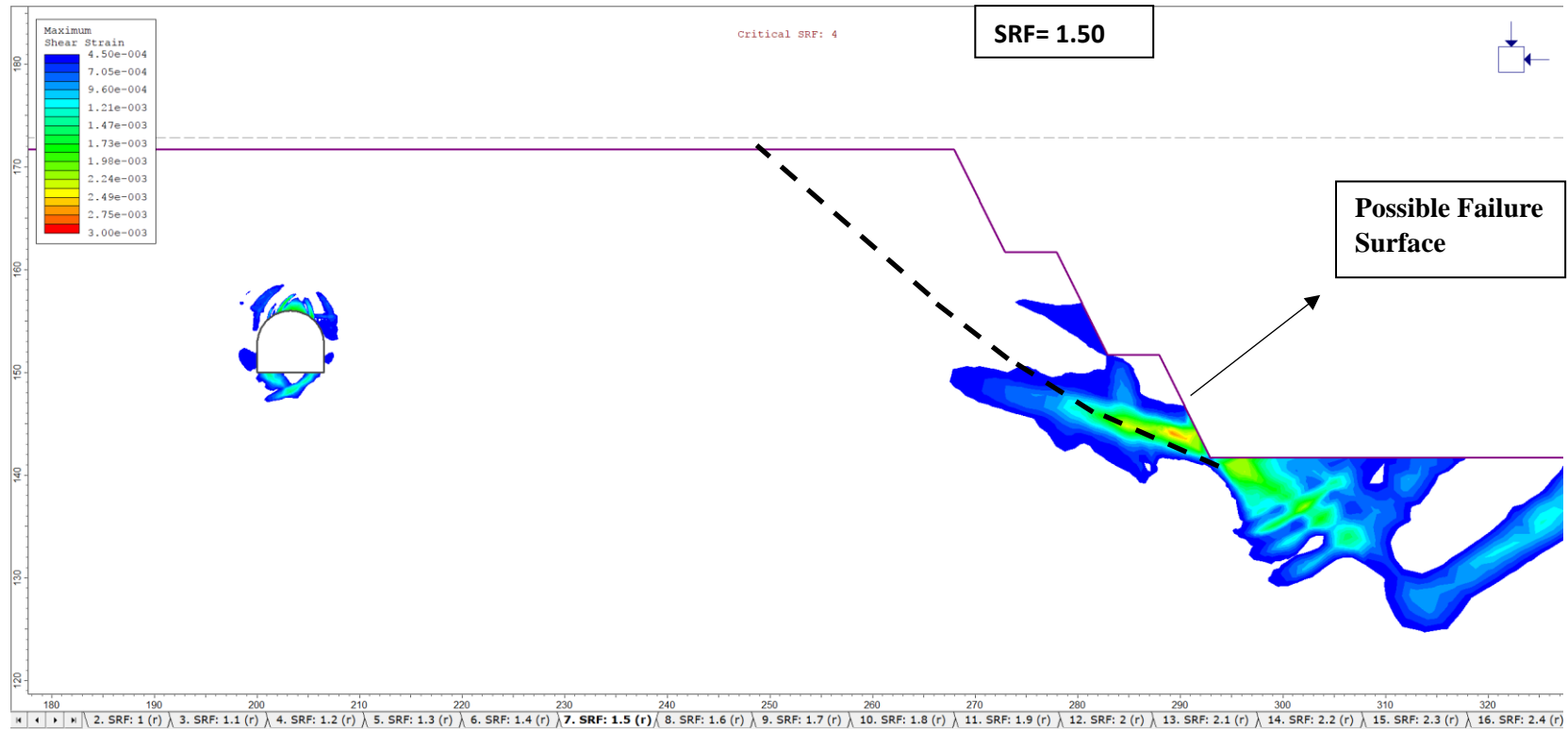
Figure 78. Maximum shear strain distribution and possible failure surface after planned slope cut at the SRF=1.50 at Km 26+690
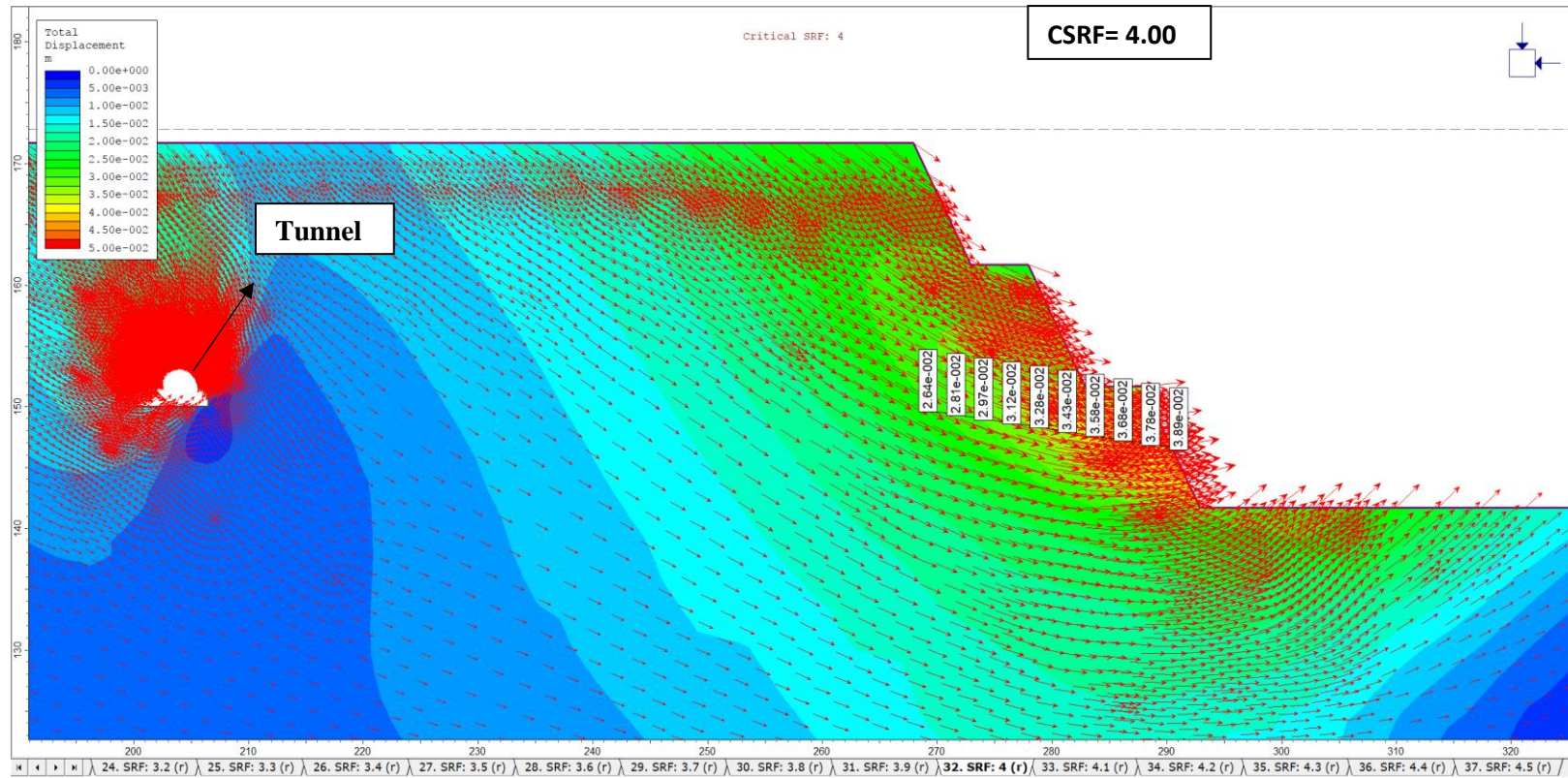
Figure 79. Displacement vectors and displacement magnitudes within planned slope cut at the CSRF=4.00 at Km 26+690
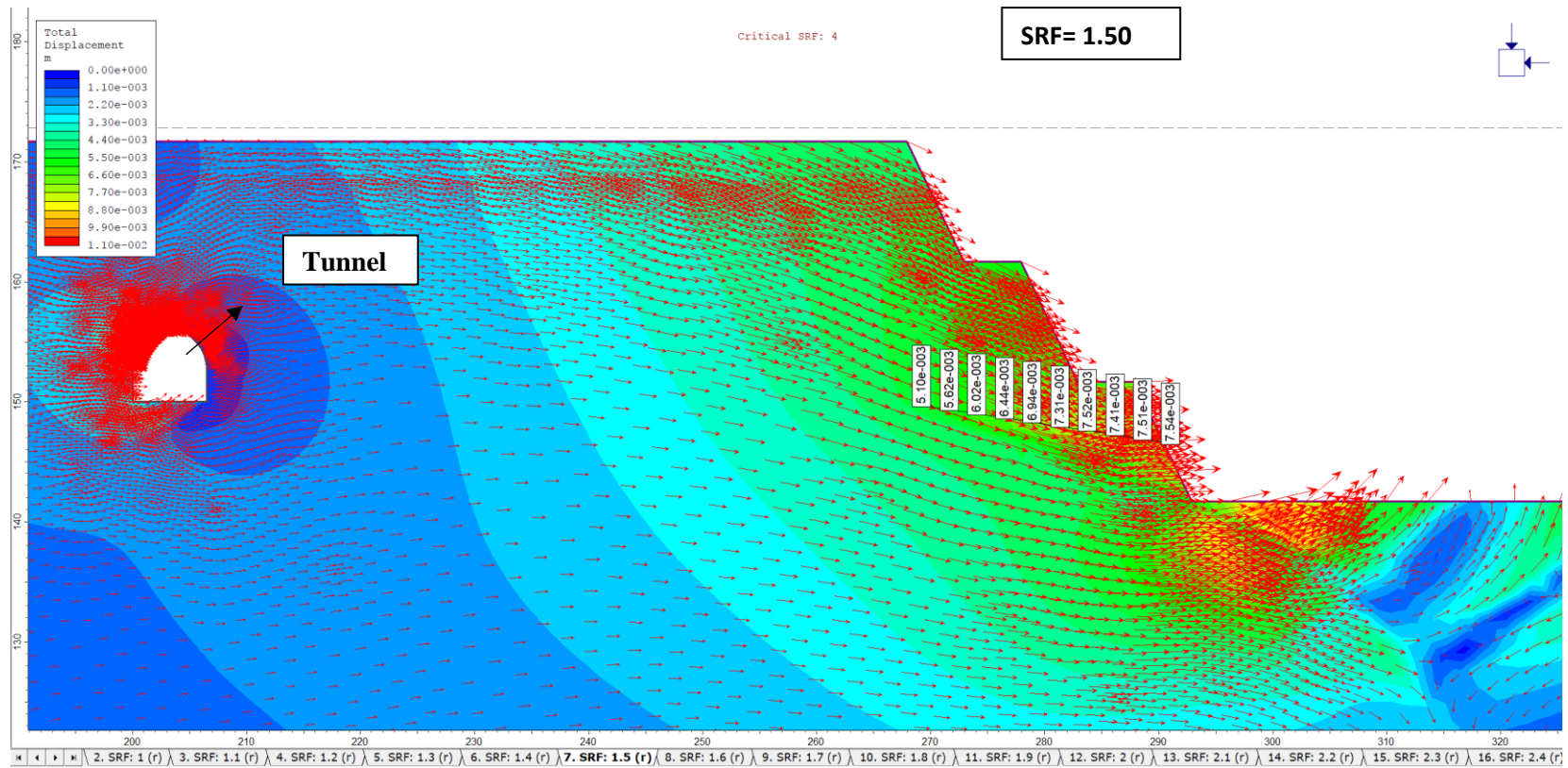
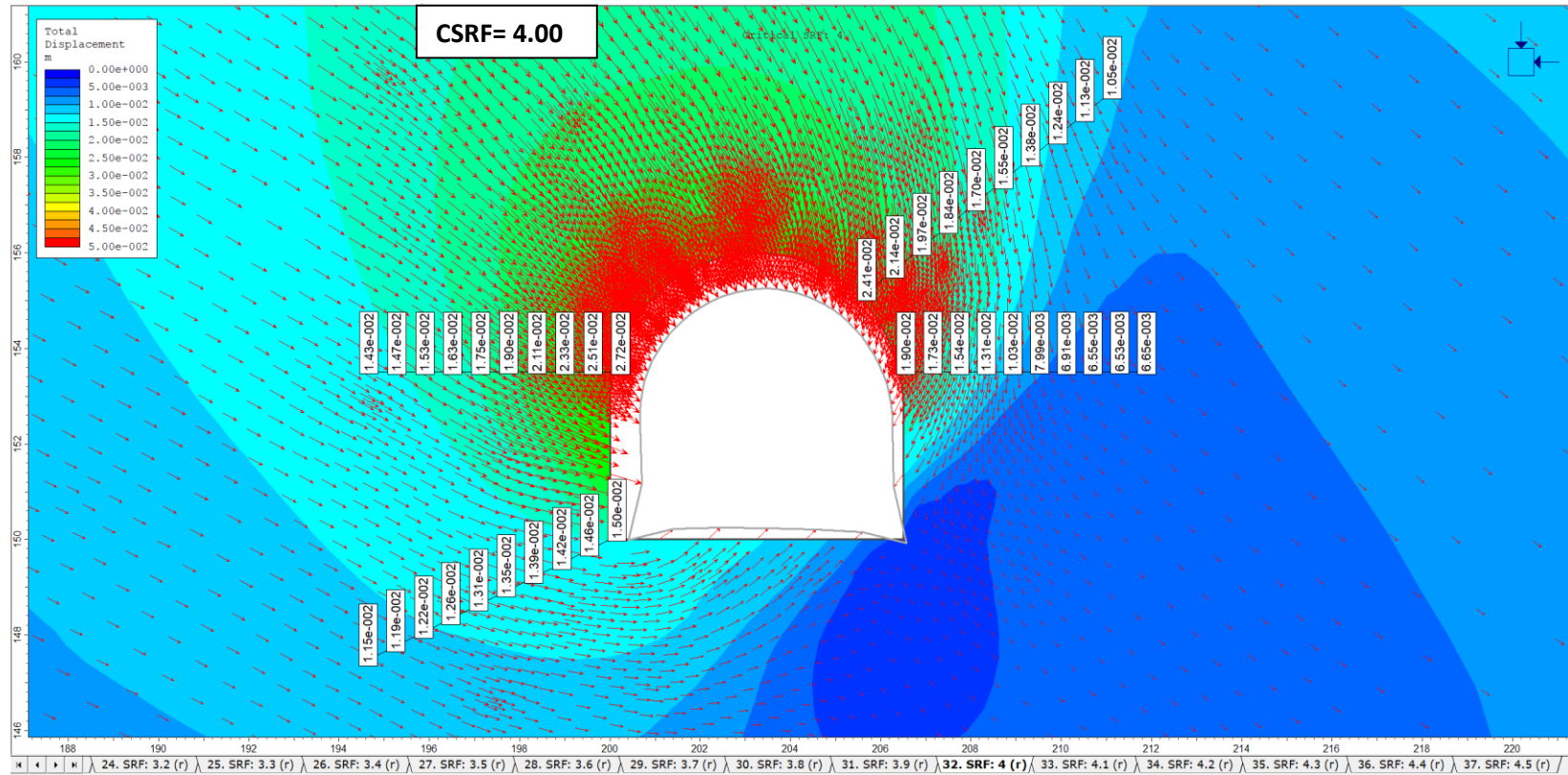*Figure 80. Displacement vectors and displacement magnitudes within planned slope cut at the SRF=1.50 at Km 26+690*

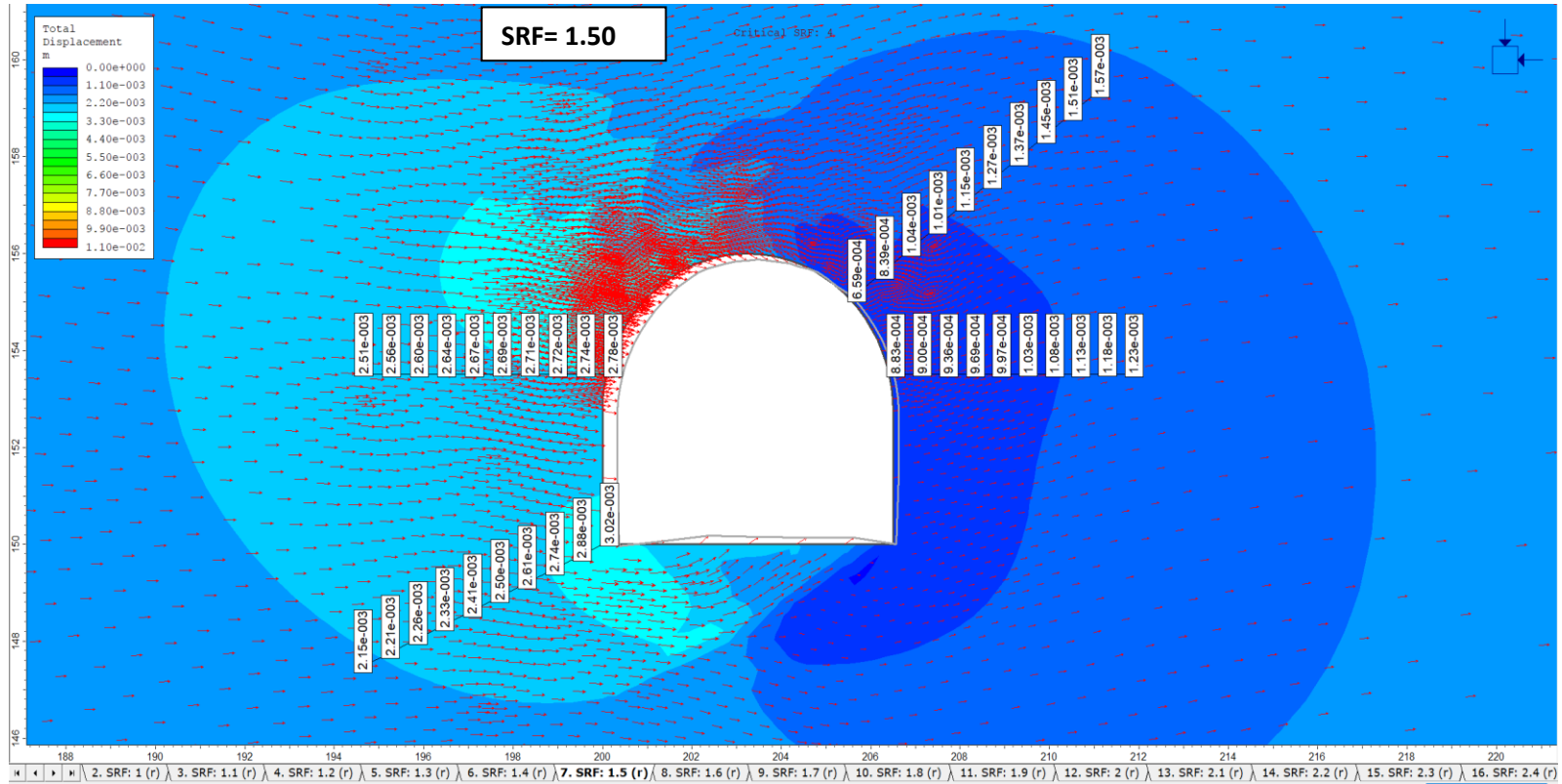*Figure 81. Deformations around the tunnel at the CSRF=4.00 at Km 26+690*

Figure 82. Deformations around the tunnel at the SRF=1.50 at Km 26+690